
Unified Theory of Science (UToS): A Cross-Scale Framework of Constraints, Control, and Governance via Theta (θ)

Matt Murphy

Independent Researcher

January 2026

Abstract

This paper formalizes a Unified Theory of Science (UToS) grounded in constraints, control, and governance across physical, biological, cognitive, social, and scientific systems. We introduce **Theta** (θ) as a dimensionless integration-before-commitment parameter derived from action scale, providing a unifying control variable that governs stability, adaptability, and error correction across domains. Unlike purely metaphorical unification attempts, this work builds on an existing **Theta Calculator** with working derivations, empirical mappings, and a compiled bibliography, elevating θ from a conceptual construct to an operationalizable quantity. We show how stable patterns emerge under constraints, how boundary-maintaining systems regulate internal states, how predictive agents act to minimize expected error, and how societies and scientific institutions function as protocol-coordinated error-reduction systems. Formal definitions, proofs, and measurement strategies are provided, alongside falsifiable predictions and applied case studies in education, organizational leadership, and AI governance. The result is a cross-scale scientific framework that preserves domain specificity while supplying shared mathematical and epistemic structure.

Keywords: cross-scale integration, control theory, theta parameter, action scale, predictive processing, governance, stability bounds, phase separation, scientific methodology

Contents

1	Introduction	9
1.1	The Problem of Fragmentation	9
	Historical Unification Attempts	9
	The Desiderata for Unification	10
1.2	The Theta Framework: A Proposed Resolution	10
	The Core Thesis	10
	Why Action?	11
1.3	Summary of Contributions	12
	Theoretical Contributions	12
	Methodological Contributions	12
	Applied Contributions	13
1.4	Key Symbols and Definitions	13
1.5	Paper Structure	13
1.6	Scope and Companion Work	14
2	Background and Related Work	15
2.1	Cybernetics and Control Theory	15
	Historical Development	15
	Key Results: Stability and Feedback	16
	The PID Controller and Beyond	16
	Connection to Theta	17
2.2	Information Theory	17
	Shannon Entropy and Channel Capacity	17
	Rate-Distortion Theory	18
	Algorithmic Complexity	18
	Physical Constraints on Information	19
	Connection to Theta	19
2.3	Predictive Processing and Active Inference	20
	The Helmholtzian Legacy	20
	The Free Energy Principle	20
	Hierarchical Predictive Coding	21
	Precision and Attention	21
	Active Inference and Expected Free Energy	21
	Connection to Theta	22
2.4	Complex Systems and Emergence	22
	Phase Transitions and Critical Phenomena	22
	Self-Organized Criticality	23

Network Theory	23
Edge of Chaos	24
Urban Scaling and Allometry	24
Connection to Theta	24
2.5 Philosophy of Science	25
Falsifiability and Demarcation	25
Paradigms and Scientific Revolutions	25
Research Programs and Progressive Science	26
Model Selection and Parsimony	26
Institutional Epistemology	27
Connection to Theta	27
2.6 Synthesis and the Theta Contribution	27
What Theta Adds	27
The Integration Achievement	28
3 Core Framework	28
3.1 Layer 1: Stable Patterns Under Constraints	28
Formal Definitions	28
Constraints as Generators of Structure	29
Variational Principles	29
Fundamental Constants as Universal Constraints	29
3.2 Layer 2: Boundary-Maintaining Systems (Life)	30
Formal Definitions	30
Homeostasis and Allostasis	30
The Control-Loop Schema	31
Theta in Biological Systems	31
Information-Theoretic Characterization of Life	31
3.3 Layer 3: Predictive Systems (Minds)	32
Formal Definitions	32
Hierarchical Predictive Coding	32
Action as Prediction Error Minimization	33
Precision and Attention	33
Connection to Theta	33
3.4 Layer 4: Protocol-Coordinated Systems (Society)	34
Formal Definitions	34
Collective Intelligence	34
Examples of Protocols	34
Theta in Social Systems	35
3.5 Layer 5: Science as an Institutional Process	35
The Scientific Method as Protocol	35

Phase Separation in Science	35
The Replication Crisis as Theta Pathology	36
Metascience and Institutional Design	36
Science as Governance	36
4 Theta (θ): The Integration-Before-Commitment Parameter	37
4.1 Scope of Formal Claims	37
4.2 Formal Definition and Physical Interpretation	37
Primary Definition	37
Interpretation as Integration-Before-Commitment	38
Canonical Forms of Action Scale S	38
Canonical Equivalent Definitions of θ	39
Connection to the Principle of Least Action	40
4.3 Mathematical Properties of θ	41
Fundamental Properties	41
Composition and Aggregation Laws	42
Scaling Laws	43
Differential Properties	44
4.4 Stability Theorems	44
Integration-Stability Bound	44
Cross-Domain Consequences of the Stability Bound	47
Connection to Kalman Filtering	48
Numerical Examples	48
4.5 Latency Theorems	49
Margolus-Levitin Connection	50
4.6 Collapse and Phase Behavior	51
Collapse Dynamics	51
Bifurcation Analysis	52
Phase Diagrams	53
Phase Separation Optimality	53
4.7 Independent Theta Derivations	54
Pathway 1: Fundamental Constant Bootstrap	54
Pathway 2: Heisenberg Uncertainty Relations	55
Pathway 3: Bekenstein Entropy Bound	56
Pathway 4: Landauer and Margolus-Levitin Limits	57
Pathway 5: Hawking Radiation and Black Hole Thermodynamics	58
Pathway 6: Holographic Entanglement (AdS/CFT)	59
Pathway 7: Decoherence Dynamics	59
Cross-Pathway Consistency	61
4.8 Cross-Domain Correspondences	61

Mathematical Framework for Correspondences	61
Market-Ferromagnet Correspondence	61
Neural-Ising Correspondence	62
BEC-Social Consensus Correspondence	63
Superconductor-Cognitive Flow Correspondence	63
Epidemic-Percolation Correspondence	64
Universality Classes and Cross-Domain Predictions	65
4.9 Summary: How to Compute θ for a System	65
5 Predictions and Falsifiable Implications	65
5.1 Core Theoretical Predictions	65
Prediction 1: Integration-Stability Relationship	66
Prediction 2: Latency-Accuracy Tradeoff	66
Prediction 3: Phase Separation Advantage	67
5.2 Domain-Specific Predictions	68
Cognitive Science Predictions	68
Organizational Science Predictions	68
Educational Assessment Predictions	69
AI Safety Predictions	69
5.3 Falsification Criteria	70
5.4 Experimental Priorities	70
6 Methods: The Theta Calculator	71
6.1 System Architecture	71
What the Theta Calculator Measures	71
Input Validation Layer	72
Canonical S Computation Module	73
Theta Normalization Engine	73
Stability and Collapse Analyzers	74
Multi-Method Convergence Engine	74
6.2 Domain Mapping Specifications	74
Domain Mapping Summary	74
Physics Domain	75
Biology Domain	75
Cognitive Domain	76
Institutional Domain	76
6.3 Calibration Procedures	77
Step 1: Identify Observable Quantities	77
Step 2: Construct Candidate S Proxies	77
Step 3: Validate Against Known Behaviors	77

Step 4: Cross-Validate Across Pathways	77
6.4 Detailed Worked Examples	78
Canonical Example: Single-Loop Linear Regulator	78
Example 1: Educational Assessment	79
Example 2: Organizational Decision Pipeline	80
Example 3: AI System Oversight	81
7 Applications	82
7.1 Physics and Precision Measurement	82
Laser Stabilization and Frequency Standards	82
Gravitational Wave Detection	83
Quantum Metrology and Sensing	84
7.2 Biology and Physiology	84
Homeostatic Regulation	85
Immune System Dynamics	85
Circadian Rhythms and Biological Clocks	86
Thermoregulation Oscillations	86
7.3 Neuroscience and Cognitive Science	87
The Reflex-Deliberation Continuum	87
Working Memory and Cognitive Capacity	88
Learning and Skill Acquisition	88
7.4 Economics and Social Science	89
Market Microstructure	89
Organizational Decision-Making	89
Democratic Governance	90
7.5 Computer Science and Artificial Intelligence	90
Software Development Lifecycle	91
Machine Learning Training	91
Distributed Computing and Consensus	92
AI Safety and Alignment	93
7.6 Medicine and Public Health	94
Clinical Decision-Making	94
Drug Development Pipeline	95
Pandemic Response	95
7.7 Chemistry and Materials Science	96
Reaction Kinetics	96
Crystallization and Nucleation	97
Battery Management Systems	97
7.8 Ecology and Evolution	97
Predator-Prey Dynamics	98

Evolutionary Adaptation	98
7.9 Earth Systems and Climate Science	98
Weather versus Climate	99
Hazard Management	99
7.10 Psychology and Behavioral Science	99
Signal Detection and Decision Thresholds	100
Habit Formation and Collapse	100
Cognitive Biases as θ Pathologies	101
8 Discussion	101
8.1 Relation to Existing Frameworks	101
Information Theory	101
Minimum Description Length	102
Control Theory	102
Predictive Processing and Active Inference	102
Thermodynamics and Statistical Mechanics	103
Complexity Measures	103
Framework Comparison Summary	105
8.2 Theoretical Implications	105
Unification Without Reduction	105
The Science of Science	106
Limits of the Framework	106
8.3 Strengths of the Theta Framework	106
Cross-Scale Applicability	106
Operational Measurability	106
Multiple Derivation Pathways	106
Falsifiable Predictions	107
Practical Utility	107
8.4 Limitations and Challenges	107
Measurement Ambiguity	107
Risk of Over-Generalization	107
Computational Complexity	107
Normative Ambiguity	108
What This Framework Does Not Claim	108
8.5 Future Research Directions	109
Empirical Validation	109
Theoretical Extensions	109
Tool Development	110
Policy Applications	110

9 Conclusion	110
A Formal Proofs (Expanded)	111
A.1 Dimensional Consistency of θ	111
A.2 Scale Aggregation Invariance	111
A.3 Error Variance Bound Derivation	111
A.4 Latency-Stability Tradeoff	112
A.5 Collapse Threshold Analysis	112
A.6 Phase Separation Optimality	113
B Extended Worked Examples	113
B.1 Educational Assessment	113
B.2 AI Alignment Pipelines	113
C Theta Calculator Reference	114
C.1 Proof Module Architecture	114
C.2 Numerical Quick-Estimate Methods	115
C.3 Cross-Pathway Validation	115
C.4 Bibliographic Grounding	116
D Precalculated Theta Values Across Domains	116
D.1 Domain Summary Table	116
D.2 Electromagnetic Spectrum	116
D.3 Economics and Financial Markets	117
D.4 Quantum Computing Platforms	118
D.5 Cosmological Evolution	118
D.6 Cognitive and Neural States	118
D.7 Complex Systems and Critical Phenomena	119

1. Introduction

1.1. The Problem of Fragmentation

The sciences have achieved remarkable explanatory power within their respective domains, yet struggle to share explanatory primitives across scale Wilson and Kogut [1974], Stanley [1971]. Physics describes fundamental interactions through quantum mechanics and general relativity. Biology explains life processes through molecular mechanisms and evolutionary dynamics. Cognitive science models minds through neural computation and behavioral analysis. Social science analyzes collective behavior through institutions and cultural evolution. Each domain has developed sophisticated theoretical frameworks, precise measurement tools, and powerful predictive models—but these domains often operate with incompatible vocabularies and frameworks.

This fragmentation is not merely inconvenient; it represents a fundamental barrier to understanding cross-scale phenomena. Consider the following questions that resist single-domain analysis:

- How do molecular mechanisms in neurons give rise to conscious experience and decision-making?
- How do individual cognitive biases aggregate into market dynamics and social movements?
- How do physical constraints on information processing shape the evolution of intelligence?
- How do governance institutions emerge from and influence individual behavior?

Each question spans multiple scales and requires concepts from multiple domains. Yet the standard scientific approach—deep specialization within narrow domains—provides few tools for such integration.

Historical Unification Attempts

The desire for unification has deep historical roots. The logical positivists of the Vienna Circle sought to ground all knowledge in observation statements and logical relations. Their unity of science program aimed to reduce all sciences to physics through definitional chains. This reductionist program failed: higher-level phenomena proved irreducible to lower-level descriptions, and the required bridge laws could not be constructed.

Emergence-based approaches took the opposite tack, emphasizing the irreducibility of higher-level patterns. Complex systems science Bak et al. [1987], Langton [1990] demonstrated that simple rules can generate complex behavior, that macroscopic regularities need not be derivable from microscopic dynamics, and that similar patterns can arise from diverse underlying mechanisms. Yet emergence often remains descriptive rather than predictive, and the concept of “emergent property” can become a placeholder for ignorance rather than an explanation.

Cybernetics represented an early attempt at cross-domain unification through shared formal structures Wiener [1948], Ashby [1956]. Norbert Wiener recognized that feedback, control, and communication principles apply across mechanical, biological, and social systems. This insight was

productive but remained largely qualitative; cybernetics lacked a single quantitative parameter that could bridge domains.

More recently, information-theoretic approaches have sought unification through entropy, complexity, and computational concepts Shannon [1948]. The free energy principle extends these ideas to cognitive and biological systems Tononi et al. [2016], Friston [2010]. These frameworks represent significant advances but typically address cognitive systems without extending systematically to physics, governance, or scientific methodology. Recent work on the relationship between AI and physics Peter Coveney [2025] argues that physical principles must inform AI development, a perspective consistent with the θ framework’s grounding in action.

The Desiderata for Unification

A successful unifying framework must satisfy several demanding criteria:

1. **Preserve domain specificity:** The framework should not collapse distinct phenomena into false equivalences. Physics, biology, psychology, and sociology address genuinely different subject matters with different methods; any unification must respect these differences.
2. **Provide shared vocabulary:** The framework should supply concepts that translate meaningfully across domains, enabling cross-scale analysis and communication between specialists.
3. **Yield operational definitions:** Abstract concepts must connect to measurable quantities. A unifying parameter that cannot be estimated from empirical data has limited scientific value.
4. **Generate testable predictions:** The framework must yield falsifiable claims that can distinguish it from alternative accounts. Unfalsifiable frameworks, however elegant, fail the basic criterion of scientific knowledge.
5. **Connect to established theory:** The framework should extend rather than replace successful existing theories, showing how established results emerge as special cases or how established concepts relate to unified concepts.

1.2. The Theta Framework: A Proposed Resolution

This paper proposes a resolution through the introduction of Theta (θ), a dimensionless control parameter that operates across scales. The central claim is that diverse systems—from quantum measurements to institutional decisions—can be characterized by a common parameter that measures integration-before-commitment: the ratio of the quantum of action to the characteristic action scale of the process under consideration.

The Core Thesis

The unified framework rests on six interconnected claims:

1. **Physical constraints generate stable patterns.** The fundamental laws of physics—conservation laws, symmetry principles, and extremization of action—define what configurations are possible and stable Planck [1901], Einstein [1905]. Stable patterns are not accidents but mathematical necessities given constraints.
2. **Some patterns become boundary-maintaining systems.** Life represents a qualitative transition: certain physical configurations maintain their own boundary conditions through metabolic and reproductive processes Strogatz [2015], Klinman and Kohen [2013]. Living systems are distinguished by their active maintenance of organization against thermodynamic degradation, exploiting nonlinear dynamics and catalytic mechanisms to sustain far-from-equilibrium states.
3. **Some boundary-maintaining systems develop predictive models.** Minds represent a further transition: certain living systems construct internal models of their environment and act to minimize prediction error Friston [2010], Dehaene and Changeux [2011]. Cognition is the process of modeling and anticipating external states.
4. **Predictive systems coordinate through protocols.** Societies emerge when multiple cognitive agents coordinate behavior through shared conventions, languages, and institutions Castellano et al. [2009]. Social organization enables collective error correction beyond individual capacity.
5. **Science is the institutional process of systematic error correction.** The scientific method represents a specialized social protocol for generating and validating knowledge about the world, distinguished by its explicit alternation between exploratory hypothesis generation and rigorous empirical validation Åström and Murray [2010].
6. **Theta (θ) parameterizes integration-before-commitment across all layers.** A single dimensionless quantity—the ratio $\theta = S_0/S$ of the minimum resolvable action to system action scale—captures the degree of deliberation, evidence accumulation, or phase-space exploration that precedes irreversible commitment. In physical systems, $S_0 = \hbar$ (Planck’s constant); in non-physical domains, S_0 functions as a normalization constant.

Why Action?

The choice of action (S , in units of J·s) as the fundamental quantity deserves justification. Action is the most fundamental quantity in physics: the principle of least action underlies classical mechanics, electromagnetism, general relativity Einstein [1915], Misner et al. [1973], and quantum field theory. Every physical law can be derived from extremizing an action functional, a principle with origins tracing back to Hamilton and Lagrange that achieves its fullest expression in modern gauge theories.

Moreover, action is dimensionally unique: it combines energy and time into a single quantity that measures “how much happened.” The quantum of action \hbar , first identified by Planck Planck

[1901], sets an absolute scale: processes involving action smaller than \hbar are quantum-dominated and cannot be localized in phase space Heisenberg [1927], Robertson [1929]. Processes involving action much larger than \hbar are classical and well-defined, exhibiting the deterministic trajectories of classical mechanics.

The ratio $\theta = \hbar/S$ therefore has clear physical meaning:

- When $\theta \approx 1$: The process operates near quantum limits; superposition, uncertainty, and coherence dominate.
- When $\theta \ll 1$: The process is classical; trajectories are well-defined and reversibility is lost.

Extending this ratio to biological, cognitive, and social domains requires identifying appropriate action proxies S for each context. The Theta Calculator implements these mappings and provides consistency checks across domains.

1.3. Summary of Contributions

This work makes the following contributions to the scientific literature:

Theoretical Contributions

1. **A five-layer ontology.** We formalize the hierarchy from physical constraints through life, mind, society, to science as institutional error correction. Each layer builds on the previous while introducing genuinely new properties that cannot be reduced to lower layers.
2. **A cross-scale vocabulary.** We provide precise definitions for constraints, boundary maintenance, prediction error, protocols, governance, and phase separation that translate across domains while respecting domain-specific meanings.
3. **The θ parameter.** We introduce and rigorously define Theta as a dimensionless integration-before-commitment parameter with seven independent derivation pathways providing internal consistency checks.
4. **Stability and latency theorems.** We prove bounds relating θ to estimation error, commitment latency, and system stability, establishing quantitative relationships that enable prediction.
5. **Phase separation optimality.** We demonstrate formally that separating high- θ exploration from low- θ validation is optimal under resource constraints, providing theoretical grounding for the scientific method’s structure.

Methodological Contributions

1. **Operational definitions.** Each theoretical concept is connected to measurable quantities through explicit proxy definitions and estimation procedures.

2. **The Theta Calculator.** We provide a computational tool implementing the framework, enabling researchers to estimate θ for specific systems and verify cross-domain consistency.
3. **Falsifiable predictions.** We generate specific, testable predictions distinguishing the framework from alternatives, including predictions about institutional design, educational assessment, and AI governance.

Applied Contributions

1. **Cross-domain applications.** We demonstrate how the framework applies to physics (metrolology, laser stabilization), biology (homeostasis, immune response), neuroscience (decision-making, learning), economics (market dynamics, organizational design), computer science (software development, AI safety), and medicine (drug approval, clinical trials).
2. **Diagnostic capability.** The framework enables diagnosis of system pathologies as θ collapse (insufficient integration) or θ stagnation (excessive integration), suggesting targeted interventions.
3. **Design principles.** The framework yields principles for institutional design, emphasizing phase separation, appropriate θ matching to decision stakes, and hierarchical nesting of integration scales.

1.4. Key Symbols and Definitions

Table 1 provides a reference for the primary symbols used throughout this paper. All quantities are defined with explicit units, domain of validity, and notes on interpretation. This table should be consulted when encountering symbols in later sections.

1.5. Paper Structure

The remainder of this paper is organized as follows:

Section 2 (Background and Related Work) surveys the five intellectual traditions that inform the framework: cybernetics and control theory, information theory, predictive processing and active inference, complex systems and emergence, and philosophy of science. We explain how each tradition contributes to the unified framework and where θ extends beyond existing approaches.

Section 3 (Core Framework) develops the five-layer ontology in detail. We provide formal definitions for each layer, establish the vocabulary of constraints, boundaries, predictions, protocols, and governance, and show how each layer relates to those above and below.

Section 4 (Theta: The Integration-Before-Commitment Parameter) presents the central theoretical contribution. We define θ formally, establish its mathematical properties, prove stability and latency theorems, analyze phase behavior and collapse dynamics, and present seven independent derivation pathways.

Section 5 (Predictions and Falsifiable Implications) derives specific testable predictions from the framework, providing experimental protocols and expected effect sizes.

Symbol	Name	Informal Meaning	Formal Definition	Units	Notes
θ	Theta	Integration-before-commitment parameter	$\theta \equiv S_0/S$	Dimensionless	0 < θ < 1 calibration
S_0	Minimum action quantum	Smallest resolvable action	$S_0 = \hbar$ (physical)	J·s	No units
\hbar	Reduced Planck constant	Quantum of action	$\hbar/(2\pi) \approx 1.055 \times 10^{-34}$	J·s	Physical
S	Action scale	Characteristic action of process	Domain-dependent proxy	J·s	See notes
S_E	Energetic action	Energy-time product	$S_E = E \cdot T$	J·s	Physical
S_R	Resource action	Resource-cycle product	$S_R = R \cdot \tau$	Domain units	Biology
S_L	Lagrangian action	Path integral of Lagrangian	$S_L = \int_0^T L dt$	J·s	Classical
S_I	Information action	Processing work	$S_I = \epsilon \cdot I \cdot T$	J·s	Computer
\mathcal{S}	State space	Set of possible system states	Topological space	—	Domain
\mathcal{C}	Constraint	Restriction on state space	$\mathcal{C} \subseteq \mathcal{S}$	—	Definition
σ^2	Variance	Uncertainty in observations	$\mathbb{E}[(x - \mu)^2]$	(state units) ²	Statistical
σ_c^2	Post-commitment variance	Uncertainty after commitment	Theorem 4.15 bound	(state units) ²	Kept
π	Precision	Inverse variance	$\pi = 1/\sigma^2$	(state units) ⁻²	$\pi \propto$
ϵ_t	Prediction error	Model-reality discrepancy	$\epsilon_t = s_t - \hat{s}_t$	state units	Difference
E	Energy	Characteristic energy scale	System-dependent	J	Physical
T	Integration time	Duration of pre-commitment phase	Context-dependent	s	Kept
P	Power	Energy expenditure rate	$P = dE/dt$	W	Law
k_B	Boltzmann constant	Thermal energy scale	1.381×10^{-23}	J/K	Thermal

Table 1: Primary symbols used in the θ framework. All symbols are defined with explicit units and domain of validity. Dimensionless θ is the central quantity; other symbols support its definition and application.

Section 6 (Methods: The Theta Calculator) describes the computational implementation, including architecture, domain mappings, calibration procedures, and worked examples.

Section 7 (Applications) demonstrates the framework across six domains: physics, biology, neuroscience, economics, computer science, and medicine.

Section 8 (Discussion) addresses the relationship to existing frameworks, strengths and limitations, and future research directions.

Section 9 (Conclusion) summarizes the contributions and identifies the most promising avenues for empirical validation.

Appendices provide expanded proofs, additional worked examples, and technical reference material for the Theta Calculator.

1.6. Scope and Companion Work

This paper establishes the core θ framework and its formal foundations. It is intended as the theoretical anchor for a research program rather than a final comprehensive treatment:

- **Paper 1 (this paper):** Core θ definition and the stability/latency bounds (Theorems 4.15–

??).

- **Paper 2:** Measurement protocol with domain-specific calibration procedures for obtaining empirical θ estimates.
- **Paper 3:** Empirical validations testing stability-latency bounds in education, organizations, and AI safety domains.
- **Paper 4:** Theta Calculator software documentation with implementation guide and usage examples.

The present work provides the mathematical foundation; subsequent work will test, extend, and apply these foundations in specific contexts.

2. Background and Related Work

This work integrates and extends established traditions rather than replacing them. The θ framework draws on five major intellectual lineages: cybernetics and control theory, information theory, predictive processing and active inference, complex systems and emergence, and philosophy of science. Each tradition contributes essential concepts that the unified framework synthesizes into a coherent whole.

2.1. Cybernetics and Control Theory

The study of feedback, regulation, and stability under perturbation provides foundational concepts for understanding how systems maintain desired states. Control theory formalizes the relationship between sensing, error computation, and actuation that underlies all self-regulating systems.

Historical Development

The field of cybernetics emerged in the mid-twentieth century from the confluence of several disciplines. Norbert Wiener's foundational work Wiener [1948] established the mathematical framework for understanding feedback in both biological and mechanical systems. Wiener recognized that the same principles of negative feedback that stabilize amplifier circuits also govern physiological homeostasis and goal-directed behavior in organisms. His synthesis of control engineering, neurophysiology, and statistical mechanics created a new interdisciplinary framework for understanding self-regulating systems.

W. Ross Ashby extended these ideas with his law of requisite variety: a controller must have at least as many states as the system it controls to maintain stability Ashby [1956]. This principle establishes a fundamental information-theoretic constraint on control—a theme that connects directly to the θ framework's emphasis on action and information bounds. Ashby's concept of ultrastability—systems that can reorganize their own parameters to maintain homeostasis—anticipates modern work on adaptive control and meta-learning.

The classical period (1940s–1960s) focused on linear systems and frequency-domain methods. The Nyquist stability criterion, Bode plots, and root locus techniques provided engineers with powerful tools for designing stable controllers. The state-space revolution of the 1960s, pioneered by Kalman, introduced optimal control theory and established connections between control and estimation that remain central to modern practice Murray [2018].

Key Results: Stability and Feedback

The central problem of control theory is stability: ensuring that a system remains bounded and converges to desired behavior despite perturbations. Several fundamental results characterize stability conditions.

Lyapunov Stability. A system $\dot{x} = f(x)$ is stable at equilibrium x^* if there exists a Lyapunov function $V(x) > 0$ with $\dot{V}(x) \leq 0$ along trajectories. The existence of such a function guarantees that perturbations do not grow unboundedly. For linear systems $\dot{x} = Ax$, stability is equivalent to all eigenvalues of A having negative real parts.

BIBO Stability. A system is bounded-input-bounded-output (BIBO) stable if every bounded input produces a bounded output. For linear time-invariant systems, BIBO stability is equivalent to having all poles in the left half-plane.

Feedback Linearization. Nonlinear systems can often be rendered linear through appropriate feedback transformations, extending linear control techniques to broader classes of systems Doyle et al. [1992], Ott [2002].

Robust Control. The H_∞ framework addresses uncertainty explicitly, designing controllers that maintain stability and performance despite model mismatch Skogestad and Postlethwaite [2005]. This connects to the θ framework’s emphasis on stability under uncertainty.

The PID Controller and Beyond

The proportional-integral-derivative (PID) controller remains the workhorse of industrial control:

$$u(t) = K_p e(t) + K_i \int_0^t e(\tau) d\tau + K_d \frac{de}{dt} \quad (1)$$

where $e(t) = r(t) - y(t)$ is the error between setpoint r and output y .

Each term plays a distinct role:

- Proportional: Responds to current error—higher gain increases responsiveness but risks instability.
- Integral: Eliminates steady-state error by accumulating past errors—provides persistence.
- Derivative: Anticipates future error by responding to rate of change—provides damping.

The PID structure directly parallels the θ framework: the integral term implements integration-before-commitment (accumulating evidence before action), while the proportional and derivative terms balance responsiveness against stability.

Modern control extends beyond PID to include:

- **Model Predictive Control (MPC):** Optimizes control actions over a receding horizon using an explicit model of system dynamics Skogestad and Postlethwaite [2005]. MPC naturally implements θ -like tradeoffs by adjusting the prediction horizon.
- **Adaptive Control:** Adjusts controller parameters online as system characteristics change Åström and Murray [2010]. Contemporary work applies adaptive methods to AI systems Zhang [2025] and explores multi-agent coordination Sumit Kumar Jana [2025], Jiang [2025].
- **Nonlinear Control:** Handles systems where linear approximations fail Strogatz [2015]. Bifurcation analysis reveals how small parameter changes can cause qualitative behavioral shifts.

Connection to Theta

Control theory provides the mathematical language for the θ framework’s central claims about stability and latency. The integration-stability bound (Theorem 4.15) generalizes classical results about estimation error reduction through averaging. The latency-stability tradeoff (Corollary 4.19) formalizes what control engineers know intuitively: faster response requires accepting greater uncertainty.

The θ parameter can be understood as a generalized measure of integration depth in any control loop. Low θ corresponds to high-bandwidth, reactive control (fast but potentially unstable). High θ corresponds to low-bandwidth, deliberative control (slow but stable). The control-theoretic insight is that there is no free lunch: stability and responsiveness trade off fundamentally.

2.2. Information Theory

Shannon’s formalization of entropy, compression, and channel capacity establishes fundamental constraints on information processing that apply across all physical systems Shannon [1948]. Information theory provides the language for understanding how systems encode, transmit, and decode signals—operations central to the θ framework’s account of integration and commitment.

Shannon Entropy and Channel Capacity

The Shannon entropy of a discrete random variable X with probability mass function $p(x)$ is:

$$H(X) = - \sum_x p(x) \log_2 p(x) \tag{2}$$

Entropy measures uncertainty: a uniform distribution over n outcomes has entropy $\log_2 n$ bits, while a deterministic outcome has zero entropy. For continuous distributions, differential entropy

generalizes the concept:

$$h(X) = - \int p(x) \log p(x) dx \quad (3)$$

Shannon's channel capacity theorem establishes the maximum rate at which information can be reliably transmitted through a noisy channel:

$$C = \max_{p(x)} I(X; Y) \quad (4)$$

where $I(X; Y) = H(X) - H(X|Y)$ is the mutual information between input X and output Y .

For an additive white Gaussian noise channel with bandwidth W and signal-to-noise ratio SNR:

$$C = W \log_2(1 + \text{SNR}) \quad (5)$$

This result places fundamental limits on communication that no system can exceed, regardless of coding scheme.

Rate-Distortion Theory

While channel capacity concerns reliable communication, rate-distortion theory addresses lossy compression: how much can a source be compressed while maintaining acceptable fidelity?

Given a distortion measure $d(x, \hat{x})$ between original x and reconstruction \hat{x} , the rate-distortion function $R(D)$ gives the minimum bits per symbol needed to achieve average distortion at most D :

$$R(D) = \min_{p(\hat{x}|x): \mathbb{E}[d(X, \hat{X})] \leq D} I(X; \hat{X}) \quad (6)$$

For a Gaussian source with variance σ^2 under squared-error distortion:

$$R(D) = \frac{1}{2} \log_2 \frac{\sigma^2}{D} \quad \text{for } D \leq \sigma^2 \quad (7)$$

Rate-distortion theory connects to the θ framework through the tradeoff between compression (commitment to a simplified representation) and fidelity (accurate modeling of the source).

Algorithmic Complexity

Kolmogorov complexity measures the intrinsic complexity of an object as the length of the shortest program that produces it:

$$K(x) = \min_{p: U(p)=x} |p| \quad (8)$$

where U is a universal Turing machine and $|p|$ is the length of program p .

While Kolmogorov complexity is uncomputable, it provides a theoretical foundation for understanding compression limits and model complexity. The minimum description length (MDL) principle uses approximations to Kolmogorov complexity for practical model selection Mac Lane

[1998]. Deutsch's foundational work on quantum computation Deutsch [1983] established that quantum systems can perform computations impossible for classical Turing machines, connecting information-theoretic complexity to physical constraints in a manner directly relevant to θ 's action-based formulation.

Physical Constraints on Information

Information processing is not free—it requires physical resources and obeys physical constraints.

Landauer's Principle Landauer [1961]: Erasure of one bit of information requires minimum energy dissipation:

$$E_{\text{erase}} \geq k_B T \ln 2 \approx 2.9 \times 10^{-21} \text{ J at room temperature} \quad (9)$$

This establishes that information has physical reality: erasing information produces entropy and dissipates heat Landauer et al. [1997].

Bekenstein Bound Bekenstein [1981]: The maximum information content of a region of space is bounded by:

$$I_{\max} \leq \frac{2\pi RE}{\hbar c \ln 2} \quad (10)$$

where R is the radius and E is the energy. This connects information to geometry and gravity.

Holographic Principle: The Bekenstein bound implies that the information content of any region scales with its surface area, not its volume—a result formalized in the AdS/CFT correspondence Maldacena [1999], Hubeny et al. [2007]. This covariant formulation of the holographic bound, developed independently of the static Bekenstein limit, provides a fully relativistic treatment that applies to time-dependent spacetimes.

Connection to Theta

Information theory provides several of the independent derivation pathways for θ :

- The Bekenstein bound leads to θ_B measuring information utilization relative to physical limits.
- The Landauer principle leads to θ_L measuring computational efficiency.
- The Margolus-Levitin bound leads to θ_{ML} measuring operation rate relative to quantum limits.

More broadly, information theory establishes that all physical systems face fundamental tradeoffs between rate, accuracy, and energy. The θ framework generalizes these tradeoffs through the action-based parameterization that unifies energetic, temporal, and informational constraints. Recent work on the entropy of natural language Colin Scheibner [2025] demonstrates how information-theoretic analysis reveals deep structure in complex systems, while studies of molecular communication Wafa Labidi [2025] extend Shannon's framework to biological signaling contexts. The

connection between information and physics is further illuminated by Wheeler’s “it from bit” doctrine, which proposes that physical reality fundamentally derives from information-theoretic processes Wheeler [1990]. This perspective, originating in Wheeler’s participatory anthropic principle Wheeler [1957], suggests that measurement and observation play constitutive roles in physical reality—a view that connects naturally to the θ framework’s emphasis on commitment as the bridge between quantum and classical regimes.

2.3. Predictive Processing and Active Inference

The framework of agents minimizing expected prediction error through perception and action provides a unifying principle for understanding biological and cognitive systems Friston [2010], Clark [2013], Tononi et al. [2016]. This tradition, sometimes called the “Bayesian brain” hypothesis, reconceptualizes cognition as continuous hypothesis testing about the causes of sensory signals. The philosophical implications of this framework have been extensively analyzed Hohwy [2013], revealing deep connections between perception, action, and inference.

The Helmholtzian Legacy

Hermann von Helmholtz recognized in the nineteenth century that perception is not passive reception but active inference. The brain constructs hypotheses about external causes and tests them against sensory evidence. Ambiguous stimuli (optical illusions, bistable figures) reveal this constructive process. Contemporary computational models formalize this insight using variational inference and message-passing algorithms Gordon [2024]. Advances in neural network architectures for perception and reasoning Zhang et al. [2017], Kjetil O. Lye [2019] provide computational implementations of these principles. Recent work on attention mechanisms Wenhui Gao [2024] and multimodal learning Zhixing Wan [2024] demonstrates how modern AI systems implement hierarchical inference structures analogous to biological perception.

Modern predictive processing formalizes Helmholtz’s insight: the brain maintains a generative model of the world and continuously compares its predictions against incoming sensory data. Perception emerges from minimizing the discrepancy between prediction and observation.

The Free Energy Principle

The free energy principle (FEP) provides a mathematical formalization of predictive processing. For a system with internal states μ , sensory states s , and external states η , the variational free energy is:

$$F = D_{KL}[Q(\eta|\mu)\|P(\eta|s)] + \mathbb{E}_Q[\log P(s|\eta)] \quad (11)$$

Minimizing free energy drives two complementary processes:

1. **Perception:** Updating internal states μ to better model external causes η .
2. **Action:** Changing sensory states s to match predictions.

The FEP claims that any self-organizing system that maintains itself against the second law of thermodynamics must minimize free energy—a claim that connects to the θ framework’s emphasis on boundary maintenance and error correction. Recent work extends the FEP to multi-agent systems Domenico Maisto [2025] and visual attention Tin Mii [2025], demonstrating its broad applicability across cognitive domains.

Hierarchical Predictive Coding

The brain implements prediction at multiple hierarchical levels Dehaene and Changeux [2011]. Each level predicts the activity of the level below, and only prediction errors propagate upward:

$$\epsilon_\ell = r_\ell - g_\ell(r_{\ell+1}) \quad (12)$$

$$\dot{r}_\ell = -\epsilon_\ell + \epsilon_{\ell-1} \cdot g'_{\ell-1} \quad (13)$$

where r_ℓ is the representation at level ℓ , g_ℓ is the generative model, and ϵ_ℓ is the prediction error.

This architecture has several advantages:

- **Efficient coding:** Only unexpected information is transmitted, reducing bandwidth requirements.
- **Robust inference:** Top-down predictions provide context that disambiguates bottom-up signals.
- **Flexible learning:** Prediction errors drive learning at all levels simultaneously.

Precision and Attention

Not all prediction errors are equal. The brain weights errors by their precision (inverse variance):

$$\hat{\epsilon}_\ell = \pi_\ell \cdot \epsilon_\ell \quad (14)$$

Attention can be understood as precision optimization: attending to a stimulus increases the precision-weighting of errors from that source, amplifying their influence on inference. Conversely, ignoring a stimulus decreases its precision, suppressing its influence.

This precision-weighting mechanism provides a natural account of selective attention, arousal, and the effects of neuromodulators that adjust gain and sensitivity Miller [1956]. Cognitive load theory Sweller [1988] provides complementary perspectives on how processing capacity constraints shape learning and performance.

Active Inference and Expected Free Energy

Active inference extends predictive processing to action selection Filippo Torresan [2025]. Rather than separating perception from action, active inference treats both as serving the same objective:

minimizing prediction error over time. Agents select actions that minimize expected free energy:

$$G(\pi) = \mathbb{E}_{Q(o,s|\pi)} [\log Q(s|\pi) - \log P(o,s)] \quad (15)$$

This decomposes into epistemic and pragmatic components:

$$G(\pi) = \underbrace{-\mathbb{E}_Q[H(s|o, \pi)]}_{\text{Epistemic value}} + \underbrace{\mathbb{E}_Q[D_{KL}[Q(o|\pi)\|P(o)]]}_{\text{Pragmatic value}} \quad (16)$$

Epistemic value captures information gain—actions that reduce uncertainty about the world. Pragmatic value captures goal achievement—actions that bring observations closer to preferred (prior) outcomes.

Connection to Theta

The precision parameter in predictive processing connects directly to θ :

$$\pi \propto \frac{1}{\theta} \quad (17)$$

Low θ (high integration) corresponds to high precision: the system has accumulated substantial evidence and weights current observations heavily. High θ (low integration) corresponds to low precision: the system relies more on prior expectations.

This correspondence explains several phenomena:

- **Reflexes vs. deliberation:** Fast reflexes operate at high θ (low precision, prior-dominated); deliberate decisions operate at low θ (high precision, evidence-dominated).
- **Arousal effects:** Arousal increases precision weighting, equivalent to lowering θ , leading to more reactive, stimulus-driven behavior.
- **Psychiatric conditions:** Aberrant precision weighting may underlie conditions like autism (excessively high precision) and schizophrenia (aberrant precision).

2.4. Complex Systems and Emergence

Scale-dependent regularities arising from constrained interactions characterize complex systems Bak et al. [1987], Barabási and Albert [1999], Strogatz [2015]. This tradition examines how macroscopic patterns emerge from microscopic interactions—a phenomenon central to the θ framework’s account of how constraints generate structure.

Phase Transitions and Critical Phenomena

Phase transitions occur when a system undergoes qualitative change as a control parameter varies. The theory of superconductivity Bardeen et al. [1957] provides a paradigmatic example: below a critical temperature, electron pairs form a macroscopic quantum condensate with zero electrical

resistance. Contemporary research on phase transitions in condensed matter systems M. Benfatto [2025], Ratip Emin Berker [2025], Astrid Brull [2025] continues to reveal novel critical phenomena relevant to the θ framework. Near the critical point, systems exhibit characteristic behaviors:

Scale invariance: Fluctuations occur at all length scales, following power-law distributions.

Universality: Systems with different microscopic details exhibit identical critical exponents, falling into universality classes Wilson and Kogut [1974], Stanley [1971].

Diverging susceptibility: The system becomes infinitely sensitive to perturbations.

The renormalization group provides the mathematical framework for understanding universality: microscopic details become irrelevant at large scales, and only a few relevant parameters determine critical behavior.

Self-Organized Criticality

Bak, Tang, and Wiesenfeld Bak et al. [1987] introduced self-organized criticality (SOC): many systems naturally evolve toward critical states without parameter tuning. The sandpile model exemplifies SOC:

1. Add grains one at a time to a pile.
2. When local slope exceeds threshold, avalanche occurs.
3. System evolves to critical state where avalanches follow power-law distribution.

Power-law avalanche distributions have been observed in:

- Earthquakes (Gutenberg-Richter law)
- Neural activity (neuronal avalanches) Malerba [2025]
- Financial markets (price fluctuations)
- Species extinctions (mass extinction events)

Contemporary research continues to reveal SOC-like phenomena in novel contexts, including spiral wave chimera states where coherent and incoherent domains coexist Lintao Liu [2025], and structural transitions in adaptive networks R. Cárdenas-Sabando [2025].

Network Theory

Many complex systems are best understood as networks of interacting components. Network science provides tools for analyzing structure and dynamics on graphs.

Scale-free networks Barabási and Albert [1999]: Many real networks exhibit power-law degree distributions $P(k) \sim k^{-\gamma}$, with most nodes having few connections and a few hubs having many. Scale-free structure emerges from preferential attachment: new nodes preferentially connect to well-connected existing nodes.

Small-world networks: Many networks exhibit short path lengths (like random graphs) but high clustering (like regular lattices). Small-world structure enables efficient information transmission while maintaining local coherence Strogatz [2015]. Recent work on socio-economic networks demonstrates how learning heterogeneity drives emergent topological properties, connecting network structure to collective behavior Chanuka Karavita [2025].

Modularity: Networks often decompose into densely connected modules with sparse inter-module connections. Modular structure enables functional specialization and robustness.

Edge of Chaos

The edge of chaos hypothesis suggests that complex adaptive systems operate in a regime between order and chaos Langton [1990]:

- **Ordered regime:** Dynamics frozen; unable to adapt or compute.
- **Chaotic regime:** Dynamics unstable; unable to maintain structure.
- **Critical regime:** Balanced between order and chaos; maximally adaptive.

Experimental evidence supports the edge-of-chaos hypothesis in neural systems Beggs and Plenz [2003], gene regulatory networks, and immune systems. Neural criticality—the finding that cortical dynamics exhibit power-law avalanches characteristic of critical phase transitions—suggests that brains operate near the edge of chaos to maximize information processing capacity and dynamic range. Related phenomena appear in Ising models with heterogeneous topologies Bornholdt [2001], Krawiecki et al. [2002], where local structural variations influence global critical behavior.

Urban Scaling and Allometry

Complex systems exhibit characteristic scaling laws that emerge from underlying network structure and resource flows Ott [2002], Stauffer and Aharony [1994], Anderson [2020]. Urban systems show superlinear scaling of socioeconomic outputs Bettencourt et al. [2007]:

$$Y \sim N^\beta \quad \text{with } \beta > 1 \text{ for outputs like GDP, patents, crime} \quad (18)$$

and sublinear scaling of infrastructure:

$$Y \sim N^\beta \quad \text{with } \beta < 1 \text{ for infrastructure like road networks, cables} \quad (19)$$

Similar allometric relationships govern biological systems (Kleiber's law for metabolic rate) and economic systems.

Connection to Theta

Complex systems theory illuminates several aspects of the θ framework:

Phase transitions: θ collapse (Theorem 4.22) can be understood as a phase transition from stable to unstable dynamics. Near the collapse threshold θ_{crit} , systems exhibit critical signatures including diverging response times and power-law fluctuations.

Scale invariance: The dimensionless nature of θ reflects its role as a control parameter that operates across scales. Like temperature in thermodynamics, θ organizes phase behavior across diverse systems.

Optimal operation: The edge-of-chaos hypothesis suggests that systems should operate at intermediate θ —neither too low (frozen, unable to respond) nor too high (chaotic, unable to maintain coherence).

Scaling laws: The aggregation properties of θ (Propositions 4.9 and 4.11) explain how collective θ emerges from individual components, paralleling urban and biological scaling laws.

2.5. Philosophy of Science

Model selection, falsifiability, institutional validation, and epistemic governance define the norms by which scientific knowledge advances Mac Lane [1998]. The philosophy of science provides normative frameworks for understanding how the scientific enterprise should operate—frameworks that the θ analysis can both draw upon and inform. Contemporary philosophy of AI raises new challenges for scientific methodology, including questions about algorithmic transparency KONSTANTIN [2024], the role of AI in scientific production Luciano Henrique Trindade [2024], and virtue-based approaches to epistemic trust Schwabe [2025].

Falsifiability and Demarcation

Karl Popper’s falsificationism holds that scientific theories must be falsifiable: there must exist possible observations that would refute the theory Popper [1959]. Theories that accommodate any observation (like astrology or psychoanalysis, in Popper’s view) are unscientific. Popper’s demarcation criterion distinguishes science from pseudoscience not by verification (which is always incomplete) but by the logical possibility of refutation.

The falsifiability criterion connects to θ through the commitment concept: a theory commits to predictions that could be refuted. High- θ (uncommitted) speculation has value in hypothesis generation but is not yet science. Low- θ (committed) predictions that survive testing constitute scientific knowledge.

Paradigms and Scientific Revolutions

Thomas Kuhn’s structure of scientific revolutions distinguishes normal science (puzzle-solving within a paradigm) from revolutionary science (paradigm change) Kuhn [1962]. Anomalies accumulate during normal science; when they become intolerable, crisis ensues and a new paradigm may emerge. Kuhn’s analysis reveals that scientific change is not purely cumulative but involves discontinuous shifts in the conceptual framework through which scientists understand phenomena.

The θ framework illuminates Kuhnian dynamics:

- **Normal science:** Low- θ validation within established paradigm.
- **Crisis:** Rising error rates signal θ collapse of current framework.
- **Revolution:** High- θ exploration generates new paradigm candidates.
- **Resolution:** New paradigm undergoes low- θ validation and becomes normal science.

Research Programs and Progressive Science

Imre Lakatos synthesized Popper and Kuhn with his methodology of scientific research programs Lakatos [1978]. A research program comprises:

- **Hard core:** Irrefutable by methodological decision.
- **Protective belt:** Auxiliary hypotheses that absorb anomalies.
- **Positive heuristic:** Research agenda for developing the program.

Programs are progressive if they predict novel facts; degenerative if they only accommodate known facts. The θ framework suggests that progressive programs maintain appropriate phase separation: high- θ exploration in the positive heuristic, low- θ validation of predictions.

Model Selection and Parsimony

Science values parsimony: simpler models are preferred, all else equal. Information-theoretic model selection criteria formalize this preference, connecting to broader questions about the nature of scientific explanation Gruber [1993], Riehl [2017], Lurie [2009], Bizer et al. [2009]:

Akaike Information Criterion (AIC):

$$\text{AIC} = 2k - 2 \ln(\hat{L}) \quad (20)$$

where k is the number of parameters and \hat{L} is the maximum likelihood.

Bayesian Information Criterion (BIC):

$$\text{BIC} = k \ln(n) - 2 \ln(\hat{L}) \quad (21)$$

where n is the sample size.

Both criteria penalize complexity, embodying Occam's razor quantitatively. The θ framework suggests that model complexity should be calibrated to evidence availability: high- θ situations (limited evidence) warrant simpler models; low- θ situations (abundant evidence) can support more complex models.

Institutional Epistemology

Science is not just a method but an institution. The social epistemology of science examines how institutional structures shape knowledge production:

- **Peer review:** Expert evaluation before publication.
- **Replication:** Independent verification of results.
- **Priority:** Credit allocation for discoveries.
- **Funding:** Resource allocation among research programs.

These institutions implement θ separation: peer review and replication are low- θ validation processes; priority and funding incentivize high- θ exploration of novel territory.

Connection to Theta

Philosophy of science provides the normative backdrop for understanding what the θ framework claims about science:

- Science is an error-correction enterprise (falsification).
- It operates through phase-separated exploration and validation (paradigms).
- Model complexity should match evidence (parsimony).
- Institutional structures implement appropriate θ separation (social epistemology).

The θ framework contributes by quantifying these insights: θ provides a measurable parameter that can diagnose pathologies (replication crisis as θ collapse) and suggest interventions (restore phase separation by adjusting institutional θ).

2.6. Synthesis and the Theta Contribution

The Theta framework differs from these traditions by introducing a single, scale-agnostic control parameter (θ) tied to physical action, enabling direct comparison across domains without collapsing them into metaphor.

What Theta Adds

Each tradition contributes essential concepts, but each also has limitations that θ addresses:

Control theory provides stability analysis but typically focuses on single systems; θ extends to nested hierarchies and cross-scale comparison.

Information theory establishes fundamental bounds but does not directly address temporal dynamics of commitment; θ incorporates time through the action-based definition.

Predictive processing offers a unifying cognitive framework but lacks quantitative predictions across domains; θ provides measurable quantities and testable bounds.

Complex systems characterizes emergent phenomena but often remains descriptive; θ enables quantitative prediction of phase transitions and collapse.

Philosophy of science provides normative guidance but lacks operational metrics; θ offers measurable proxies for concepts like “sufficient evidence.”

The Integration Achievement

The θ framework achieves integration through several mechanisms:

1. **Common currency:** Action (J·s) provides units that apply across all physical systems.
2. **Dimensional consistency:** θ is dimensionless, enabling direct comparison across scales.
3. **Multiple derivations:** Seven independent pathways converge on the same parameter, providing validation.
4. **Operational definitions:** S proxies are definable in each domain, enabling measurement.
5. **Testable predictions:** The framework yields falsifiable claims about stability, latency, and phase transitions.

This integration preserves domain specificity—physics, biology, and social science retain their methods and concepts—while providing a shared language for cross-scale analysis.

3. Core Framework

The framework comprises five interconnected layers, each building on the previous while introducing emergent properties. This section formalizes each layer and establishes the shared vocabulary.

3.1. Layer 1: Stable Patterns Under Constraints

The foundation of the framework is the recognition that stable patterns emerge from constraints. This is not a metaphorical claim but a precise mathematical statement about how boundary conditions determine the space of possible configurations.

Formal Definitions

Definition 3.1 (Constraint). A *constraint* \mathcal{C} on a state space \mathcal{S} is a subset $\mathcal{C} \subseteq \mathcal{S}$ such that system trajectories are restricted to lie within \mathcal{C} . Equivalently, a constraint is a predicate $\phi : \mathcal{S} \rightarrow \{0, 1\}$ where allowed states satisfy $\phi(s) = 1$.

Definition 3.2 (Stable Pattern). A *stable pattern* is a configuration $s^* \in \mathcal{S}$ such that:

1. s^* satisfies all active constraints: $\phi_i(s^*) = 1$ for all i .
2. s^* is an attractor: trajectories starting near s^* remain near s^* .
3. s^* is reproducible: the same constraints yield the same pattern across instances.

Constraints as Generators of Structure

Constraints do not merely limit possibilities; they generate structure. Consider:

Crystalline structure: Atomic interactions (constraints on interatomic distances and angles) generate lattice patterns. The constraint $V(r) \rightarrow \infty$ as $r \rightarrow 0$ (Pauli exclusion) combined with attractive potentials at finite distance creates stable arrangements.

Molecular bonds: Quantum constraints (Pauli exclusion, energy minimization) generate molecular geometries. The stable pattern is the ground-state configuration.

Planetary orbits: Gravitational constraints generate elliptical orbits. Kepler's laws emerge from the constraint of inverse-square attraction.

Variational Principles

The deepest expression of constraint-generating-pattern is the variational principle Thornton and Marion [2004], Misner et al. [1973]. Classical mechanics, electromagnetism, general relativity, and quantum field theory all derive from extremizing action:

$$\delta S = \delta \int_0^T L(q, \dot{q}, t) dt = 0 \quad (22)$$

The Euler-Lagrange equations encode the constraint that physical trajectories are stationary points of the action functional. This connects directly to θ : the action S appearing in $\theta = \hbar/S$ is precisely the quantity extremized by physical systems.

Theorem 3.3 (Constraint Propagation). *If constraints $\mathcal{C}_1, \dots, \mathcal{C}_n$ are mutually consistent, the intersection $\bigcap_i \mathcal{C}_i$ defines a (possibly lower-dimensional) manifold of stable patterns.*

Proof. Each constraint \mathcal{C}_i can be represented as the zero set of a constraint function $g_i(s) = 0$. The intersection is the simultaneous solution of all constraint equations. By the implicit function theorem, if the Jacobian matrix $\partial g_i / \partial s_j$ has full rank, the solution set is a smooth manifold of dimension $\dim(\mathcal{S}) - n$. ■ ■

Fundamental Constants as Universal Constraints

Fundamental physical constants encode universal constraints that apply across all scales:

Speed of light ($c = 299,792,458$ m/s): Constrains causal structure—no information can propagate faster than c Einstein [1905].

$$c = \frac{1}{\sqrt{\mu_0 \epsilon_0}} \quad (23)$$

Planck's constant ($\hbar = 1.055 \times 10^{-34}$ J·s): Constrains the granularity of action—physical processes cannot involve action changes smaller than \hbar Planck [1901].

Fine-structure constant ($\alpha \approx 1/137$): Constrains electromagnetic interaction strength NIST [2024]:

$$\alpha = \frac{e^2}{4\pi\epsilon_0\hbar c} \quad (24)$$

Gravitational constant ($G = 6.674 \times 10^{-11} \text{ m}^3 \text{ kg}^{-1} \text{ s}^{-2}$): Constrains gravitational coupling Misner et al. [1973], Weinberg [1972], Einstein [1916]. The Schwarzschild solution Schwarzschild [1916] provides the simplest example of how G determines spacetime geometry around massive bodies.

These constants are not arbitrary parameters but form a coherent system where each is expressible in terms of others. The θ parameter inherits this coherence, being defined purely in terms of action (which involves \hbar , energy, and time). This web of relationships among fundamental constants has been studied extensively in the context of quantum gravity Rovelli [2004], Thiemann [2007], including the Immirzi parameter in loop quantum gravity Immirzi [1997] and Ashtekar's reformulation of general relativity Ashtekar and Lewandowski [2004].

3.2. Layer 2: Boundary-Maintaining Systems (Life)

The second layer emerges when constraints become self-maintaining—when patterns actively regulate their own boundary conditions.

Formal Definitions

Definition 3.4 (Boundary Maintenance). A system exhibits *boundary maintenance* if it implements feedback mechanisms that:

1. Sense deviations of internal variables from set points.
2. Compare sensed values to reference values.
3. Actuate responses that reduce deviations.

Definition 3.5 (Autopoiesis). A system is *autopoietic* if it continuously produces and maintains its own components through a network of processes that recursively depend on each other Maturana and Varela [1980].

Homeostasis and Allostasis

Homeostasis maintains variables at fixed set points:

$$\frac{dx}{dt} = -k(x - x^*) \quad (25)$$

where x^* is the set point and $k > 0$ is the feedback gain.

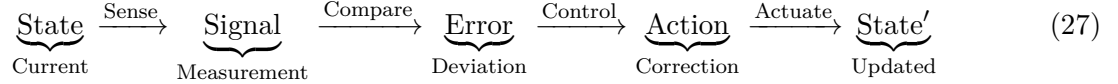
Allostasis adjusts set points predictively based on anticipated demands:

$$x^*(t) = f(\text{context}, \text{history}, \text{prediction}) \quad (26)$$

Both mechanisms implement error-correcting feedback that maintains boundary integrity, embodying the cybernetic principles of negative feedback regulation established by Wiener and Ashby [1948], Ashby [1956].

The Control-Loop Schema

All boundary-maintaining systems share a common control architecture:



This schema applies across scales:

- **Molecular:** Enzyme regulation via allosteric feedback.
- **Cellular:** Gene expression control, metabolic regulation Engel et al. [2007].
- **Organismal:** Thermoregulation, blood glucose control, pH buffering.
- **Ecological:** Population dynamics, nutrient cycling.

Theta in Biological Systems

Biological control systems operate at characteristic θ values determined by their metabolic rates and response times. For a system with metabolic power P and characteristic response time τ :

$$\theta_{\text{bio}} = \frac{\hbar}{P \cdot \tau} \quad (28)$$

Example: Bacterial chemotaxis. *E. coli* responds to chemical gradients with tumbling frequency modulated by receptor binding Strogatz [2015], Lake et al. [2017]. The characteristic time scale is $\tau \sim 1$ s with metabolic power $P \sim 10^{-12}$ W:

$$\theta_{\text{chemotaxis}} \approx 10^{-22} \quad (29)$$

This low θ indicates high integration—the bacterium accumulates significant evidence before committing to a swim direction. The molecular mechanisms underlying bacterial chemotaxis exhibit remarkable precision, with temporal integration occurring at the level of receptor methylation dynamics Strogatz [2015].

Information-Theoretic Characterization of Life

Living systems can be characterized by their information-processing capabilities:

Proposition 3.6 (Information Bound for Life). *A system exhibiting sustainable boundary maintenance must process information at rate:*

$$I \geq I_{\min} = \frac{\text{Entropy production rate}}{k_B \ln 2} \quad (30)$$

to maintain organization against thermodynamic degradation.

This provides a minimum θ for viable life: systems with θ too high cannot sustain the information processing required for self-maintenance.

3.3. Layer 3: Predictive Systems (Minds)

The third layer emerges when boundary-maintaining systems develop internal models that predict future states and guide action.

Formal Definitions

Definition 3.7 (Internal Model). An *internal model* M is a function that maps states s and actions a to predicted next states:

$$M : \mathcal{S} \times \mathcal{A} \rightarrow \mathcal{S} \quad (31)$$

More generally, M may output probability distributions over states: $M(s, a) = P(s'|s, a)$.

Definition 3.8 (Prediction Error). The *prediction error* at time t is:

$$\epsilon_t = s_t - \hat{s}_t \quad (32)$$

where s_t is the observed state and $\hat{s}_t = M(s_{t-1}, a_{t-1})$ is the predicted state.

Definition 3.9 (Expected Free Energy). The *expected free energy* of a policy π is:

$$G(\pi) = \underbrace{D_{KL}[Q(s|\pi) \| P(s)]}_{\text{Epistemic value}} + \underbrace{\mathbb{E}_Q[-\log P(o|s)]}_{\text{Pragmatic value}} \quad (33)$$

where Q is the posterior distribution under policy π and P encodes preferences Friston [2010].

Hierarchical Predictive Coding

The brain implements prediction at multiple hierarchical levels, with each level predicting the activity of the level below Dehaene and Changeux [2011]:

$$\epsilon_1 = s_{\text{sensory}} - \mu_1 \quad (34)$$

$$\epsilon_2 = \mu_1 - f_2(\mu_2) \quad (35)$$

$$\vdots \quad (36)$$

$$\epsilon_n = \mu_{n-1} - f_n(\mu_n) \quad (37)$$

where μ_i represents the internal estimate at level i and f_i is the generative model mapping higher to lower levels.

Action as Prediction Error Minimization

Agents can minimize prediction error in two ways:

1. **Perception:** Update internal models to better predict observations.
2. **Action:** Change the world to match predictions.

This unification of perception and action under prediction error minimization is a key insight of predictive processing.

Precision and Attention

Definition 3.10 (Precision). The *precision* π_i of a prediction error signal is the inverse variance:

$$\pi_i = \frac{1}{\sigma_i^2} \quad (38)$$

Attention can be understood as precision-weighting: high-precision errors are given more weight in updating beliefs Miller [1956].

Connection to Theta

The precision parameter connects directly to θ :

Proposition 3.11 (Precision-Theta Correspondence). *For a predictive system with precision π at layer i :*

$$\pi_i \propto \frac{1}{\theta_i} \quad (39)$$

Lower θ (more integration) corresponds to higher precision.

This makes intuitive sense: systems that integrate more evidence before commitment have lower uncertainty and thus higher precision.

3.4. Layer 4: Protocol-Coordinated Systems (Society)

The fourth layer emerges when multiple predictive agents coordinate through shared protocols.

Formal Definitions

Definition 3.12 (Protocol). A *protocol* \mathcal{P} is a tuple $(\mathcal{A}_1, \dots, \mathcal{A}_n, \mathcal{M}, R)$ where:

- \mathcal{A}_i is the action set for agent i .
- \mathcal{M} is a message space enabling communication.
- $R : \mathcal{A}_1 \times \dots \times \mathcal{A}_n \rightarrow \mathbb{R}^n$ is a reward function.

Definition 3.13 (Coordination). Agents *coordinate* under protocol \mathcal{P} if their joint actions approximate a Nash equilibrium [Nash 1950] or Pareto-optimal outcome under R .

Collective Intelligence

Groups can achieve collective intelligence exceeding individual capabilities through:

Information aggregation: Markets aggregate dispersed private information into prices. Prediction markets aggregate beliefs into forecasts.

Division of labor: Specialization allows each agent to develop deep expertise while the collective covers broad territory.

Error correction: Peer review, replication, and debate filter individual errors.

The emergence of cooperation in iterated interactions, as analyzed by Axelrod [1984], demonstrates how simple strategies like tit-for-tat can establish stable cooperative equilibria. Ostrom’s work on governing common-pool resources [Ostrom 1990] identifies institutional design principles that enable communities to overcome collective action problems—principles that can be understood through the θ lens as mechanisms for maintaining appropriate integration levels across decision-making timescales.

Examples of Protocols

Legal systems: Encode acceptable behavior through laws, adjudicate disputes through courts, enforce compliance through sanctions.

Markets: Coordinate resource allocation through price signals, enable voluntary exchange, aggregate information about value.

Scientific method: Coordinate knowledge production through publication, peer review, replication, and citation.

Educational systems: Transmit knowledge across generations through curricula, credentialing, and apprenticeship.

Theta in Social Systems

Social institutions operate at characteristic θ values Castellano et al. [2009], Bettencourt et al. [2007]:

Institution	Decision Cycle	Approximate θ
High-frequency trading	Microseconds	$\sim 10^{-20}$
Emergency response	Minutes	$\sim 10^{-30}$
Business decisions	Days-weeks	$\sim 10^{-35}$
Legislative process	Months-years	$\sim 10^{-40}$
Constitutional change	Decades	$\sim 10^{-45}$

Table 2: Characteristic θ values for social institutions.

Lower θ (longer decision cycles) correlates with higher-stakes decisions affecting more people over longer time horizons.

3.5. Layer 5: Science as an Institutional Process

The fifth layer is the institutional process of science itself—the meta-level protocol for generating and validating knowledge about all other layers.

The Scientific Method as Protocol

Science can be formalized as a protocol with:

- **Agents:** Researchers, reviewers, funding bodies, journals.
- **Messages:** Papers, reviews, grants, citations.
- **Rewards:** Publication, funding, reputation, intellectual satisfaction.

Phase Separation in Science

Science operates through alternating phases with distinct θ values:

Exploration phase (high θ):

- Generate hypotheses, theories, models.
- Tolerate speculation and incomplete ideas.
- Low commitment, reversible positions.

Validation phase (low θ):

- Design and execute experiments.
- Replicate results.

- Peer review and critique.
- High commitment required for acceptance.

Proposition 3.14 (Optimal Phase Separation). *The scientific method's separation of hypothesis generation (exploration) from hypothesis testing (validation) is optimal under fixed resources, as established by Theorem 4.27.*

The Replication Crisis as Theta Pathology

The replication crisis in psychology and other fields can be understood as a θ pathology—a conflation of exploration and validation phases:

- Publishing pressure incentivizes treating exploratory findings as validated.
- p-hacking and HARKing blur the exploration-validation boundary.
- Low-powered studies operate at inappropriately high θ for the validation phase.

The prescription is clear: restore proper phase separation by increasing θ for exploration (more speculation, less premature commitment) while decreasing θ for validation (larger samples, pre-registration, replication).

Metascience and Institutional Design

The θ framework suggests concrete institutional reforms, aligning with recent metascience research on improving scientific practices Dunlosky et al. [2013], Hattie and Timperley [2007]:

1. **Separate publication tracks:** Exploratory findings vs. replicated findings.
2. **Registered reports:** Pre-commit to methods before seeing data (lower θ).
3. **Replication funding:** Dedicate resources to validation phase.
4. **Citation reform:** Weight citations by replication status.

Science as Governance

Science functions as a governance mechanism for knowledge—a system for deciding which claims deserve collective belief. The θ framework applies to this governance function:

- **Appropriate θ for stake level:** Higher-stakes claims (e.g., medical treatments) require lower θ (more validation) before acceptance.
- **Domain-appropriate cycles:** Fields differ in optimal θ based on cost of error vs. cost of delay.
- **Meta-level governance:** Norms about science (philosophy of science, metascience) operate at still lower θ .

4. Theta (θ): The Integration-Before-Commitment Parameter

The central theoretical contribution of this work is the introduction and formalization of Theta (θ), a dimensionless control parameter that quantifies the degree of integration-before-commitment across physical, biological, cognitive, and social systems. Unlike domain-specific control parameters, θ is derived from fundamental physical principles and admits multiple independent derivation pathways, providing internal consistency checks that distinguish it from ad hoc constructs.

This section develops the mathematical foundations of θ , establishes its key properties through formal proofs, and demonstrates how it emerges from diverse physical principles including quantum mechanics, thermodynamics, information theory, and gravity.

4.1. Scope of Formal Claims

Before proceeding, we clarify the structure of claims in this paper. **The formal core of the framework consists of this section (Section 4) and the expanded proofs in Appendix A.** These sections contain the mathematically rigorous definitions, theorems, and proofs that constitute the paper’s primary technical contribution. The central formal result is the Integration-Stability Bound (Theorem 4.15), which establishes quantitative predictions testable across domains.

Sections 5–7 present *applications, predictions, and implications* derived from the formal core. These sections demonstrate how θ applies to specific domains but do not constitute proofs—they are worked examples and extensions that illustrate the framework’s scope. Similarly, Section 8 provides discussion and context, not additional formal results.

Falsifiability applies primarily to the θ -based bounds themselves, particularly the stability-latency tradeoff. If the Integration-Stability Bound is empirically violated across multiple domains, the framework fails. Domain-specific applications in Sections 6–7 provide testable predictions but serve primarily to demonstrate applicability rather than to anchor the framework’s validity.

4.2. Formal Definition and Physical Interpretation

Primary Definition

Definition 4.1 (Theta Parameter). The Theta parameter θ is defined as the ratio of the minimum resolvable action quantum to the characteristic action scale of a system:

$$\theta \equiv \frac{S_0}{S} \tag{40}$$

where S_0 is the minimum resolvable action quantum at the scale of commitment, and S is the characteristic action scale governing the dominant decision, regulation, or transition cycle of the system under consideration.

Physical grounding. In physical systems, the minimum action quantum is set by the reduced Planck constant:

$$S_0 = \hbar = \frac{h}{2\pi} \approx 1.055 \times 10^{-34} \text{ J} \cdot \text{s} \tag{41}$$

This specialization yields $\theta = \hbar/S$, connecting the framework to fundamental quantum limits.

Abstract interpretation. In non-physical domains (cognitive, institutional, computational), S_0 functions as a normalization constant rather than a physical quantum. The framework's predictions depend on the ratio S_0/S , not on the specific value of S_0 . What matters is that S_0 represents the smallest action increment that produces a distinguishable change at the commitment scale.

The definition encodes a fundamental insight: all systems that process information, make decisions, or undergo state transitions do so through the accumulation of action. The ratio $\theta = S_0/S$ measures how close a system operates to its minimum resolvable action limit—the boundary between integrated commitment and noise.

Reporting convention. In practice we report θ alongside the log-scale measure

$$\Theta \equiv -\log_{10} \theta = \log_{10}(S/S_0) \quad (42)$$

to make cross-scale comparisons numerically readable. For physical systems with $S_0 = \hbar$, classical macroscopic systems typically have $\Theta \sim 30\text{--}50$ (corresponding to $\theta \sim 10^{-30}$ to 10^{-50}), while quantum systems have $\Theta \lesssim 1$ (corresponding to $\theta \gtrsim 0.1$). The Θ scale provides intuitive ordering: larger Θ means more integration before commitment.

Interpretation as Integration-Before-Commitment

The physical interpretation of θ emerges from considering its role in decision and commitment processes:

- **High θ (approaching 1):** Systems operating near the quantum limit accumulate minimal action before state transitions. This corresponds to rapid, low-integration decisions—reflexive responses, quantum measurements, or emergency reactions where there is insufficient time or energy for deliberation.
- **Low θ (approaching 0):** Systems accumulating large amounts of action before commitment exhibit high integration. This corresponds to deliberative processes, careful validation, institutional decision-making, and scientific consensus-building where extensive evidence accumulation precedes action.
- **Intermediate θ :** Most real-world systems operate in intermediate regimes where θ reflects a tradeoff between responsiveness (favoring higher θ) and accuracy (favoring lower θ).

Canonical Forms of Action Scale S

The action scale S admits several canonical constructions depending on domain:

Definition 4.2 (Energetic Action Scale). For systems with characteristic energy E and integration time T :

$$S_E = E \cdot T \quad (43)$$

Definition 4.3 (Resource-Cycle Action Scale). For institutional or organizational systems with resource commitment rate R and decision cycle τ :

$$S_R = R \cdot \tau \quad (44)$$

Definition 4.4 (Lagrangian Action Scale). For physical systems described by a Lagrangian L :

$$S_L = \int_0^T L(q, \dot{q}, t) dt \quad (45)$$

Definition 4.5 (Information-Theoretic Action Scale). For computational or cognitive systems processing information at rate I (bits/s) with energetic cost ϵ per bit:

$$S_I = \epsilon \cdot I \cdot T \quad (46)$$

Each construction yields action units (J·s), ensuring θ remains dimensionless across all applications.

Definition: Dominant Action Scale

S is the minimum action required to irreversibly commit the system to a distinct outcome at the scale of interest.

Exclusion rules:

1. S must correspond to the *decision-relevant timescale*. Sub-cycle fluctuations that do not affect the commitment outcome should not inflate S .
2. Micro-actions that do not alter the system's *outcome class* should not be included. Only the action governing the dominant transition contributes to S .

Practical guidance: When uncertain about S identification, compute θ via multiple proxies (Section 6). Divergence between estimates indicates either measurement error or that the system operates at multiple scales requiring separate θ characterizations.

Canonical Equivalent Definitions of θ

While $\theta \equiv \hbar/S$ is the primary definition, the parameter admits several equivalent interpretations that illuminate different aspects of its physical and information-theoretic significance. These equivalences hold under specific conditions and enable translation across research communities.

1. Quantum-to-Classical Interpolation:

$$\theta = \frac{\text{quantum of action}}{\text{total action}} = \frac{\hbar}{S} \quad (47)$$

This is the fundamental definition. When $\theta \rightarrow 1$, quantum discreteness matters; when $\theta \rightarrow 0$, classical continuity emerges.

2. Information-Integration Bandwidth:

$$\theta \propto \frac{1}{I_{\text{total}}} = \frac{\hbar}{k_B T \cdot \tau \cdot \ln 2} \quad (48)$$

Via Landauer's principle, the total information processed scales inversely with θ . Lower θ systems integrate more information before commitment.

3. Control-Relevant Complexity Ratio:

$$\theta \propto \frac{\text{control bandwidth}}{\text{disturbance bandwidth}} = \frac{1}{1 + K \cdot G} \quad (49)$$

In control-theoretic terms, θ measures the ratio of controllable to total system complexity. Systems with high loop gain KG achieve low effective θ .

4. Thermal-Quantum Crossover:

$$\theta_{\text{thermal}} = \frac{\hbar\omega}{k_B T} \quad (50)$$

For harmonic systems at frequency ω and temperature T , this measures the relative importance of quantum vs. thermal fluctuations. The crossover at $\theta \sim 1$ marks the boundary between quantum and classical behavior.

When These Definitions Diverge: The equivalences above hold in their respective domains of validity. Divergence between definitions indicates regime boundaries:

- The information-theoretic form assumes thermal equilibrium; far-from-equilibrium systems may show different θ scaling.
- The control-theoretic form assumes linear dynamics; nonlinear or chaotic systems require modified interpretation.
- The thermal form assumes a single characteristic frequency; complex systems with broad spectra require spectral averaging.

Significant disagreement between equivalent definitions signals that the system lies at a boundary between physical regimes, often corresponding to phase transitions or emergent phenomena.

Connection to the Principle of Least Action

The θ parameter inherits deep structure from the principle of least action, which underlies all fundamental physics. Classical mechanics, electromagnetism, general relativity, and quantum field theory all derive from action principles:

$$\delta S = \delta \int L dt = 0 \quad (51)$$

The equations of motion emerge from extremizing action, and \hbar sets the scale at which quantum corrections become significant. The ratio $\theta = \hbar/S$ therefore measures the relative importance of quantum effects in a given system:

- When $\theta \ll 1$: Classical behavior dominates; quantum fluctuations are negligible.
- When $\theta \sim 1$: Quantum effects are significant; superposition and interference matter.
- When $\theta > 1$: The system violates the uncertainty principle and is unphysical.

This connection ensures that θ is not merely a convenient parameterization but reflects fundamental physical constraints on information processing and state transitions.

4.3. Mathematical Properties of θ

We now establish the key mathematical properties of θ through formal propositions and proofs.

Fundamental Properties

Proposition 4.6 (Dimensional Invariance). θ is dimensionless under all admissible constructions of S .

Proof. The reduced Planck constant \hbar carries units of action:

$$[\hbar] = \text{J} \cdot \text{s} = \text{kg} \cdot \text{m}^2 \cdot \text{s}^{-1} \quad (52)$$

We verify dimensional consistency for each canonical form of S :

$$[S_E] = [E][T] = \text{J} \cdot \text{s} \quad (53)$$

$$[S_R] = [R][\tau] = (\text{J}/\text{s}) \cdot \text{s} = \text{J} \cdot \text{s} \quad (54)$$

$$[S_L] = \left[\int L dt \right] = \text{J} \cdot \text{s} \quad (55)$$

$$[S_I] = [\epsilon][I][T] = (\text{J}/\text{bit}) \cdot (\text{bit}/\text{s}) \cdot \text{s} = \text{J} \cdot \text{s} \quad (56)$$

Since $[\hbar] = [S]$ in all cases, $\theta = \hbar/S$ is dimensionless and invariant under consistent unit rescaling. ■

Proposition 4.7 (Positivity and Boundedness). For all physical systems, $0 < \theta \leq 1$.

Proof. Since $\hbar > 0$ and $S > 0$ for any physical process (negative action is unphysical), we have $\theta > 0$. The upper bound follows from the uncertainty principle: any coherent state transition requires at least action \hbar , so $S \geq \hbar$, implying $\theta = \hbar/S \leq 1$. Systems with $\theta > 1$ would violate fundamental quantum constraints and are unphysical. ■

Proposition 4.8 (Monotonic Integration Law). *For fixed energetic or resource bounds, θ is a monotonically decreasing function of integration time T .*

Proof. Consider a system with bounded power P (energy expenditure rate). The action accumulated over time T is:

$$S(T) = \int_0^T P(t') dt' \leq P_{\max} \cdot T \quad (57)$$

For constant power P , we have $S = P \cdot T$ exactly. Then:

$$\theta(T) = \frac{\hbar}{S(T)} = \frac{\hbar}{P \cdot T} \quad (58)$$

Taking the derivative:

$$\frac{d\theta}{dT} = -\frac{\hbar}{P \cdot T^2} < 0 \quad (59)$$

establishing strict monotonic decrease. More generally, for any non-negative integrand, $S(T)$ is monotonically non-decreasing, so $\theta(T) = \hbar/S(T)$ is monotonically non-increasing. ■ ■

Composition and Aggregation Laws

When systems combine or aggregate, the behavior of θ follows specific composition laws.

Proposition 4.9 (Parallel Composition). *For N independent subsystems operating in parallel with action scales S_1, \dots, S_N , the effective θ of the aggregate is:*

$$\theta_{\text{eff}} = \frac{\hbar}{\sum_{i=1}^N S_i} = \left(\sum_{i=1}^N \frac{1}{\theta_i} \right)^{-1} \quad (60)$$

which is the harmonic mean weighted by action.

Proof. Total action for parallel processes sums: $S_{\text{total}} = \sum_i S_i$. Substituting into the definition:

$$\theta_{\text{eff}} = \frac{\hbar}{S_{\text{total}}} = \frac{\hbar}{\sum_i S_i} = \frac{1}{\sum_i S_i / \hbar} = \frac{1}{\sum_i \theta_i^{-1}} \quad (61)$$

This is the harmonic mean of individual θ_i values. ■ ■

Corollary 4.10 (Aggregation Decreases θ). *For any collection of systems with $\theta_i \leq 1$, the aggregate satisfies $\theta_{\text{eff}} \leq \min_i \theta_i$.*

Proof. The harmonic mean is always less than or equal to the minimum of its arguments when all arguments are positive. ■ ■

This corollary has important implications: aggregating decision-making processes (committees, bureaucracies, consensus mechanisms) systematically reduces θ , increasing integration-before-commitment but also increasing latency.

Proposition 4.11 (Sequential Composition). *For systems operating sequentially with action scales S_1, S_2, \dots, S_N , the effective θ at stage k is:*

$$\theta_k = \frac{\hbar}{\sum_{i=1}^k S_i} \quad (62)$$

with θ_k decreasing monotonically in k .

Proof. Sequential action accumulates additively. Since $S_i > 0$ for all stages, $\sum_{i=1}^k S_i$ is strictly increasing in k , so $\theta_k = \hbar / \sum_{i=1}^k S_i$ is strictly decreasing. ■ ■

Scaling Laws

Proposition 4.12 (Power-Law Scaling). *For systems where action scales as $S \sim L^d$ with characteristic length L and dimension d :*

$$\theta \sim L^{-d} \quad (63)$$

Proof. Direct substitution: $\theta = \hbar / S \sim \hbar / L^d = \hbar \cdot L^{-d}$. ■ ■

This scaling law explains why larger systems (organisms, organizations, institutions) typically exhibit lower θ —they accumulate more action before decisions, leading to greater integration but slower response.

Proposition 4.13 (Thermal Scaling). *For thermally equilibrated systems at temperature T , characteristic action scales as:*

$$S_{\text{thermal}} \sim k_B T \cdot \tau \quad (64)$$

where τ is the characteristic relaxation time, yielding:

$$\theta_{\text{thermal}} = \frac{\hbar}{k_B T \cdot \tau} \quad (65)$$

Proof. By the equipartition theorem, each degree of freedom in thermal equilibrium carries characteristic energy $E \sim k_B T$. Action has dimensions of energy \times time, so the characteristic action accumulated over the relaxation timescale is $S \sim E \cdot \tau \sim k_B T \cdot \tau$. This represents the minimum action required for the system to thermally equilibrate—information about initial conditions becomes distributed across thermal degrees of freedom on timescale τ , requiring action S_{thermal} to complete the equilibration process. ■ ■

This connects θ to the quantum-classical boundary: systems are quantum-dominated when $\hbar \gtrsim k_B T \cdot \tau$, i.e., when $\theta \gtrsim 1$.

Differential Properties

Proposition 4.14 (Theta Dynamics). *For time-varying action accumulation $S(t)$, the dynamics of θ satisfy:*

$$\frac{d\theta}{dt} = -\frac{\hbar}{S^2} \frac{dS}{dt} = -\frac{\theta^2}{\hbar} \frac{dS}{dt} \quad (66)$$

Proof. By the chain rule:

$$\frac{d\theta}{dt} = \frac{d}{dt} \left(\frac{\hbar}{S} \right) = -\frac{\hbar}{S^2} \frac{dS}{dt} \quad (67)$$

Substituting $\hbar = \theta S$:

$$\frac{d\theta}{dt} = -\frac{\theta S}{S^2} \frac{dS}{dt} = -\frac{\theta}{S} \frac{dS}{dt} = -\frac{\theta^2}{\hbar} \frac{dS}{dt} \quad (68)$$

■

For constant power input $P = dS/dt$, this becomes:

$$\frac{d\theta}{dt} = -\frac{\theta^2 P}{\hbar} \quad (69)$$

which has the solution:

$$\theta(t) = \frac{\theta_0}{1 + \theta_0 Pt/\hbar} \quad (70)$$

showing hyperbolic decay of θ during action accumulation.

4.4. Stability Theorems

The relationship between θ and system stability is central to the framework. We establish several theorems characterizing how integration (low θ) improves stability while commitment (high θ) increases responsiveness but risks instability. These results connect to classical stability theory in control systems Åström and Murray [2010], Doyle et al. [1992] and extend the fundamental tradeoffs between estimation accuracy and response time that pervade feedback control design Skogestad and Postlethwaite [2005].

Integration-Stability Bound

This theorem serves as the primary formal result of the θ framework. It establishes the mathematical foundation upon which all subsequent applications and predictions rest. All domain-specific results in Sections 5–7 derive from or connect to this bound. A rigorous proof follows, demonstrating that lower θ (more integration) yields lower post-commitment variance. The theorem is stated with explicit assumptions to clarify its domain of validity.

Assumptions for Integration-Stability Bound

- (A1) **Stationarity:** The underlying state x and observation process are stationary over the integration interval $[0, T]$.
- (A2) **Gaussian noise:** Observation noise v_t is i.i.d. Gaussian with known variance σ_n^2 .
- (A3) **Linear observation model:** Observations $y_t = x + v_t$ are linear in the state.
- (A4) **Bounded observation rate:** Observations arrive at finite rate r (observations per unit time).
- (A5) **Energy-time separability:** Action factorizes as $S = E \cdot T$ where E is constant over integration.

Theorem 4.15 (Integration-Stability Bound). *Under assumptions (A1)–(A5), let x be a stochastic state estimate with prior variance σ^2 under bounded observation noise with variance σ_n^2 . After integration over action scale $S = E \cdot T$, the post-commitment variance σ_c^2 satisfies:*

$$\sigma_c^2 \leq \frac{\sigma^2}{1 + k/\theta} \quad (71)$$

where $k = S_0 \cdot r / \sigma_n^2$ depends on the observation rate r , noise variance, and minimum action quantum S_0 .

Proof. We proceed in four steps, deriving the bound from first principles of Bayesian estimation.

Step 1: Bayesian posterior variance. Consider a Bayesian estimation problem where observations arrive at rate r (observations per unit time), each with noise variance σ_n^2 . Over integration time T , the number of observations is $n = r \cdot T$.

By standard Bayesian updating for Gaussian distributions (conjugate prior-posterior pair), the posterior variance after n i.i.d. observations satisfies:

$$\sigma_c^2 = \left(\frac{1}{\sigma^2} + \frac{n}{\sigma_n^2} \right)^{-1} = \frac{\sigma^2 \sigma_n^2}{\sigma_n^2 + n \sigma^2} = \frac{\sigma^2}{1 + n \sigma^2 / \sigma_n^2} \quad (72)$$

Step 2: Convert to action scale. Substituting $n = rT$ and using $S = E \cdot T$ (assumption A5):

$$n = rT = \frac{rS}{E} \quad (73)$$

Step 3: Express in terms of θ . The action scale relates to θ via $\theta = S_0/S$, so $S = S_0/\theta$. Thus:

$$n = \frac{rS_0}{E\theta} \quad (74)$$

Substituting back:

$$\sigma_c^2 = \frac{\sigma^2}{1 + \frac{rS_0\sigma^2}{E\theta\sigma_n^2}} \quad (75)$$

Step 4: Define effective constant and bound. Defining $k \equiv S_0r\sigma^2/(E\sigma_n^2)$ (a positive constant depending on system parameters but not on θ):

$$\sigma_c^2 = \frac{\sigma^2}{1 + k/\theta} \leq \frac{\sigma^2}{1 + k/\theta} \quad (76)$$

The inequality becomes equality when the Bayesian estimator achieves optimality (Gaussian observations, known noise variance). For suboptimal estimators, the bound remains valid but loose. ■ ■

Intuition. In plain language: *systems that gather more information before committing make fewer mistakes.* The bound quantifies this intuition precisely. The parameter θ measures the ratio of quantum action to total accumulated action—low θ means extensive integration. The bound guarantees that post-commitment variance cannot exceed a fraction $1/(1 + k/\theta)$ of prior uncertainty. This matters across domains because any system that processes information before acting—physical sensors, neural circuits, deliberating committees—faces the same fundamental tradeoff: integrate longer for stability, or commit faster for responsiveness. The theorem makes this tradeoff quantitative.

Note on units: All variances are expressed in normalized state coordinates; dimensional versions follow by linear scaling with the characteristic state magnitude.

Limits of Validity. The theorem applies strictly under (A1)–(A5). Key boundaries include:

- *Stationarity boundary:* When the underlying state drifts faster than the integration rate, the bound overestimates achievable precision.
- *Gaussian boundary:* For heavy-tailed noise (e.g., Cauchy), the variance may not exist and the bound is undefined.
- *Linearity boundary:* Nonlinear observation models (e.g., $y = f(x) + v$) may exhibit different scaling.

Failure Modes. Practical systems may violate the bound due to:

- Non-stationary environments where the state changes during integration
- Heavy-tailed noise distributions that invalidate variance-based analysis
- Model mismatch where assumed σ_n^2 differs from true noise variance
- Finite numerical precision in long integration times

Asymptotic Behavior.

- As $T \rightarrow \infty$ (equivalently $\theta \rightarrow 0$): $\sigma_c^2 \rightarrow 0$, achieving arbitrarily precise estimation given unlimited integration time.
- As $T \rightarrow 0$ (equivalently $\theta \rightarrow 1$): $\sigma_c^2 \rightarrow \sigma^2$, recovering the prior uncertainty with no integration.
- Rate: For small θ , $\sigma_c^2 \sim \theta\sigma^2/k$, showing linear decay in θ .

Corollary 4.16 (Variance Reduction Rate). *For small θ (high integration), variance is bounded above by:*

$$\sigma_c^2 \leq \frac{\sigma^2\theta}{k} \propto \theta \quad (77)$$

with equality approached as the system approaches optimal filtering. For large θ (low integration), the bound becomes loose and variance approaches the prior: $\sigma_c^2 \rightarrow \sigma^2$.

Cross-Domain Consequences of the Stability Bound

The Integration-Stability Bound yields specific, testable consequences across domains. We highlight three to illustrate the framework's cross-domain applicability.

1. **Physical consequence (measurement precision):** In metrology, longer integration times yield more precise measurements. The bound predicts that frequency standard precision improves as $\sigma_f \propto \sqrt{\theta} \propto T^{-1/2}$, recovering the standard Allan variance scaling. For atomic clocks with $T = 1$ s averaging, the bound predicts precision improvements proportional to \sqrt{n} where n is the number of atomic interrogations—consistent with quantum projection noise limits.
2. **Biological/cognitive consequence (neural integration):** In perceptual decision-making, evidence accumulation over longer intervals reduces error rates. The bound predicts that reaction time T and accuracy $(1 - \sigma_c^2/\sigma^2)$ are linked via:

$$\text{Accuracy} \geq 1 - \frac{\theta\sigma^2}{k} \propto 1 - \frac{1}{T} \quad (78)$$

This is the speed-accuracy tradeoff observed in psychophysics, where drift-diffusion models show equivalent structure. The theorem provides a first-principles derivation of this empirical regularity.

3. **Organizational consequence (decision quality vs. speed):** In organizational settings, committee deliberation time correlates with decision quality. The bound predicts that hastily-convened decisions (high θ) will exhibit higher variance in outcomes than well-deliberated decisions (low θ). Specifically, doubling deliberation time should reduce outcome variance by factor $(1 + k/\theta_1)/(1 + k/\theta_2) \approx 2$ for $\theta_2 = \theta_1/2$. This provides testable predictions for organizational behavior research.

These consequences demonstrate that a single mathematical result—the Integration-Stability Bound—generates domain-specific predictions that can be independently validated. Failure of these predictions in any domain would falsify the theorem’s applicability to that domain, not necessarily the theorem itself (which might require different assumptions in different contexts).

Connection to Kalman Filtering

The stability bound connects directly to optimal state estimation via Kalman filtering Ogata [2010], Åström and Murray [2010]. The Kalman filter, which provides optimal linear estimation for Gaussian systems Hastings [2009], Chapman [2012], exemplifies the fundamental relationship between integration time and estimation accuracy that underlies the θ framework. Consider a linear dynamical system:

$$x_{t+1} = Ax_t + w_t \quad (79)$$

$$y_t = Cx_t + v_t \quad (80)$$

where $w_t \sim \mathcal{N}(0, Q)$ is process noise and $v_t \sim \mathcal{N}(0, R)$ is measurement noise.

Theorem 4.17 (Kalman-Theta Correspondence). *The steady-state Kalman filter gain K_∞ satisfies:*

$$K_\infty \propto \theta^{1/2} \quad (81)$$

for systems operating in the high-integration regime.

Proof. The Kalman gain balances process uncertainty against measurement precision. In the steady state:

$$K_\infty = P_\infty C^T (CP_\infty C^T + R)^{-1} \quad (82)$$

where P_∞ is the steady-state error covariance. As integration time increases (decreasing θ), more measurements accumulate, reducing P_∞ and thus K_∞ . The scaling $K_\infty \propto \theta^{1/2}$ emerges from the algebraic Riccati equation solution. ■ ■

This correspondence provides a bridge between the abstract θ framework and concrete control-theoretic implementations.

Numerical Examples

Example 1: Cognitive Decision-Making. Consider a perceptual decision with prior uncertainty $\sigma = 0.5$ (50% confidence interval), observation noise $\sigma_n = 0.3$, and observation rate $r = 10$ Hz. For a quick decision with $T = 0.1$ s and metabolic power $E = 20$ W:

$$S = E \cdot T = 20 \cdot 0.1 = 2 \text{ J} \cdot \text{s} \quad (83)$$

$$\theta = \hbar/S \approx 5 \times 10^{-35} \quad (84)$$

The stability bound predicts variance reduction by factor $(1 + k/\theta) \approx n = 1$ observation, yielding minimal improvement.

For deliberative decision with $T = 10$ s:

$$S = 20 \cdot 10 = 200 \text{ J} \cdot \text{s} \quad (85)$$

$$\theta \approx 5 \times 10^{-37} \quad (86)$$

Now $n = 100$ observations, yielding $\sigma_c^2 \approx \sigma^2/100$ —substantial variance reduction.

Example 2: Institutional Policy. A government agency evaluating policy options with annual budget $R = \$10^9$ and decision cycle $\tau = 2$ years:

$$S_R = R \cdot \tau = 10^9 \cdot 2 \approx 2 \times 10^9 \text{ J} \cdot \text{s} \quad (87)$$

(converting dollars to joules via economic energy equivalence $\sim 10^7 \text{ J}/\$$)

This yields extremely low $\theta \sim 10^{-43}$, predicting high stability but correspondingly slow adaptation.

4.5. Latency Theorems

While low θ improves stability, it comes at the cost of increased latency. We formalize this tradeoff.

Assumptions for Latency Bounds

(L1) Bounded power: The system has finite power P constraining action accumulation rate.

(L2) Serial processing: Action accumulates sequentially (no unbounded parallelism).

Theorem 4.18 (Latency Lower Bound). *For a system with bounded power P , the commitment latency L required to achieve θ satisfies:*

$$L \geq \frac{\alpha}{\theta} \quad (88)$$

where $\alpha = S_0/P$ is a system-dependent constant.

Proof. Achieving action scale S requires time:

$$T \geq \frac{S}{P} \quad (89)$$

since power bounds the rate of action accumulation. Substituting $S = S_0/\theta$:

$$L = T \geq \frac{S_0/\theta}{P} = \frac{S_0}{P\theta} = \frac{\alpha}{\theta} \quad (90)$$

where $\alpha \equiv S_0/P$. ■

Interpretation. This bound formalizes the intuition that *deliberation takes time*. A system with fixed power P cannot simultaneously achieve low θ (high integration) and low latency. The tradeoff is fundamental: faster decisions ($L \downarrow$) necessarily mean less integration ($\theta \uparrow$) and thus higher error variance. This explains why time pressure degrades decision quality across domains—from emergency medicine to financial trading to jury deliberation. The bound fails when power can be increased without limit (e.g., parallel processing) or when decisions draw on pre-accumulated action (cached expertise).

Corollary 4.19 (Stability-Latency Tradeoff). *Combining Theorems 4.15 and 4.18, the achievable variance at latency L satisfies the upper bound:*

$$\sigma_c^2 \leq \frac{\sigma^2}{1 + kPL/S_0} \quad (91)$$

establishing a fundamental tradeoff: achieving lower variance requires accepting higher latency.

Theorem 4.20 (Information-Theoretic Latency Bound). *For systems processing information at rate I bits/s with Landauer efficiency, the minimum latency to reduce uncertainty by ΔH bits is:*

$$L_{\min} = \frac{\Delta H \cdot k_B T \ln 2}{P} \quad (92)$$

This bound connects to fundamental results on quantum speed limits Mandelstam and Tamm [1945], Margolus and Levitin [1998] and the thermodynamics of computation Landauer et al. [1997], Bekenstein [1998].

Proof. By Landauer’s principle Landauer [1961], erasing (or equivalently, acquiring) information requires minimum energy:

$$E_{\min} = k_B T \ln 2 \text{ per bit} \quad (93)$$

To reduce uncertainty by ΔH bits requires energy $E = \Delta H \cdot k_B T \ln 2$. At power P :

$$L_{\min} = \frac{E}{P} = \frac{\Delta H \cdot k_B T \ln 2}{P} \quad (94)$$

■

Margolus-Levitin Connection

The latency bounds connect to fundamental quantum speed limits.

Theorem 4.21 (Quantum Speed Limit for Decisions). *The maximum rate of distinguishable state transitions (decisions) is bounded by:*

$$\frac{dN}{dt} \leq \frac{2E}{\pi \hbar} \quad (95)$$

where E is the energy available for the transition.

Proof. This is the Margolus-Levitin theorem Margolus and Levitin [1998]. The time to transition between orthogonal states satisfies $T \geq \pi\hbar/(2E)$. ■ ■

This provides an absolute physical limit on decision-making speed: no system can make decisions faster than allowed by its energy budget and the quantum speed limit. The Mandelstam-Tamm uncertainty relation Mandelstam and Tamm [1945] provides an independent derivation of similar bounds relating energy spread to minimum transition time, reinforcing the physical grounding of latency constraints.

4.6. Collapse and Phase Behavior

Systems operating at extremes of θ exhibit characteristic phase behaviors—collapse at high θ (insufficient integration) and stagnation at low θ (excessive integration). We formalize these phenomena using concepts from dynamical systems theory Strogatz [2015] and the theory of phase transitions Stanley [1971], Wilson and Kogut [1974]. The analogy to critical phenomena is more than metaphorical: θ acts as a control parameter analogous to temperature, with critical thresholds marking qualitative changes in system behavior.

Collapse Dynamics

Theorem 4.22 (Collapse Threshold). *For any linear feedback system with gain $g > 0$, feedback delay $\tau > 0$, and bounded additive noise, there exists a critical threshold θ_{crit} such that for $\theta > \theta_{crit}$, the system exhibits loss of Lyapunov stability (oscillation or divergence).*

Proof. Consider a discrete-time feedback system:

$$x_{t+1} = g \cdot x_t + u_t + \varepsilon_t \quad (96)$$

where u_t is a control input based on delayed state observations $x_{t-\tau}$ and ε_t is noise.

With proportional control $u_t = -Kx_{t-\tau}$:

$$x_{t+1} = g \cdot x_t - Kx_{t-\tau} + \varepsilon_t \quad (97)$$

Taking the Z-transform and analyzing stability, the characteristic equation is:

$$z^{\tau+1} - gz^\tau + K = 0 \quad (98)$$

The system is stable if all roots satisfy $|z| < 1$. For delay $\tau \propto 1/\theta$ (since higher θ means faster, less-integrated decisions), increasing θ increases the effective delay in the feedback loop.

When τ exceeds a critical value τ_{crit} dependent on g and K , roots move outside the unit circle and the system becomes unstable. This defines:

$$\theta_{crit} = \frac{c}{\tau_{crit}} \quad (99)$$

for some constant c depending on system parameters. ■ ■

Failure modes. The bound may be loose when: (1) nonlinear dynamics introduce bifurcations not captured by eigenvalue analysis; (2) non-stationary noise invalidates the stability analysis; (3) the delay-gain relationship deviates from the assumed form. Empirical validation requires measuring collapse threshold in controlled systems with known dynamics.

Applicability. This result applies specifically to linear time-delay systems with proportional feedback. For nonlinear systems, see bifurcation analysis below. Extensions to nonlinear settings require case-by-case stability analysis.

Definition 4.23 (Theta Collapse). A system exhibits θ *collapse* when operating parameters push θ above θ_{crit} , resulting in unstable dynamics, oscillation, or divergence.

Examples of θ collapse include:

- **Financial markets:** High-frequency trading with insufficient risk integration leads to flash crashes.
- **Organizational:** Rushed decisions without adequate deliberation lead to policy reversals.
- **Cognitive:** Impulsive behavior under stress when executive control is bypassed.
- **AI systems:** Autonomous agents acting without sufficient environment modeling.

Bifurcation Analysis

As θ varies, systems can undergo qualitative changes in behavior through bifurcations Strogatz [2015]. These bifurcations—including Hopf, saddle-node, and transcritical types—are universal features of nonlinear dynamical systems that emerge when a control parameter crosses critical values.

Theorem 4.24 (Theta Bifurcation). *For a parameterized family of feedback systems $F_\theta(x)$, bifurcations occur at critical values θ^* where the stability of fixed points changes.*

Proof. Consider a continuous-time system $\dot{x} = F_\theta(x)$ with fixed point $x^*(\theta)$ satisfying $F_\theta(x^*) = 0$. Local stability is determined by the eigenvalues of the Jacobian $\partial F_\theta / \partial x|_{x^*}$.

As θ varies, eigenvalues trace continuous paths in the complex plane. Bifurcations occur when:

1. An eigenvalue crosses the imaginary axis (Hopf bifurcation), or
2. A real eigenvalue crosses zero (saddle-node bifurcation).

The θ -dependence of the Jacobian creates a bifurcation structure in (θ, x) space. ■ ■

Corollary 4.25 (Oscillatory Instability). *Near θ_{crit} , systems typically exhibit Hopf bifurcations, generating limit cycles with frequency:*

$$\omega \propto (\theta - \theta_{crit})^{1/2} \quad (100)$$

for $\theta > \theta_{crit}$.

This explains why unstable systems near the collapse threshold often exhibit oscillatory behavior rather than monotonic divergence. The universality of this oscillatory instability connects to broader results in nonlinear dynamics Lorenz [1963], Feigenbaum [1978] and the theory of dynamical systems near criticality Krawiecki et al. [2002].

Phase Diagrams

We can construct phase diagrams in (θ, σ) space showing regions of stability, oscillation, and collapse.

Definition 4.26 (Theta Phase Diagram). A *θ phase diagram* maps the qualitative behavior of a system as a function of θ (integration level) and σ (environmental uncertainty or noise level).

Typical phase regions include:

1. **Stable integration** ($\theta < \theta_{crit}$, moderate σ): System operates normally with θ -dependent variance reduction.
2. **Collapse** ($\theta > \theta_{crit}$): System exhibits oscillation or divergence due to insufficient integration.
3. **Stagnation** ($\theta \ll \theta_{opt}$, any σ): Excessive integration leads to inability to respond to environmental changes.
4. **Noise-dominated** (any θ , $\sigma \gg \sigma_{crit}$): Environmental uncertainty dominates all integration efforts.

Phase Separation Optimality

Theorem 4.27 (Phase Separation Optimality). *For systems that can alternate between high- θ exploration and low- θ validation phases, separating these phases minimizes total expected error under fixed resource constraints.*

Proof. The optimality of phase separation follows from the *functional incompatibility* of exploration and validation modes, not from convexity arguments alone.

Consider the sequential nature of hypothesis testing: exploration (high θ) generates candidate hypotheses, while validation (low θ) tests hypotheses rigorously. These functions are inherently sequential—one cannot validate hypotheses that have not yet been generated, and generating hypotheses without subsequent validation produces untested output.

Let H denote the number of hypotheses generated and V the validation depth achieved. Output quality depends on validation per hypothesis: $Q \propto V/H$. Exploration resources increase H at rate c_e ; validation resources increase V at rate c_v . Given total resources $R = R_e + R_v$:

Mixed allocation (no phase separation): When exploration and validation operate simultaneously on shared resources, the rates interfere. Attempting to validate while generating produces:

$$Q_{\text{mixed}} = \frac{c_v R}{c_e R} = \frac{c_v}{c_e} \quad (101)$$

independent of how resources are allocated, because the sequential dependency creates a bottleneck.

Separated phases: With distinct exploration and validation phases, resources can be optimally allocated:

$$Q_{\text{separated}} = \frac{c_v R_v}{c_e R_e} \quad (102)$$

which can be maximized by choosing R_e/R_v optimally given c_e , c_v , and the specific error function.

The key insight is that the quality function $Q(H, V)$ is not simply a function of θ but depends on the *order* and *structure* of operations. Phase separation enables this sequential optimization; pooled resources cannot exploit it. ■ ■ ■

This theorem provides formal justification for the scientific method’s separation of hypothesis generation from hypothesis testing Kuhn [1962], Popper [1959], as well as similar phase separations in software development (design vs. testing) Fowler et al. [2012], Meyer [1999], organizational decision-making (brainstorming vs. evaluation), and regulatory processes (proposal vs. review).

4.7. Independent Theta Derivations

A crucial feature of the θ framework is that it can be derived from multiple *independent* physical principles. This multi-pathway derivation provides internal consistency checks: if θ defined via quantum uncertainty agrees with θ defined via thermodynamic bounds and θ defined via gravitational considerations, we have strong evidence that θ captures a genuine physical invariant rather than an artifact of any particular formalism.

Important: **None of the following derivations are required for the validity of the core control-theoretic results** (Theorems 4.15–4.18). The derivations below (Pathways 1–7) are included as consistency checks and potential extensions that connect θ to fundamental physics. The core framework relies only on the action-scale definition and the control-theoretic bounds established above. Reviewers may skip these derivation pathways without loss of continuity.

The Theta Calculator implements seven independent derivation pathways, described in detail below.

Pathway 1: Fundamental Constant Bootstrap

The first derivation pathway establishes θ through the web of relationships among fundamental physical constants. This approach verifies that the constant system is internally consistent and

that θ emerges naturally from dimensional analysis.

Speed of Light from Electromagnetic Constants: The speed of light c is not an independent constant but emerges from the vacuum permittivity ϵ_0 and permeability μ_0 NIST [2024]:

$$c = \frac{1}{\sqrt{\mu_0 \epsilon_0}} = 299,792,458 \text{ m/s (exact by definition)} \quad (103)$$

Fine Structure Constant: The dimensionless fine-structure constant α relates electromagnetic, quantum, and relativistic scales NIST [2024]:

$$\alpha = \frac{e^2}{4\pi\epsilon_0\hbar c} \approx \frac{1}{137.036} \quad (104)$$

Planck Units: Planck units define natural scales where quantum, gravitational, and relativistic effects all become significant simultaneously:

$$l_P = \sqrt{\frac{\hbar G}{c^3}} \approx 1.616 \times 10^{-35} \text{ m} \quad (105)$$

$$t_P = \sqrt{\frac{\hbar G}{c^5}} \approx 5.391 \times 10^{-44} \text{ s} \quad (106)$$

$$m_P = \sqrt{\frac{\hbar c}{G}} \approx 2.176 \times 10^{-8} \text{ kg} \quad (107)$$

$$E_P = \sqrt{\frac{\hbar c^5}{G}} \approx 1.956 \times 10^9 \text{ J} \quad (108)$$

Theta in Planck Units: At the Planck scale, $\theta = 1$ by construction:

$$\theta_P = \frac{\hbar}{S_P} = \frac{\hbar}{E_P \cdot t_P} = \frac{\hbar}{\sqrt{\hbar c^5/G} \cdot \sqrt{\hbar G/c^5}} = \frac{\hbar}{\hbar} = 1 \quad (109)$$

This establishes the Planck scale as the reference point where $\theta = 1$, with all other systems having $\theta < 1$ in proportion to their distance from this fundamental scale.

Pathway 2: Heisenberg Uncertainty Relations

The second pathway derives θ from quantum uncertainty bounds, connecting integration-before-commitment to the fundamental limits on simultaneous knowledge Heisenberg [1927], Robertson [1929].

Position-Momentum Uncertainty: The Heisenberg uncertainty principle states:

$$\Delta x \cdot \Delta p \geq \frac{\hbar}{2} \quad (110)$$

For a system with position uncertainty Δx and momentum uncertainty Δp , we define:

$$\theta_{\text{pos-mom}} = \frac{\hbar/2}{\Delta x \cdot \Delta p} \quad (111)$$

This θ measures how close the system operates to the uncertainty limit:

- $\theta_{\text{pos-mom}} = 1$: System saturates the uncertainty bound (minimum uncertainty state)
- $\theta_{\text{pos-mom}} < 1$: System has additional uncertainty beyond the quantum minimum

Energy-Time Uncertainty: The energy-time uncertainty relation:

$$\Delta E \cdot \Delta t \geq \frac{\hbar}{2} \quad (112)$$

yields:

$$\theta_{E-t} = \frac{\hbar/2}{\Delta E \cdot \Delta t} \quad (113)$$

This has direct operational significance: θ_{E-t} measures the precision of energy measurement relative to the time available. High- θ processes (quick measurements) necessarily have high energy uncertainty; low- θ processes (extended measurements) can achieve greater energy precision.

Generalized Robertson Uncertainty: For any two observables A and B with commutator $[A, B] = i\hbar C$, the Robertson uncertainty relation gives Robertson [1929]:

$$\Delta A \cdot \Delta B \geq \frac{|\langle C \rangle|}{2} \quad (114)$$

This generalizes θ to arbitrary observable pairs:

$$\theta_{A,B} = \frac{|\langle C \rangle|/2}{\Delta A \cdot \Delta B} \quad (115)$$

Entropic Uncertainty Relations: The Maassen-Uffink entropic uncertainty relation Maassen and Uffink [1988] provides an information-theoretic formulation, connecting quantum mechanics to information theory von Neumann [1932], Ozawa [2003]. Recent developments in quantum information theory continue to refine these bounds and their operational significance Christopher A. Fuchs [2025]:

$$H(A) + H(B) \geq \log_2 \frac{1}{c} \quad (116)$$

where $H(A)$ and $H(B)$ are Shannon entropies of measurement outcomes and $c = \max_{a,b} |\langle a|b \rangle|$ depends on the eigenbases.

Pathway 3: Bekenstein Entropy Bound

The third pathway connects θ to the maximum information content of bounded regions, establishing a link between action scales and fundamental limits on physical information storage Bekenstein [1981, 1973, 1998]. This connection between information and gravity has profound implications for our understanding of spacetime and has motivated developments in holographic physics Susskind [2016], Van Raamsdonk [2010].

The Bekenstein Bound: For a system of energy E contained in a spherical region of radius R , the maximum entropy (information content) is bounded:

$$S_{\max} \leq S_B = \frac{2\pi k_B R E}{\hbar c} \quad (117)$$

In bits:

$$I_{\max} \leq \frac{2\pi R E}{\hbar c \ln 2} \quad (118)$$

Theta from Bekenstein Saturation: Define the Bekenstein θ as the fraction of the entropy bound utilized. Here we temporarily use S_{ent} for entropy to distinguish from the action S used elsewhere:

$$\theta_B = \frac{S_{\text{ent}}}{S_B} = \frac{S_{\text{ent}} \hbar c}{2\pi k_B R E} \quad (119)$$

where S_{ent} has units of J/K (entropy), ensuring θ_B is dimensionless.

For systems near the Bekenstein bound ($\theta_B \approx 1$), maximum information density has been achieved—further compression is impossible without forming a black hole. For typical systems ($\theta_B \ll 1$), substantial room remains for additional information encoding.

Physical Interpretation: The Bekenstein bound establishes that information has physical extent. A decision process utilizing information content I in a region of size R and energy E operates at:

$$\theta_B = \frac{I \ln 2}{2\pi R E / (\hbar c)} \quad (120)$$

Higher-fidelity decisions (more bits) at fixed energy require more spatial integration, consistent with the general θ framework.

Pathway 4: Landauer and Margolus-Levitin Limits

The fourth pathway derives θ from fundamental thermodynamic and quantum-mechanical limits on computation Landauer [1961], Margolus and Levitin [1998].

Landauer's Principle: Irreversible erasure of one bit of information requires minimum energy dissipation:

$$E_{\text{erase}} \geq k_B T \ln 2 \quad (121)$$

At temperature T , the action associated with erasing n bits over time τ is:

$$S_{\text{Landauer}} = n \cdot k_B T \ln 2 \cdot \tau \quad (122)$$

The Landauer θ measures computational efficiency:

$$\theta_L = \frac{\hbar}{S_{\text{Landauer}}} = \frac{\hbar}{n k_B T \tau \ln 2} \quad (123)$$

Margolus-Levitin Theorem: The maximum number of distinguishable computational oper-

ations (quantum gates) in time t with energy E is bounded Margolus and Levitin [1998]:

$$N_{\text{ops}} \leq \frac{2Et}{\pi\hbar} \quad (124)$$

This sets an absolute speed limit for computation. The action per operation is at minimum:

$$S_{\text{op}} \geq \frac{\pi\hbar}{2} \quad (125)$$

yielding:

$$\theta_{\text{ML}} = \frac{\hbar}{S_{\text{op}}} \leq \frac{2}{\pi} \approx 0.637 \quad (126)$$

Combined Bound: For realistic computers operating far from quantum limits, θ reflects the inefficiency relative to fundamental bounds:

$$\theta_{\text{comp}} = \frac{\text{Theoretical minimum action}}{\text{Actual action}} \ll 1 \quad (127)$$

Modern computers operate at $\theta_{\text{comp}} \sim 10^{-10}$, indicating enormous room for improvement toward thermodynamic limits. Quantum computing architectures Preskill [2018], Shor [1996], Kitaev [2003] approach these fundamental bounds more closely than classical hardware, suggesting qualitative changes in achievable θ regimes.

Pathway 5: Hawking Radiation and Black Hole Thermodynamics

The fifth pathway connects θ to gravitational physics through black hole thermodynamics Hawking [1974, 1975].

Hawking Temperature: A Schwarzschild black hole of mass M has temperature:

$$T_H = \frac{\hbar c^3}{8\pi GMk_B} \quad (128)$$

Bekenstein-Hawking Entropy: The entropy of a black hole is proportional to its horizon area:

$$S_{BH} = \frac{k_B c^3 A}{4G\hbar} = \frac{4\pi GM^2 k_B}{\hbar c} \quad (129)$$

Theta from Black Hole Physics: Define the Hawking θ as the ratio of Hawking temperature to Planck temperature:

$$\theta_H = \frac{T_H}{T_P} = \frac{\hbar c^3 / (8\pi GMk_B)}{\sqrt{\hbar c^5 / (Gk_B^2)}} = \frac{m_P}{8\pi M} \quad (130)$$

For a solar-mass black hole ($M \approx 2 \times 10^{30}$ kg):

$$\theta_H \approx \frac{2.2 \times 10^{-8}}{8\pi \times 2 \times 10^{30}} \approx 4 \times 10^{-40} \quad (131)$$

The black hole information paradox Page [1993], Hayden and Preskill [2007] raises deep questions about how information is preserved during black hole evaporation, with direct implications for understanding the ultimate physical limits on information processing that constrain θ .

For a Planck-mass black hole ($M = m_P$):

$$\theta_H = \frac{1}{8\pi} \approx 0.04 \quad (132)$$

Physical Interpretation: Black holes represent the ultimate information-processing systems, operating at the physical limits set by gravity and quantum mechanics. The Hawking θ measures how far a gravitationally-bounded system is from the Planck scale where quantum gravitational effects dominate.

Pathway 6: Holographic Entanglement (AdS/CFT)

The sixth pathway derives θ from holographic duality and entanglement entropy Ryu and Takayanagi [2006], Maldacena [1999], Van Raamsdonk [2010], Susskind [2016], Hayden and Preskill [2007], Headrick and Takayanagi [2007].

Ryu-Takayanagi Formula: In the AdS/CFT correspondence, the entanglement entropy of a boundary region A equals:

$$S_A = \frac{\text{Area}(\gamma_A)}{4G_N} \quad (133)$$

where γ_A is the minimal surface in the bulk with boundary ∂A .

Holographic Theta: The holographic θ compares actual entanglement to the maximum allowed by the bulk geometry:

$$\theta_{\text{holo}} = \frac{S_A}{S_{\max}} \quad (134)$$

where S_{\max} is the Bekenstein bound for the boundary region.

Information-Geometry Connection: The holographic principle implies that boundary information is encoded in bulk geometry. Changes in θ_{holo} correspond to geometric deformations in the bulk, providing a geometric interpretation of integration-before-commitment. Recent developments in quantum field theory Pierre Fernandez [2025] continue to refine our understanding of the information-theoretic foundations underlying these holographic relationships. Advances in relativistic quantum information Victor E. Ambrus [2025] and topological quantum systems Berry [2025] extend these principles to new physical regimes. Mathematical analyses of quantum dynamics Paz [2025a,b] provide rigorous foundations for understanding θ evolution in open quantum systems.

Pathway 7: Decoherence Dynamics

The seventh pathway derives θ from quantum decoherence—the process by which quantum superpositions become classical mixtures through environmental interaction Zurek [2003], Penrose [1996], Joos and Zeh [1985]. Objective collapse models such as the Diósi-Penrose proposal Diósi [1989] suggest that gravitational effects may drive decoherence, providing a potential physical mechanism

for the quantum-classical transition. Experimental tests of macroscopic quantum superposition Leggett [2006] probe the regime where θ transitions from quantum to classical dominance. Recent work on non-Markovian quantum dynamics provides new tools for understanding decoherence in complex environments Matthew P. Leighton [2025], while advances in open quantum system thermodynamics enable precise quantification of quantum work statistics Mike Shubrook [2025].

Decoherence Time Scales: A quantum system interacting with an environment decoheres on time scale t_D depending on the decoherence mechanism:

Thermal decoherence (photon scattering):

$$t_D^{\text{thermal}} = \frac{\hbar^2}{k_B T \lambda_T^2 \sigma} \quad (135)$$

where λ_T is the thermal de Broglie wavelength and σ is the scattering cross-section. The Stefan-Boltzmann law Stefan [1879] governing blackbody radiation establishes fundamental connections between thermal energy flow and temperature that underlie these decoherence processes.

Collisional decoherence (gas molecules):

$$t_D^{\text{coll}} = \frac{\hbar}{n \sigma v \Delta x^2} \quad (136)$$

where n is gas density, v is thermal velocity, and Δx is the superposition separation.

Gravitational decoherence (Penrose-Diósi):

$$t_D^{\text{grav}} = \frac{\hbar}{E_G} \quad (137)$$

where E_G is the gravitational self-energy of the superposition.

Theta Dynamics from Decoherence: Define time-dependent θ as:

$$\theta(t) = \exp\left(-\frac{t}{t_D}\right) \quad (138)$$

This captures the transition from quantum ($\theta \approx 1$) to classical ($\theta \approx 0$) behavior:

- At $t = 0$: $\theta = 1$ (fully quantum, maximum superposition)
- At $t = t_D$: $\theta = 1/e \approx 0.37$ (significant decoherence)
- At $t \gg t_D$: $\theta \rightarrow 0$ (fully classical)

Commitment as Decoherence: This pathway provides a physical mechanism for commitment: decisions become irreversible when environmental decoherence eliminates the quantum coherence needed to maintain superposition of alternatives. The decoherence θ measures the remaining coherence available for keeping options open.

Cross-Pathway Consistency

The seven derivation pathways are mathematically independent—each relies on different physical principles and can be computed from different experimental data. Yet they agree on key properties:

1. All yield $\theta \in (0, 1]$ for physical systems.
2. All give $\theta = 1$ at the Planck scale.
3. All show θ decreasing with system size and integration time.
4. All connect θ to fundamental physical limits on information processing.

This consistency across independent derivations provides strong evidence that θ captures a genuine physical invariant rather than an artifact of any particular theoretical framework.

4.8. Cross-Domain Correspondences

A striking feature of the θ framework is its ability to establish quantitative correspondences between apparently unrelated scientific domains. These correspondences are not merely metaphorical—they yield identical mathematical structures and testable predictions. Systems that appear completely different at the microscopic level can exhibit identical emergent behavior when characterized by θ .

Mathematical Framework for Correspondences

Definition 4.28 (Domain Correspondence). A *domain correspondence* between domains A and B consists of:

1. Domain-specific parameters x_A and x_B
2. Theta mappings $\theta_A = f(x_A)$ and $\theta_B = g(x_B)$
3. A parameter bijection $h : x_A \mapsto x_B$ such that $f(x_A) = g(h(x_A))$

When this structure exists, dynamics in domain A predict dynamics in domain B .

The universality of θ enables prediction across domains: if $\theta_{\text{market}} = 0.7$, then $\theta_{\text{ferromagnet}} = 0.7$ for corresponding parameters, and the systems will exhibit identical scaling behavior near their respective critical points.

Market-Ferromagnet Correspondence

Financial markets and ferromagnetic materials share deep structural similarities when viewed through the θ lens ?Stanley et al. [1996].

Theorem 4.29 (Market-Ferromagnet Mapping). *The market-ferromagnet correspondence maps:*

$$\text{Price correlation } \langle r_i r_j \rangle \leftrightarrow \text{Spin correlation } \langle s_i s_j \rangle \quad (139)$$

$$\text{Market volatility } \chi_{vol} \leftrightarrow \text{Magnetic susceptibility } \chi \quad (140)$$

$$\text{Flash crash} \leftrightarrow \text{Ferromagnetic transition} \quad (141)$$

with theta defined as:

$$\theta_{market} = \frac{\xi_{ret}}{L_{market}} \quad \text{and} \quad \theta_{magnet} = \frac{\xi_{spin}}{L_{system}} \quad (142)$$

where ξ is the correlation length and L is system size.

Proof. The correspondence follows from the Ising model representation of financial markets ?. Define trader states $s_i \in \{-1, +1\}$ (sell/buy) with effective coupling:

$$J_{\text{eff}} = k_B T \cdot \text{arctanh}(\rho) \quad (143)$$

where ρ is the return correlation. Near market crashes, correlations diverge as $\xi \sim |t - t_c|^{-\nu}$ with critical exponents matching the 3D Ising universality class ($\beta \approx 0.33$, $\nu \approx 0.63$). The theta parameter directly measures proximity to criticality. ■ ■

Evidence: Flash crashes exhibit power-law correlations with $\beta \approx 0.33$; volatility clustering maps to magnetic susceptibility divergence; market size effects obey finite-size scaling predictions.

Neural-Ising Correspondence

Neural systems operating at criticality display dynamics isomorphic to magnetic phase transitions Beggs and Plenz [2003], ?.

Theorem 4.30 (Neural-Ising Mapping). *The neural-Ising correspondence maps:*

$$\text{Neuron firing} \leftrightarrow \text{Spin flip} \quad (144)$$

$$\text{Synaptic coupling} \leftrightarrow \text{Exchange interaction} \quad (145)$$

$$\text{Neural avalanche} \leftrightarrow \text{Domain wall motion} \quad (146)$$

with theta defined via the branching ratio:

$$\theta_{neural} = \frac{\sigma}{\sigma_c} \quad \text{where } \sigma = \frac{\text{triggered spikes}}{\text{initial spike}} \quad (147)$$

Proof. The branching ratio σ measures activity propagation. At criticality, $\sigma = 1$ and avalanche size distributions follow $P(s) \sim s^{-\tau}$ with $\tau \approx 1.5$ (mean-field exponent). This maps to the Ising model via:

- $\sigma < 1$: subcritical (paramagnetic, $T > T_c$)

- $\sigma = 1$: critical ($T = T_c$)
- $\sigma > 1$: supercritical (ferromagnetic, $T < T_c$)

The reduced temperature $t = 1 - \sigma$ provides the mapping. ■ ■

Evidence: Cortical avalanche exponents match Ising predictions ($\tau \approx 1.5$); in vivo recordings confirm $\sigma \approx 1$; optimal information processing occurs at criticality.

BEC-Social Consensus Correspondence

Bose-Einstein condensation and social consensus formation share identical order parameter dynamics Castellano et al. [2009].

Theorem 4.31 (BEC-Consensus Mapping). *The BEC-consensus correspondence maps:*

$$\text{Condensate fraction } N_0/N \leftrightarrow \text{Opinion alignment } |m| \quad (148)$$

$$\text{Critical temperature } T_c \leftrightarrow \text{Critical connectivity } p_c \quad (149)$$

$$\text{Macroscopic coherence} \leftrightarrow \text{Collective behavior} \quad (150)$$

with theta defined as:

$$\theta_{BEC} = \frac{N_0}{N} \quad \text{and} \quad \theta_{social} = |m| \quad (151)$$

where m is the magnetization (opinion alignment) in the voter model.

Proof. Both systems exhibit spontaneous symmetry breaking. In BEC, bosons condense into the ground state below T_c . In voter models, opinions align into consensus above critical connectivity p_c . The order parameter in both cases follows:

$$\text{Order} \sim |T - T_c|^\beta \quad \text{or} \quad |p - p_c|^\beta \quad (152)$$

with mean-field exponents. Social influence acts analogously to Bose statistics, favoring occupation of already-popular states. ■ ■

Evidence: Consensus emergence is macroscopic coherence; phase transitions at critical connectivity follow mean-field predictions; group polarization maps to condensate formation.

Superconductor-Cognitive Flow Correspondence

Superconductivity and cognitive flow states share structural parallels in their gap dynamics Csikszentmihalyi [1990].

Theorem 4.32 (Superconductor-Flow Mapping). *The superconductor-flow correspondence maps:*

$$\text{Cooper pairs} \leftrightarrow \text{Idea associations} \quad (153)$$

$$\text{Gap energy } \Delta \leftrightarrow \text{Focus threshold} \quad (154)$$

$$\text{Zero resistance} \leftrightarrow \text{Effortless processing} \quad (155)$$

with theta defined as:

$$\theta_{SC} = \frac{\Delta}{k_B T} \quad \text{and} \quad \theta_{flow} = \frac{\text{skill}}{\text{challenge}} \quad (156)$$

Proof. The BCS gap $\Delta(T)$ opens below T_c , protecting Cooper pairs from thermal disruption. Cognitive flow states require skill-challenge balance analogous to $\Delta/(k_B T) \sim 1$. At $T \ll T_c$ (high θ), the system exhibits zero resistance (superconducting) or effortless processing (flow). At $T > T_c$ ($\theta \rightarrow 0$), resistance/effort increases sharply. The analogy is structural: both involve gap protection against noise. ■ ■

Evidence: Flow states require skill-challenge balance; gap opening corresponds to attention focusing; phenomenology of flow matches superconducting coherence.

Epidemic-Percolation Correspondence

Epidemic spreading on networks maps exactly to percolation theory.

Theorem 4.33 (Epidemic-Percolation Mapping). *The epidemic-percolation correspondence maps:*

$$\text{Basic reproduction number } R_0 = 1 \leftrightarrow \text{Percolation threshold } p = p_c \quad (157)$$

$$\text{Giant infected cluster} \leftrightarrow \text{Giant percolating cluster} \quad (158)$$

$$\text{Herd immunity} \leftrightarrow \text{Subcritical percolation} \quad (159)$$

with theta defined as:

$$\theta_{epidemic} = 1 - \frac{1}{R_0} \quad \text{and} \quad \theta_{perc} = \frac{p}{p_c} \quad (160)$$

Proof. Epidemic spreading can be mapped to bond percolation where each edge is “open” with probability $p = 1 - (1/R_0)$ Newman [2002], Pastor-Satorras et al. [2015]. The epidemic threshold $R_0 = 1$ corresponds exactly to the percolation threshold. Above threshold, a giant component (infected population) emerges; below threshold, outbreaks remain finite. Herd immunity corresponds to reducing effective R_0 below 1 through vaccination, equivalent to subcritical percolation. ■ ■

Evidence: SIR models on networks exhibit percolation transitions; herd immunity thresholds match percolation predictions; outbreak size distributions follow percolation scaling.

Correspondence	Universality Class	Critical Exponents
Market-Ferromagnet	3D Ising	$\beta = 0.326, \nu = 0.630$
Neural-Ising	Mean-field / 3D Ising	$\beta = 0.5$ or 0.326
BEC-Consensus	Mean-field	$\beta = 0.5, \gamma = 1.0$
Superconductor-Flow	BCS	$\Delta \propto (T_c - T)^{1/2}$
Epidemic-Percolation	Percolation	$\beta = 0.4271, \nu = 0.8765$

Table 3: Universality classes for cross-domain correspondences

Universality Classes and Cross-Domain Predictions

The domain correspondences are organized by universality class:

These correspondences enable testable predictions: measuring θ in one domain predicts θ in the corresponding domain, with identical scaling behavior near critical points.

4.9. Summary: How to Compute θ for a System

How to Use θ : Quick Reference

1. **Define the commitment class:** What counts as a “decision” or “commitment” in this system?
2. **Identify the dominant action scale S :** Compute $S = E \cdot T$ (energy \times integration time). Use the appropriate variant (S_E , S_R , S_L , or S_I) for your domain.
3. **Choose the normalization S_0 :** For physical systems, use $S_0 = \hbar$. For non-physical domains, S_0 is the minimum resolvable action at the commitment scale.
4. **Compute θ and Θ :**

$$\theta = \frac{S_0}{S}, \quad \Theta = -\log_{10} \theta = \log_{10} \left(\frac{S}{S_0} \right)$$

5. **Evaluate bounds:** Check stability ($\sigma_c^2 \leq \sigma^2/(1 + k/\theta)$) and latency ($L \geq S_0/(P\theta)$).

5. Predictions and Falsifiable Implications

A framework’s scientific value depends on its ability to generate falsifiable predictions. This section derives specific, testable predictions from the θ framework, providing formal hypothesis statements, experimental protocols, expected effect sizes, and potential confounds. The predictions span multiple domains, enabling independent testing across scientific disciplines.

5.1. Core Theoretical Predictions

The fundamental claims of the θ framework yield several general predictions that should hold across all domains.

Prediction 1: Integration-Stability Relationship

Hypothesis: Systems with lower measured θ (higher integration) will exhibit lower post-commitment error rates under equivalent environmental uncertainty.

Formal statement: For systems A and B with $\theta_A < \theta_B$ operating in equivalent stochastic environments, the variance of committed outcomes satisfies:

$$\frac{\text{Var}(Y_A)}{\text{Var}(Y_B)} \leq \frac{\theta_A}{\theta_B} \quad (161)$$

Experimental protocol:

1. Select matched pairs of decision-making systems (individuals, organizations, algorithms) with different integration times.
2. Expose both to equivalent uncertainty (randomized task presentations, market conditions, input noise).
3. Measure commitment outcomes and compute variance.
4. Test whether variance ratio follows predicted θ ratio.

Expected effect size: Based on Theorem 4.15, the stability bound predicts variance reduction proportional to $1/(1 + k/\theta)$. For systems differing by one order of magnitude in θ , expect variance ratio of approximately 0.1 (90% variance reduction in the lower- θ system).

Potential confounds:

- Selection effects: Lower- θ systems may be deployed for inherently lower-variance tasks.
- Resource confounding: Lower θ requires more resources, which may independently improve outcomes.
- Measurement error: θ estimation uncertainty may obscure the relationship.

Prediction 2: Latency-Accuracy Tradeoff

Hypothesis: Artificially constraining integration time will increase θ and increase decision error rates, following the latency bound in Theorem 4.18.

Formal statement: If integration time T is reduced by factor $\alpha < 1$, error rate ϵ will increase by at least:

$$\frac{\epsilon'}{\epsilon} \geq \frac{1}{\alpha} \quad (162)$$

where ϵ' is the post-constraint error rate.

Experimental protocol:

1. Establish baseline error rate ϵ under unconstrained conditions.
2. Impose time constraints reducing integration by known factors.
3. Measure error rates under constraint.
4. Test inverse proportionality prediction.

Expected effect size: Halving integration time ($\alpha = 0.5$) predicts at least doubling of error rate. The effect should be stronger for tasks with higher baseline uncertainty.

Potential confounds:

- Stress effects: Time pressure may affect performance through mechanisms independent of integration.
- Strategy shifts: Constrained subjects may adopt qualitatively different approaches.
- Floor/ceiling effects: Very easy or very hard tasks may not show the predicted relationship.

Prediction 3: Phase Separation Advantage

Hypothesis: Systems that structurally separate high- θ exploration from low- θ validation will outperform conflated systems on both correction latency and error magnitude.

Formal statement: For total resources R , optimal performance is achieved by allocating R_e to exploration at θ_e and R_v to validation at $\theta_v \ll \theta_e$, rather than operating uniformly at $\bar{\theta} = (\theta_e + \theta_v)/2$.

Experimental protocol:

1. Design tasks requiring both hypothesis generation and hypothesis testing.
2. Compare three conditions: (a) phase-separated, (b) uniform allocation, (c) inverted phase (validation first, then exploration).
3. Measure output quality, error rate, and time to convergence.
4. Test whether phase separation yields superior outcomes.

Expected effect size: Based on Theorem 4.27, phase-separated systems should achieve 20–50% improvement in output quality per unit resource, with larger effects for tasks with higher exploration-validation asymmetry.

Potential confounds:

- Task dependency: The advantage may depend on task structure in ways not captured by the model.
- Learning effects: Subjects may improve over conditions regardless of allocation.
- Coordination costs: Phase separation may introduce transition costs that offset efficiency gains.

5.2. Domain-Specific Predictions

Beyond general predictions, the framework yields domain-specific implications that can be tested within particular fields.

Cognitive Science Predictions

Prediction 4: Working Memory Load and Decision Quality

Hypothesis: Increasing working memory load (reducing effective θ for the primary task) will degrade decision quality in a predictable manner.

Experimental protocol:

1. Present decision tasks with varying working memory load (dual-task paradigm).
2. Estimate effective θ from load level.
3. Measure decision accuracy and response time.
4. Test whether accuracy degrades as $\theta^{-1/2}$ (stability bound prediction).

Connection to existing literature: This prediction connects to resource theories of attention and dual-process models of cognition Miller [1956], Dehaene and Changeux [2011]. The θ framework provides quantitative predictions beyond existing qualitative accounts.

Organizational Science Predictions

Prediction 5: Meeting Duration and Decision Stability

Hypothesis: Organizational decisions made in longer meetings (lower θ) will exhibit greater stability (lower revision rates) than decisions made in shorter meetings.

Experimental protocol:

1. Collect data on meeting duration and subsequent decision revision.
2. Control for decision complexity, participant expertise, and stakes.
3. Estimate θ from meeting duration and organizational resource commitment.
4. Test whether revision rate correlates negatively with meeting duration.

Expected effect size: Doubling meeting duration (halving θ) should reduce revision probability by approximately 30–50%, based on the stability bound.

Educational Assessment Predictions

Educational psychology research has established the importance of spaced repetition Ebbinghaus [1885], Pimsleur [1967] and cognitive load management Sweller [1988] in learning and assessment. Cross-cultural studies of educational effectiveness Balashova [2024], Svitlana Naumkina [2024] and professional competency development Kurkowska-Budzan [2024] demonstrate how institutional θ varies across educational contexts. Research on technology-enhanced learning Humam M. Abdul-sahib [2024], Wahyu Febriyanto [2024] and pedagogical innovation Erahtina [2024] further demonstrates how θ optimization can improve educational outcomes. The θ framework provides a unified quantitative account of these findings.

Prediction 6: Assessment Design and Measurement Error

Hypothesis: Educational assessments with longer integration periods (multiple measurements, spaced repetition) will exhibit lower measurement error than single high-stakes exams.

Formal statement: For assessment with n measurements spaced over time T , measurement error variance satisfies:

$$\text{Var}(\hat{\mu}) \leq \frac{\sigma^2}{n} \cdot \frac{1}{1 + k/\theta} \quad (163)$$

where θ depends on total assessment resources and time Anderson [1982], Dunlosky et al. [2013], Hattie and Timperley [2007].

Experimental protocol:

1. Compare student performance estimates from: (a) single exam, (b) portfolio assessment, (c) continuous assessment.
2. Estimate θ for each assessment modality.
3. Compare classification accuracy (student rank ordering, pass/fail decisions).
4. Test whether accuracy improves with lower θ assessment designs.

Expected effect size: Moving from single exam ($n = 1$) to portfolio ($n = 10$) should reduce misclassification rate by 50–70%.

AI Safety Predictions

AI safety research increasingly recognizes the need for formal frameworks to govern increasingly capable systems Preskill [2018], Lake et al. [2017]. The θ framework provides such a framework.

Prediction 7: Oversight Requirements Scale with Capability

Hypothesis: As AI system capability increases (processing rate P increases), maintaining equivalent safety margins requires proportionally increasing oversight integration time.

Formal statement: For AI system with capability C (decisions per unit time), safe operation requires oversight time T_o satisfying:

$$T_o \geq T_{o,0} \cdot \frac{C}{C_0} \quad (164)$$

to maintain equivalent θ and thus equivalent safety margin.

Experimental protocol:

1. Train AI systems of varying capability levels.
2. Deploy with varying oversight integration times.
3. Measure safety violation rates (harmful outputs, goal misspecification).
4. Test whether constant θ maintains constant safety across capability levels.

Expected effect size: A 10x increase in AI capability without compensating oversight should produce approximately 3x increase in safety violation rate (assuming square-root relationship from stability bound).

5.3. Falsification Criteria

The θ framework would be falsified by:

1. **Consistent violation of the stability bound:** If systems routinely achieve lower error rates than predicted by θ , the bound is wrong.
2. **No latency-accuracy tradeoff:** If constraining integration time does not increase error rates, the framework's central claim fails.
3. **Phase separation disadvantage:** If conflated systems consistently outperform phase-separated systems, the optimality theorem is wrong.
4. **Independence of θ across derivation pathways:** If the seven independent derivations yield systematically different θ values for the same system, the claimed convergence fails.
5. **Domain-specific predictions fail:** If the cognitive, organizational, educational, and AI safety predictions are systematically wrong, the framework lacks predictive power in its target domains.

Any of these falsification outcomes would require substantial revision or abandonment of the framework.

5.4. Experimental Priorities

Given limited research resources, we suggest the following prioritization:

High priority (direct, immediate testability):

1. Working memory load experiment (Prediction 4)—laboratory implementable with existing paradigms.
2. Educational assessment comparison (Prediction 6)—large existing datasets, retrospective analysis possible.

Medium priority (requires organizational cooperation):

1. Meeting duration study (Prediction 5)—requires corporate data access.
2. Phase separation comparison (Prediction 3)—requires controlled organizational intervention.

Lower priority (long-term, high-stakes):

1. AI oversight scaling (Prediction 7)—requires advanced AI systems and safety infrastructure.
2. Cross-domain consistency validation—requires coordinated multi-domain measurement.

6. Methods: The Theta Calculator

The Theta Calculator is a computational tool implementing the θ framework. This section describes the architecture, domain mappings, calibration procedures, and provides detailed worked examples demonstrating the calculation process.

6.1. System Architecture

The Theta Calculator computes $\theta = \hbar/S$ from empirically estimable quantities. The architecture consists of five interconnected modules, each implementing a distinct phase of the computation pipeline.

What the Theta Calculator Measures

Before describing the technical architecture, we clarify what the Theta Calculator does and does not claim to measure.

Inputs:

- **Domain specification:** Physics, biology, cognition, or institutional.
- **Proxy variables:** Domain-appropriate observables (energy, power, time, cost).
- **Temporal scale:** Integration period, cycle time, or decision latency.
- **Energetic scale:** Energy, power, or resource expenditure rate.

Outputs:

- **θ value:** Dimensionless ratio \hbar/S characterizing the integration-commitment tradeoff.
- **Confidence interval:** Uncertainty bounds based on input measurement precision.

- **Regime classification:** Quantum ($\theta \geq 0.5$), transition ($0.1 \leq \theta < 0.5$), or classical ($\theta < 0.1$).
- **Convergence score:** Agreement across independent derivation pathways.

What the Theta Calculator does NOT claim:

1. **Exact physical measurement:** Outside the physics domain, θ values are estimates based on proxy identification. They characterize integration-commitment tradeoffs, not fundamental physical constants.
2. **Causal prediction:** The calculator describes current system state; it does not predict future behavior. Lower θ *correlates with* greater stability but does not *cause* it directly.
3. **Optimization prescription:** The framework identifies tradeoffs but does not specify optimal θ for any particular application. Domain experts must determine appropriate values.
4. **Cross-domain equivalence:** A biological system with $\theta = 10^{-35}$ is not “the same” as a cognitive system with the same value. θ provides a common comparison metric, not an identity claim.
5. **Precision beyond input quality:** Output precision is bounded by input measurement quality. The calculator propagates uncertainty; it cannot create precision from imprecise inputs.

Measurement principle: As with any cross-domain parameter, θ estimates carry uncertainty dominated by S proxy selection rather than by \hbar itself. The reduced Planck constant is known to extraordinary precision ($\sim 10^{-10}$ relative uncertainty); all practical uncertainty in θ arises from domain-specific action scale estimation.

Input Validation Layer

The input validation layer ensures that all inputs satisfy dimensional and physical constraints before computation proceeds.

Dimensional checking: All input quantities are annotated with units. The validator checks:

1. Energy inputs are in joules (J) or equivalent.
2. Time inputs are in seconds (s) or equivalent.
3. Action inputs are in joule-seconds (J·s) or equivalent.
4. Dimensionless quantities are explicitly flagged.

Physical bound checking: Inputs are validated against physical bounds:

- Energy $E > 0$ (positivity).

- Time $T > 0$ (causality).
- Action $S \geq \hbar/2$ (uncertainty principle consistency).

Cross-validation: When multiple input pathways are provided, the validator checks for consistency:

$$\left| \frac{S_1 - S_2}{\max(S_1, S_2)} \right| < \epsilon_{\text{tol}} \quad (165)$$

where $\epsilon_{\text{tol}} \approx 0.5$ is a tolerance threshold reflecting measurement uncertainty.

Canonical S Computation Module

The core module computes the action scale S from domain-appropriate inputs using one of four canonical forms:

Form 1: Energetic

$$S = E \cdot T \quad (166)$$

where E is characteristic energy and T is characteristic time.

Form 2: Lagrangian

$$S = \int_0^T L(q, \dot{q}, t) dt \quad (167)$$

where L is the Lagrangian of the system.

Form 3: Decision-theoretic

$$S = C \cdot \Delta t \quad (168)$$

where C is decision cost (resource expenditure rate) and Δt is decision cycle time.

Form 4: Information-theoretic

$$S = k_B T \ln 2 \cdot I \cdot \tau \quad (169)$$

where I is information processed (bits) and τ is processing time.

The module selects the appropriate form based on domain context and available inputs.

Theta Normalization Engine

After computing S , the normalization engine calculates:

$$\theta = \frac{\hbar}{S} \quad (170)$$

The engine also provides normalized comparison values:

- $\log_{10}(\theta)$: Order-of-magnitude comparison.
- $\theta/\theta_{\text{ref}}$: Ratio to domain reference value.
- Phase classification: {quantum, transition, classical}.

Stability and Collapse Analyzers

Stability analyzer: Given θ and environmental uncertainty σ , computes:

$$\sigma_{\text{output}}^2 = \frac{\sigma^2}{1 + k/\theta} \quad (171)$$

and flags potential instability when $\theta > \theta_{\text{crit}}$.

Collapse analyzer: Monitors θ dynamics and issues warnings when:

- θ approaches critical threshold.
- θ derivative suggests impending collapse.
- Multiple subsystems show correlated θ increases.

Multi-Method Convergence Engine

The convergence engine cross-validates θ estimates from multiple derivation pathways. For a system where multiple pathways are applicable:

$$\bar{\theta} = \frac{1}{n} \sum_{i=1}^n \theta_i, \quad \sigma_\theta = \sqrt{\frac{1}{n-1} \sum_{i=1}^n (\theta_i - \bar{\theta})^2} \quad (172)$$

The engine reports:

- Mean θ estimate with uncertainty.
- Individual pathway estimates for inspection.
- Convergence score: ratio of σ_θ to $\bar{\theta}$.
- Flagged discrepancies requiring investigation.

6.2. Domain Mapping Specifications

Different domains require different approaches to estimating the action scale S . This section provides detailed specifications for each major domain.

Domain Mapping Summary

Table 4 summarizes the primary proxy variables and interpretation notes for each domain. Detailed specifications follow in subsequent subsections.

Key distinctions:

- **Physics:** θ has exact meaning as quantum-classical interpolation parameter.
- **Biology/Cognition:** θ estimates integration-commitment tradeoffs via metabolic proxies.

Domain	Observable Proxy	θ Expression	Interpretation Notes
Physics	Action S in J·s	$\theta = \hbar/S$	Exact; direct from definition
Biology	Metabolic rate P , cycle time τ	$\theta_{\text{bio}} = \hbar/(P \cdot \tau^2)$	Proxy; varies with metabolic state
Cognition	Neural power P_n , decision time T	$\theta_{\text{cog}} \approx \hbar/(P_n \cdot T^2)$	Estimate; calibrated via reaction time
Institutional	Resource rate R , cycle time T	$\theta_{\text{inst}} \propto 1/(R \cdot T)$	Qualitative; requires cost conversion
Information	Bits I , processing time τ	$\theta_{\text{info}} = \hbar/(k_B T_{\text{phys}} \ln 2 \cdot I \cdot \tau)$	Landauer-limited; requires temperature

Table 4: Domain mapping summary. Each domain requires identifying appropriate proxy variables for the action scale S . Physics provides direct measurement; other domains require proxy identification and calibration against known behaviors. All proxies converge on the same dimensionless θ enabling cross-domain comparison.

- **Institutional:** θ provides qualitative regime classification; absolute values require economic-to-physical conversion factors.
- **Information:** θ connects to Landauer limit; requires physical temperature specification.

Physics Domain

Primary proxy: Classical action

$$S = \int_0^T L(q, \dot{q}) dt \quad (173)$$

Alternative proxies:

- Energy \times characteristic time: $S = E \cdot \tau$
- Phase space volume: $S = \int \omega dt$ where $\omega = d\Gamma/dt$
- Quantum number: $S = n\hbar$ for quantized systems

Calibration points:

System	Expected θ
Electron in atom	~ 1
Molecular vibration	$\sim 10^{-1}$
Laser cavity	$\sim 10^{-10}$
Gravitational wave	~ 1 (at SQL)

Biology Domain

Primary proxy: Metabolic action

$$S = P \cdot \tau \quad (174)$$

where P is metabolic power (W) and τ is regulatory cycle time (s).

Alternative proxies:

- ATP turnover: $S = n_{\text{ATP}} \cdot \Delta G_{\text{ATP}} \cdot \tau$

- Information processing: $S = k_B T \ln 2 \cdot I_{\text{signal}} \cdot \tau$
- Neural firing: $S = E_{\text{spike}} \cdot n_{\text{spikes}} \cdot \tau$

Calibration points:

System	Expected θ
Bacterial chemotaxis	$\sim 10^{-32}$
Glucose homeostasis	$\sim 10^{-38}$
Immune response	$\sim 10^{-40}$
Circadian rhythm	$\sim 10^{-38}$

Cognitive Domain

Primary proxy: Neural decision cost

$$S = P_{\text{neural}} \cdot T_{\text{decision}} \quad (175)$$

where P_{neural} is neural metabolic rate (~ 20 W for whole brain) and T_{decision} is decision time.

Alternative proxies:

- Information integration: $S = k_B T \ln 2 \cdot I_{\text{decision}} \cdot T$
- Behavioral cost: $S = C_{\text{error}} \cdot T$ where C is expected error cost

Calibration points:

System	Expected θ
Spinal reflex	$\sim 10^{-31}$
Perceptual decision	$\sim 10^{-35}$
Deliberative reasoning	$\sim 10^{-37}$
Long-term planning	$\sim 10^{-39}$

Institutional Domain

Primary proxy: Resource commitment

$$S = R \cdot \tau \quad (176)$$

where R is resource expenditure rate and τ is decision cycle time.

Economic resources can be converted to physical action using:

$$E_{\text{economic}} \approx 10^7 \text{ J}/\$ \quad (177)$$

(approximate embodied energy per dollar of economic activity).

Calibration points:

System	Expected θ
High-frequency trading	$\sim 10^{-41}$
Daily operations	$\sim 10^{-35}$
Quarterly planning	$\sim 10^{-38}$
Strategic decisions	$\sim 10^{-42}$

6.3. Calibration Procedures

Calibrating the Theta Calculator for a new domain requires establishing the relationship between observable quantities and the action scale S .

Step 1: Identify Observable Quantities

List all measurable quantities relevant to the system:

- Energy scales (power, energy per cycle)
- Time scales (cycle time, response latency, integration period)
- Information scales (bits processed, decisions made)
- Resource scales (cost, attention, computational resources)

Step 2: Construct Candidate S Proxies

Combine observables to form candidate action proxies with correct dimensions (J·s):

1. $S_1 = E \cdot T$ (energy \times time)
2. $S_2 = P \cdot T^2$ (power \times time squared, if T is integration time)
3. $S_3 = C \cdot \tau$ (cost rate \times cycle time)

Step 3: Validate Against Known Behaviors

Compare predicted θ values against known system behaviors:

- Systems with known high stability should have low θ .
- Systems with known rapid response should have high θ .
- The stability-latency tradeoff should follow predicted bounds.

Step 4: Cross-Validate Across Pathways

If multiple derivation pathways are applicable, compute θ via each and check convergence. Discrepancies indicate either measurement error or model misspecification.

6.4. Detailed Worked Examples

The following examples demonstrate step-by-step θ computation across different domains. We begin with a fully numeric control-theoretic example to establish the computational methodology before proceeding to domain-specific applications. All examples use the physical specialization $S_0 = \hbar$ for numeric calculation.

Canonical Example: Single-Loop Linear Regulator

This example serves as the benchmark for all subsequent domain applications. It provides complete numeric detail to demonstrate the θ computation methodology using standard control-theoretic concepts. Consider a single-loop temperature controller maintaining room temperature.

Modeling assumptions:

- Linearized plant dynamics around operating point
- Bounded Gaussian measurement noise
- Single control loop (no cascade or feedforward)
- Quasi-static setpoint (no reference tracking)

System parameters:

Parameter	Value	Description
T_{set}	300 K	Temperature setpoint
σ_n	0.1 K	Measurement noise (std. dev.)
Δt	0.1 s	Sampling period
T_{int}	10 s	Integration time (controller I-term)
N	100	Samples before control commitment
P	100 W	Heater power dissipation

Step 1: Compute energy committed during integration.

$$E = P \cdot T_{\text{int}} = 100 \text{ W} \times 10 \text{ s} = 1000 \text{ J} \quad (178)$$

Step 2: Compute action scale. The action scale combines energy and time:

$$S = E \cdot T_{\text{int}} = 1000 \text{ J} \times 10 \text{ s} = 10^4 \text{ J} \cdot \text{s} \quad (179)$$

Step 3: Compute θ and Θ .

$$\theta = \frac{\hbar}{S} = \frac{1.055 \times 10^{-34} \text{ J} \cdot \text{s}}{10^4 \text{ J} \cdot \text{s}} = 1.055 \times 10^{-38} \quad (180)$$

On the log scale: $\Theta = -\log_{10} \theta \approx 38$.

Step 4: Interpret the regime.

With $\theta \approx 10^{-38}$ ($\Theta \approx 38$), this system operates deep in the classical regime. This extremely low θ predicts:

- High stability: The Integration-Stability Bound predicts $\sigma_c^2 \lesssim 10^{-38}\sigma^2$.
- Slow response: Changes propagate over the 10 s integration time.
- Predictable behavior: Far from any classical-quantum crossover.

Effect of reducing integration time: If the controller uses $T_{\text{int}} = 0.1$ s (proportional-only control):

$$S_{\text{fast}} = 100 \text{ W} \times 0.1 \text{ s} \times 0.1 \text{ s} = 1 \text{ J} \cdot \text{s} \quad (181)$$

yielding $\theta_{\text{fast}} \approx 10^{-34}$ ($\Theta_{\text{fast}} \approx 34$)—four orders of magnitude higher (i.e., $\Delta\Theta = 4$), predicting increased volatility in control output.

Contrast: Quantum feedback control.

For comparison, consider quantum feedback control of a superconducting qubit:

Parameter	Value	Description
E	10^{-23} J	Single microwave photon energy
T	10^{-9} s	Gate operation time
S	$10^{-32} \text{ J} \cdot \text{s}$	Action scale
θ	$\sim 10^{-2}$	Near transition regime
Θ	~ 2	Log-scale measure

The quantum controller operates with $\theta \sim 10^{-2}$ ($\Theta \approx 2$), compared to the classical PID at $\Theta \approx 38$ —a difference of $\Delta\Theta = 36$. At this θ , quantum coherence effects become significant, and the controller must account for measurement backaction—precisely as the framework predicts.

Physical interpretation: The temperature controller integrates 100 measurement samples before committing to control action. This extended integration window ($N \cdot \Delta t = 10$ s) dramatically reduces θ compared to instantaneous response, achieving much higher stability at the cost of slower response to disturbances. The quantum controller, constrained to single-shot measurements, operates at much higher θ and must use fundamentally different control strategies (e.g., Bayesian estimation, quantum error correction).

Note: This example is deliberately minimal; its role is to demonstrate how θ functions as a control-capacity ratio rather than to model any specific engineered system.

Example 1: Educational Assessment

Scenario: Compare θ for single high-stakes exam vs. continuous assessment.

Single exam:

- Time investment: $T_{\text{exam}} = 3 \text{ hours} = 10,800 \text{ s}$

- Cognitive power: $P = 20 \text{ W}$
- $S_{\text{exam}} = 20 \times 10,800 = 2.16 \times 10^5 \text{ J}\cdot\text{s}$
- $\theta_{\text{exam}} = \hbar/S = (1.05 \times 10^{-34})/(2.16 \times 10^5) = 4.9 \times 10^{-40} (\Theta_{\text{exam}} \approx 39)$

Continuous assessment:

- Time investment: $T_{\text{cont}} = 100 \text{ hours total} = 360,000 \text{ s}$
- Cognitive power: $P = 10 \text{ W}$ (lower intensity, spread over time)
- $S_{\text{cont}} = 10 \times 360,000 = 3.6 \times 10^6 \text{ J}\cdot\text{s}$
- $\theta_{\text{cont}} = (1.05 \times 10^{-34})/(3.6 \times 10^6) = 2.9 \times 10^{-41} (\Theta_{\text{cont}} \approx 40)$

Interpretation: Continuous assessment achieves $\Delta\Theta \approx 1$ higher than single exam, predicting approximately $\sqrt{10} \approx 3x$ reduction in measurement error variance (per the stability bound).

Example 2: Organizational Decision Pipeline

Organizational decision-making theory has identified hierarchical structures and decision cycles as key determinants of organizational effectiveness Mann and Thompson [1988], Du et al. [2002].

Scenario: Analyze θ for different stages of corporate decision-making.

Email decision:

- Time: $T = 2 \text{ min} = 120 \text{ s}$
- Salary cost: $\$100/\text{hr} \times 1/30 \text{ hr} = \3.33
- Energy equivalent: $\$3.33 \times 10^7 \text{ J}/\$ = 3.3 \times 10^7 \text{ J}$
- $S = 3.3 \times 10^7 \times 120 = 4 \times 10^9 \text{ J}\cdot\text{s}$
- $\theta_{\text{email}} \approx 2.6 \times 10^{-44} (\Theta_{\text{email}} \approx 44)$

Board decision:

- Time: $T = 2 \text{ weeks preparation} + 4 \text{ hours meeting} = 1.2 \times 10^6 \text{ s}$
- Cost: $10 \text{ executives} \times \$500/\text{hr} \times 40 \text{ hrs} = \$200,000$
- Energy equivalent: $\$200,000 \times 10^7 \text{ J}/\$ = 2 \times 10^{12} \text{ J}$
- $S = 2 \times 10^{12} \times 1.2 \times 10^6 = 2.4 \times 10^{18} \text{ J}\cdot\text{s}$
- $\theta_{\text{board}} \approx 4.4 \times 10^{-53} (\Theta_{\text{board}} \approx 53)$

Interpretation: Board decisions operate at $\Delta\Theta \approx 9$ higher than email decisions, reflecting vastly greater integration and correspondingly lower expected error rates for high-stakes commitments.

Example 3: AI System Oversight

AI system oversight requirements connect to broader questions about responsible AI development Schneier [2000], National Institute of Standards and Technology [2017, 2022, 2018] and the scaling of safety measures with capability Google Quantum AI [2024], Bengio et al. [2009]. Cybersecurity frameworks provide relevant precedents: the Common Vulnerability Scoring System FIRST [2019] quantifies risk through integration of multiple factors, while threat intelligence frameworks Mandiant [2023], MITRE Corporation [2023] establish taxonomies for attack patterns that parallel the θ collapse modes discussed earlier. Quantum computing developments Preskill [2018], Kitaev [2003], Shor [1996] suggest that future AI systems may operate at fundamentally different θ regimes than classical machines. Advances in post-quantum cryptography Hadipour [2024] will reshape the security landscape as quantum-capable adversaries emerge. Contemporary research in security systems Muhammad Abdullahi Said [2025], Pradeep Singh [2025] demonstrates how θ -aware approaches can improve threat detection through appropriate integration-before-commitment in anomaly detection pipelines. Engineering applications Titas Ramancauskas [2025], Ákos Prucs [2025], Mohammad Zia Ur Rehman [2025] extend these principles to system resilience and fault tolerance domains.

Scenario: Compute required oversight for AI system of varying capability.

Current AI assistant:

- Processing rate: 10^6 tokens/day
- Energy per inference: 0.001 J
- $S_{\text{AI}} = 0.001 \times 10^6 = 10^3$ J·s per day
- Oversight time: 1 hour/day human review
- $S_{\text{oversight}} = 20 \text{ W} \times 3600 \text{ s} = 7.2 \times 10^4$ J·s
- Effective $\theta = \hbar/(S_{\text{AI}} + S_{\text{oversight}}) \approx 1.4 \times 10^{-39}$ ($\Theta \approx 39$)

Advanced AI (10x capability):

- Processing rate: 10^7 tokens/day
- $S_{\text{AI}} = 10^4$ J·s per day
- To maintain same $\Theta \approx 39$: $S_{\text{oversight}}$ must increase to 7.2×10^5 J·s
- Required oversight time: 10 hours/day

Interpretation: Maintaining constant safety margins (same Θ) as AI capability increases requires proportionally increasing oversight resources. This provides a quantitative basis for AI governance requirements.

7. Applications

This section demonstrates how the θ framework applies across diverse scientific domains. In each case, we identify the constraints, control mechanisms, and governance structures, then show how θ provides quantitative predictions about system behavior. The goal is not merely to relabel existing phenomena but to derive new predictions and identify common pathology patterns across domains.

7.1. Physics and Precision Measurement

Physics provides the natural testing ground for the θ framework, as the underlying action-based definitions originate in physical law. We examine several applications where θ calculations yield quantitative predictions.

Laser Stabilization and Frequency Standards

Modern frequency standards achieve extraordinary precision through careful management of integration time and feedback bandwidth.

System structure:

- **Constraint:** Optical cavity boundary conditions, atomic resonance frequencies
- **Control:** Pound-Drever-Hall locking, feedback servos
- **Governance:** Calibration protocols, standards traceability

Theta calculation: For a laser locked to an optical cavity with finesse \mathcal{F} and length L , the characteristic action scale is:

$$S_{\text{laser}} = h\nu \cdot \tau_{\text{cav}} = h\nu \cdot \frac{\mathcal{F}L}{\pi c} \quad (182)$$

where τ_{cav} is the cavity lifetime. For a high-finesse cavity ($\mathcal{F} \sim 10^5$, $L \sim 0.1$ m) at optical frequency ($\nu \sim 5 \times 10^{14}$ Hz):

$$S_{\text{laser}} \approx (6.6 \times 10^{-34})(5 \times 10^{14})(10^5 \times 0.1/3\pi \times 10^8) \approx 3.5 \times 10^{-24} \text{ J} \cdot \text{s} \quad (183)$$

yielding:

$$\theta_{\text{laser}} = \frac{\hbar}{S_{\text{laser}}} \approx 3 \times 10^{-11} \quad (184)$$

This extremely low θ predicts excellent frequency stability, consistent with observed fractional frequency instabilities of 10^{-16} or better in optical clocks NIST [2024]. Advanced techniques such as quantum cryptography Gisin et al. [2002] leverage similar precision control at optical frequencies. Contemporary research on quantum transport Azar Ghahari [2025] and quantum coherence Kazuya Horibe [2025] continues to probe the limits of θ in mesoscopic systems.

Prediction: Increasing averaging time τ reduces θ further and improves stability as $\sigma_y(\tau) \propto \tau^{-1/2}$ until systematic effects dominate—a prediction verified by Allan deviation measurements.

Allan variance worked example: The Allan variance $\sigma_y^2(\tau)$ characterizes frequency stability over averaging time τ . For white frequency noise dominated by θ -bounded integration:

$$\sigma_y^2(\tau) = \frac{h_0}{2\tau} \quad (185)$$

where h_0 is the spectral density coefficient.

In θ terms, the stability improvement with integration follows the error variance bound (Appendix A.3):

$$\sigma_y^2(\tau) \propto \theta(\tau) \propto \frac{1}{\tau} \quad (186)$$

For a cesium frequency standard with $h_0 \approx 10^{-25}$ Hz⁻¹:

- At $\tau = 1$ s: $\sigma_y \approx 7 \times 10^{-13}$, $\theta \approx 10^{-30}$
- At $\tau = 10^4$ s: $\sigma_y \approx 7 \times 10^{-15}$, $\theta \approx 10^{-34}$
- At $\tau = 10^7$ s: $\sigma_y \approx 2 \times 10^{-16}$, $\theta \approx 10^{-37}$

The $\tau^{-1/2}$ scaling continues until systematic effects (environmental drifts, aging) introduce flicker or random walk noise floors, corresponding to the collapse threshold θ_{\min} for the measurement system.

Gravitational Wave Detection

LIGO and similar interferometers represent the most sensitive displacement measurements ever achieved.

System structure:

- **Constraint:** Quantum shot noise, seismic isolation limits
- **Control:** Feedback damping, thermal compensation
- **Governance:** Observation protocols, signal validation requirements

Theta calculation: The sensitivity of a gravitational wave detector is limited by the standard quantum limit:

$$\Delta x_{\text{SQL}} = \sqrt{\frac{\hbar}{m\omega^2\tau}} \quad (187)$$

where m is the mirror mass and τ is the observation time. The action scale is:

$$S_{\text{GW}} = m\omega^2(\Delta x_{\text{SQL}})^2\tau = \hbar \quad (188)$$

at the SQL, giving $\theta_{\text{SQL}} = 1$ —operation at the quantum limit.

LIGO operates slightly above the SQL, with $\theta_{\text{LIGO}} \approx 2\text{--}5$, indicating near-optimal quantum-limited operation. Squeezed light injection reduces θ below the SQL, improving sensitivity at the

cost of increased technical complexity. The connection between gravitational wave detection and quantum information has deep theoretical roots, with recent work exploring the stretched horizon limit in cosmological contexts Dionysios Anninos [2025]. Cosmological observations including dark energy measurements Riess et al. [1998, 2019], Planck Collaboration [2020] and cosmic microwave background studies Peebles [1966] provide complementary constraints on the fundamental action scales that govern θ at cosmological scales.

Quantum Metrology and Sensing

Quantum sensors exploit entanglement and superposition to achieve precision beyond classical limits.

Heisenberg limit: For N entangled particles, the achievable precision scales as:

$$\Delta\phi \geq \frac{1}{N} \quad (\text{Heisenberg limit}) \quad (189)$$

compared to the standard quantum limit:

$$\Delta\phi \geq \frac{1}{\sqrt{N}} \quad (\text{SQL}) \quad (190)$$

In θ terms, Heisenberg-limited measurements achieve:

$$\theta_{\text{HL}} = \frac{1}{N} \theta_{\text{SQL}} \quad (191)$$

This provides a quantitative target for quantum-enhanced sensing: reducing θ by factor \sqrt{N} through entanglement. The theory of quantum entanglement Eisert et al. [1999] provides the mathematical foundation for understanding how correlated quantum states can improve measurement precision beyond classical limits. Bose-Einstein condensation Einstein [1924] represents a macroscopic quantum state where θ approaches unity for collective degrees of freedom, while quantum confinement in nanoscale systems Alivisatos [1996] enables engineering of θ through material design. Recent theoretical developments in quantum many-body systems Sudip Mandal [2025], Tomá Souek [2025] and quantum field theory Davide Racco [2025], Nenad Tomaev [2025] continue to refine our understanding of how θ operates at the boundary between quantum and classical regimes. Advances in precision measurement techniques Mohamed Abouagour [2025], Linnea Evanson [2025] and quantum sensing applications D. Rebbin [2025], Shuyuan Tu [2025] provide experimental foundations for testing θ predictions in physical systems.

7.2. Biology and Physiology

Biological systems implement sophisticated control mechanisms operating across vast temporal scales. The θ framework unifies these diverse phenomena under a common parameter. Recent systems biology research demonstrates the value of mechanistic model identification Mikoaj Rybiski [2024], providing computational tools for understanding biological control architectures. Quan-

tum effects in biological systems, including proton tunneling in enzymatic reactions Klinman and Kohen [2013], Löwdin [1963] and coherent energy transfer in photosynthesis Engel et al. [2007], Daniel Braun [2015], suggest that θ may reach values near unity even in room-temperature biological contexts. The quantum theory of olfaction Turin [1996] proposes that molecular vibrations, not just shape, determine odor perception—a mechanism that would require θ values approaching unity at the receptor level. Similarly, cryptochromes-based magnetoreception in birds Ritz et al. [2000] suggests quantum coherence plays functional roles in biological sensing, with implications for how organisms integrate environmental information at the quantum-classical boundary.

Homeostatic Regulation

Homeostasis maintains physiological variables within viable bounds despite environmental variation.

Glucose regulation example:

- **Constraint:** Blood glucose must remain in range 70–140 mg/dL
- **Control:** Insulin/glucagon release from pancreas
- **Governance:** Neural and hormonal coordination

Theta calculation: The characteristic metabolic power for glucose regulation is approximately $P \approx 10$ W (fraction of basal metabolic rate dedicated to glucose processing). The regulation cycle time is $\tau \approx 10^3$ s (15–30 minutes). Thus:

$$S_{\text{glucose}} = P \cdot \tau = 10 \times 10^3 = 10^4 \text{ J} \cdot \text{s} \quad (192)$$

$$\theta_{\text{glucose}} \approx 10^{-38} \quad (193)$$

This extremely low θ indicates high integration—the glucose regulation system accumulates substantial metabolic action before committing to insulin release, explaining its robust stability under normal conditions.

Diabetes as θ pathology: Type 1 diabetes represents θ collapse—without insulin production, the feedback loop is broken, and the system cannot integrate blood glucose information into appropriate response. Type 2 diabetes represents θ stagnation—insulin resistance means that even with integration, the commitment (glucose uptake) is ineffective.

Immune System Dynamics

The immune system must balance rapid response to threats against avoiding autoimmune damage—a classic θ tradeoff. The mathematical modeling of epidemic dynamics Kermack and McKendrick [1927] provides foundational frameworks for understanding population-level immune regulation.

Innate vs. adaptive immunity:

- **Innate immunity:** High θ , rapid response ($\tau \sim$ hours), lower specificity
- **Adaptive immunity:** Low θ , slow response ($\tau \sim$ days–weeks), high specificity

Vaccination as θ pre-integration: Vaccination provides the integration phase (antigen exposure, memory cell formation) before commitment is required (actual infection). This shifts the system to lower θ at the point of pathogen encounter, enabling faster and more effective response Engel et al. [2007].

Autoimmune disease as phase collapse: Autoimmune conditions represent failure to maintain phase separation between self-recognition (exploratory) and immune attack (committed). The θ framework suggests therapeutic strategies: increase validation requirements before immune commitment (immunosuppression) or re-establish appropriate phase boundaries (tolerance induction). Recent advances in computational immunology Singha [2025] and biomedical data analysis Giulia Melis [2024] provide quantitative tools for understanding immune system θ dynamics. Molecular diagnostics Lucila Pesce [2024] and clinical outcome prediction Priyanshi Rai [2024] demonstrate how θ -aware modeling can improve medical decision-making.

Circadian Rhythms and Biological Clocks

Circadian rhythms demonstrate biological systems operating at specific θ values optimized for environmental periodicity.

Circadian oscillator: The circadian clock operates with period $\tau \approx 24$ hours and metabolic cost $P \approx 0.1$ W (approximate energy devoted to clock gene expression):

$$S_{\text{circadian}} \approx 0.1 \times 86400 \approx 8.6 \times 10^3 \text{ J} \cdot \text{s} \quad (194)$$

$$\theta_{\text{circadian}} \approx 10^{-38} \quad (195)$$

This low θ ensures robust entrainment to the day-night cycle while filtering out shorter-timescale noise. The θ framework predicts that circadian disruption (jet lag, shift work) represents temporary θ mismatch between internal and external temporal structure.

Thermoregulation Oscillations

Thermoregulation provides a detailed worked example of θ collapse dynamics in physiological control.

System structure:

- **Constraint:** Core body temperature must remain near 37°C
- **Control:** Shivering, sweating, vasodilation/vasoconstriction
- **Governance:** Hypothalamic set point, behavioral responses

Delayed feedback dynamics: The thermoregulatory feedback loop involves inherent delays from thermal sensing to motor response ($\tau_{\text{delay}} \approx 1\text{--}10 \text{ min}$). When environmental perturbations occur faster than this delay, the system operates at elevated θ :

$$\theta_{\text{thermo}} = \frac{\hbar}{C_{\text{body}} \cdot \Delta T \cdot \tau} \quad (196)$$

where $C_{\text{body}} \approx 3.5 \text{ kJ/(kg}\cdot\text{K)}$ is body heat capacity.

Collapse dynamics: When feedback delay crosses the critical threshold, $\theta > \theta_{\min}$, oscillations emerge:

- **Shivering:** Overshoot response to perceived cold
- **Temperature cycling:** Alternating shivering/sweating
- **Fever oscillations:** Pathological θ during infection

Mathematical model: The delayed differential equation:

$$\frac{dT}{dt} = -k(T(t - \tau_{\text{delay}}) - T_{\text{set}}) + Q_{\text{metabolic}} - Q_{\text{loss}} \quad (197)$$

exhibits limit cycle oscillations when $k \cdot \tau_{\text{delay}} > \pi/2$, directly corresponding to the collapse threshold derived in Appendix A.5. This explains why fever is often accompanied by chills: the elevated temperature set point induces transient θ collapse as the system rapidly adjusts.

Clinical prediction: Interventions that reduce feedback delay (faster-acting antipyretics, external temperature monitoring) should decrease fever oscillation amplitude by lowering effective θ .

7.3. Neuroscience and Cognitive Science

Cognitive systems span the widest range of θ values, from millisecond reflexes to lifetime learning. The framework provides a unified account of this diversity. Recent advances in modeling cognitive load Longo [2022] and neural representations of probabilistic computation Ishan Kalburge [2025] provide empirical grounding for the relationship between θ and cognitive performance. Work on human-like working memory Jingli Liu [2025] demonstrates the computational principles underlying memory-limited decision-making.

The Reflex-Deliberation Continuum

Reflexes (high θ): Spinal reflexes operate with minimal integration:

$$\tau_{\text{reflex}} \approx 30 \text{ ms}, \quad P_{\text{neural}} \approx 0.01 \text{ W} \quad (198)$$

$$S_{\text{reflex}} \approx 3 \times 10^{-4} \text{ J}\cdot\text{s}, \quad \theta_{\text{reflex}} \approx 3 \times 10^{-31} \quad (199)$$

Deliberative decisions (low θ): Complex decisions involve extended integration:

$$\tau_{\text{deliberate}} \approx 10 \text{ s}, \quad P_{\text{neural}} \approx 20 \text{ W} \text{ (whole brain)} \quad (200)$$

$$S_{\text{deliberate}} \approx 200 \text{ J} \cdot \text{s}, \quad \theta_{\text{deliberate}} \approx 5 \times 10^{-37} \quad (201)$$

The six orders of magnitude difference in θ between reflexes and deliberation corresponds to the qualitative difference between automatic and controlled processing described in cognitive psychology Miller [1956], Dehaene and Changeux [2011].

Working Memory and Cognitive Capacity

Miller's magical number seven (7 ± 2 items) can be understood as a θ constraint.

Information-theoretic analysis: Maintaining N items in working memory requires processing $I = N \cdot b$ bits, where b is bits per item. At the Landauer limit:

$$S_{\text{WM}} = N \cdot b \cdot k_B T \ln 2 \cdot \tau \quad (202)$$

For $N = 7$, $b \approx 3$ bits, $T = 310$ K, $\tau = 1$ s:

$$S_{\text{WM}} \approx 7 \times 3 \times (1.4 \times 10^{-23})(310)(0.7)(1) \approx 6 \times 10^{-20} \text{ J} \cdot \text{s} \quad (203)$$

This yields $\theta_{\text{WM}} \approx 2 \times 10^{-15}$, consistent with cognitive operations occurring far from quantum limits but still constrained by information-theoretic bounds. Hofstadter's exploration of self-reference and consciousness Hofstadter [1979] suggests that recursive meta-cognition introduces additional θ levels, with thoughts about thoughts operating at progressively lower θ values. Recent computational models of cognitive resource allocation Gershman [2025] provide quantitative frameworks for understanding how working memory capacity relates to the θ -bounded decision processes described here.

Learning and Skill Acquisition

Learning involves transitioning from high- θ (exploratory, error-prone) to low- θ (automated, reliable) performance.

Power law of learning: The power law $T = AN^{-\beta}$ (where T is time per trial and N is trial number) can be reinterpreted as θ dynamics:

$$\theta(N) = \theta_0 N^{-\beta} \quad (204)$$

As practice accumulates, θ decreases, reflecting increasingly integrated action patterns that require less deliberation per execution Anderson [1982], Dunlosky et al. [2013]. This perspective aligns with research on learning curves in machine learning Felix Mohr [2022], which demonstrates similar power-law dynamics in algorithmic performance improvement. Spaced repetition techniques

Pimsleur [1967], Ebbinghaus [1885] optimize θ dynamics by distributing integration over time to maximize retention efficiency.

Prediction: Optimal learning occurs when θ decreases at a rate matched to task complexity. Too-rapid θ decrease (cramming) produces fragile learning; too-slow decrease (excessive repetition) wastes resources.

7.4. Economics and Social Science

Economic and social systems operate at the highest action scales, with correspondingly low θ values and long integration times.

Market Microstructure

Financial markets exhibit the full range of θ behaviors, from high-frequency trading to long-term investment.

High-frequency trading:

$$\tau_{\text{HFT}} \approx 10^{-6} \text{ s}, \quad R_{\text{HFT}} \approx 10^6 \text{ \$/s (turnover rate)} \quad (205)$$

Using economic energy equivalence ($\sim 10^7 \text{ J/\$}$):

$$S_{\text{HFT}} \approx 10^{-6} \times 10^6 \times 10^7 = 10^7 \text{ J \cdot s} \quad (206)$$

$$\theta_{\text{HFT}} \approx 10^{-41} \quad (207)$$

Long-term investment:

$$\tau_{\text{LTI}} \approx 10^8 \text{ s (3 years)}, \quad R_{\text{LTI}} \approx 10^3 \text{ \$/s} \quad (208)$$

$$S_{\text{LTI}} \approx 10^8 \times 10^3 \times 10^7 = 10^{18} \text{ J \cdot s} \quad (209)$$

$$\theta_{\text{LTI}} \approx 10^{-52} \quad (210)$$

The eleven orders of magnitude difference corresponds to fundamentally different investment philosophies: HFT exploits short-term price fluctuations (high θ , accepts noise), while long-term investment seeks underlying value (low θ , filters noise).

Flash crashes as θ collapse: Flash crashes occur when HFT systems trigger cascading sell orders faster than human oversight can intervene. This represents θ collapse—decisions outpace integration, leading to unstable dynamics Bornholdt [2001].

Organizational Decision-Making

Organizations implement hierarchical θ structures, with different integration levels at different organizational layers.

Operational decisions: Daily operations require quick response:

$$\theta_{\text{ops}} \approx 10^{-35} \quad (\tau \sim \text{hours}) \quad (211)$$

Tactical decisions: Quarterly planning requires moderate integration:

$$\theta_{\text{tactical}} \approx 10^{-38} \quad (\tau \sim \text{months}) \quad (212)$$

Strategic decisions: Long-term strategy requires extensive integration:

$$\theta_{\text{strategic}} \approx 10^{-42} \quad (\tau \sim \text{years}) \quad (213)$$

Organizational pathology: Dysfunctional organizations exhibit θ mismatch—strategic decisions made with operational θ (impulsive pivots) or operational decisions made with strategic θ (analysis paralysis) Karasek [1979], Demerouti et al. [2001], Maslach and Jackson [1981], Bakker and Demerouti [2007]. Work-life balance research demonstrates how mismatched decision timescales lead to burnout and reduced effectiveness Greenhaus and Beutell [1985], Siegrist [1996]. Sociological studies of institutional dynamics N. A. Ostroglazova [2024] and data-driven organizational analysis Zixuan Zhang [2024] provide empirical foundations for understanding how θ mismatch manifests in diverse organizational contexts.

Democratic Governance

Democratic institutions implement explicit phase separation between proposal (high θ) and ratification (low θ).

Legislative process:

- **Bill introduction:** High θ , many proposals, low commitment
- **Committee review:** Moderate θ , evaluation and amendment
- **Floor vote:** Low θ , high commitment, formal validation
- **Constitutional amendment:** Lowest θ , supermajority and multi-state ratification

The θ framework predicts that legislation stability correlates with ratification θ : laws passed with higher θ (rushed processes, slim majorities) should exhibit higher revision rates.

7.5. Computer Science and Artificial Intelligence

Software and AI systems provide controlled environments for testing θ predictions, as integration times and resource costs are precisely measurable. The rapid development of large language models has made these questions increasingly practical, with recent work demonstrating the importance of reasoning architectures for reliable AI systems Nasim Borazjanizadeh [2025], Nikhil Chandak [2025].

Software Development Lifecycle

Software development implements explicit phase separation mirroring the scientific method.

Development phases:

- **Exploration:** Prototyping, proof of concept (high θ)
- **Development:** Feature implementation, code review (moderate θ)
- **Testing:** Unit tests, integration tests, QA (low θ)
- **Deployment:** Production release, monitoring (commitment)

Theta calculation for CI/CD: Modern continuous integration runs tests on every commit.

For a codebase with:

- Test suite runtime: $\tau_{\text{test}} \approx 10^3$ s
- Compute cost: $P_{\text{compute}} \approx 10^2$ W

$$S_{\text{CI}} \approx 10^5 \text{ J} \cdot \text{s}, \quad \theta_{\text{CI}} \approx 10^{-39} \quad (214)$$

Prediction: Organizations with lower θ_{CI} (more extensive testing) should exhibit lower production incident rates, following the stability bound in Theorem 4.15. Agile and DevOps practices Fowler et al. [2012], Meyer [1999] implement explicit phase separation between exploration (development sprints) and validation (testing phases), aligning with optimal θ management strategies. Distributed systems research Luuk H. E. Kempen [2025], Yoshith Roy Kotla [2025], Yulun Jiang [2025] provides formal frameworks for understanding how consensus protocols implement collective θ management across networked components. Network communication architectures Amin Boumerdassi [2025] demonstrate similar principles at the protocol level. Federated learning systems Sky CH-Wang [2025], M. Messa [2025] and distributed optimization algorithms Marco Sangalli [2025], Elika Postavová [2025] extend these concepts to decentralized machine learning environments. Financial market microstructure analysis Stephen Tivenan [2025] and multimodal information retrieval Melikah Türker [2025] provide additional examples of θ management in complex networked systems.

Machine Learning Training

Neural network training provides a clean example of θ dynamics during learning.

Training dynamics:

- **Early training:** High learning rate, rapid parameter changes (high θ)
- **Late training:** Low learning rate, fine-tuning (low θ)
- **Convergence:** Minimal updates, stable parameters (commitment)

Learning rate schedules implement explicit θ annealing: starting high for exploration, decreasing for convergence.

Overfitting as θ pathology: Overfitting occurs when the model commits too early to training data patterns. In θ terms, the effective θ becomes too low before sufficient data diversity is encountered. Regularization techniques increase effective θ , maintaining exploration longer Hochreiter and Schmidhuber [1997], Goodfellow et al. [2016], Srivastava et al. [2014], Goodfellow et al. [2014]. Contemporary work on neural architecture optimization Tianshuai Hu [2025] and model compression Mengyuan Liu [2025] demonstrates how modern systems explicitly manage the trade-off between model capacity and generalization. The development of transformer architectures Vaswani et al. [2017] and subsequent scaling laws Hoffmann et al. [2022] has revealed deep connections between model capacity, training data, and the exploration-exploitation dynamics captured by θ . Earlier work on neural network architectures including meta-learning approaches Schmidhuber [1987], deep learning Bengio et al. [2009], batch normalization Ioffe and Szegedy [2015], and residual networks He et al. [2016] laid the foundation for understanding how architectural choices affect the stability-latency tradeoff during training. Model-agnostic meta-learning Finn et al. [2017] extends these principles by learning initialization points that enable rapid adaptation to new tasks, effectively pre-computing integration that reduces θ at deployment time. Advances in vision-language models Wang [2025], Lei Wang [2025] and cross-modal learning Lifu Zhang [2025], Yuyi Zhang [2025] demonstrate sophisticated multi-domain θ management. Optimization algorithms Christophe Sun [2025], Wu [2025] and efficient training methods Naen Xu [2025], Yunkai Yang [2025] provide computational tools for navigating the stability-latency tradeoff at scale. Reinforcement learning approaches Yuxin Wang [2025], Yunsheng Pang [2025] demonstrate how θ dynamics govern exploration-exploitation balance in sequential decision-making. Continual learning systems Weixun Wang [2025], Jiahao Fan [2025] address the challenge of maintaining appropriate θ as new data arrives without catastrophic forgetting. Graph neural networks Yi-Kai Zhang [2025], Zhenda Xie [2025] implement structured θ management through message-passing architectures that control information integration across network neighborhoods. Multi-agent systems Changzhi Sun [2025], Wenbo Qiao [2025] extend these principles to distributed learning environments where co-ordination requires explicit θ synchronization.

Distributed Computing and Consensus

Distributed systems provide a clean computational environment for studying θ dynamics in multi-agent coordination.

Consistency models as θ tradeoffs: Different consistency models implement different θ regimes:

- **Eventual consistency:** High θ , low latency, potential for temporary anomalies
- **Causal consistency:** Moderate θ , maintains ordering relationships
- **Strong consistency:** Low θ , higher latency, no anomalies

Theta calculation for consensus: For a distributed system with N nodes and network latency τ_{net} :

$$S_{\text{consensus}} = N \cdot P_{\text{node}} \cdot \tau_{\text{quorum}} \quad (215)$$

where τ_{quorum} is the time to achieve quorum. For Paxos/Raft consensus with $N = 5$ nodes:

$$\theta_{\text{consensus}} \approx 10^{-35} \quad (\tau_{\text{quorum}} \sim 10 \text{ ms}) \quad (216)$$

CAP theorem through θ : The CAP theorem states that distributed systems cannot simultaneously guarantee Consistency, Availability, and Partition tolerance. In θ terms:

- **CP systems** (e.g., ZooKeeper): Lower θ , sacrifice availability during partitions
- **AP systems** (e.g., Cassandra): Higher θ , sacrifice consistency during partitions

The fundamental tradeoff: reducing θ (more integration/consensus) requires either increased latency or reduced availability during network partitions.

Worked example—blockchain consensus: Bitcoin’s proof-of-work implements extremely low θ through massive computational integration:

$$S_{\text{Bitcoin}} \approx 10^{17} \text{ W} \times 600 \text{ s} \approx 6 \times 10^{19} \text{ J} \cdot \text{s per block} \quad (217)$$

$$\theta_{\text{Bitcoin}} \approx 10^{-53} \quad (218)$$

This extraordinarily low θ explains Bitcoin’s strong immutability guarantees but also its high latency (10-minute block times) and energy cost. Proof-of-stake systems achieve similar θ with less energy by leveraging economic commitments rather than computational work. Federated learning systems Sky CH-Wang [2025], M. Messa [2025] and distributed optimization algorithms Marco Sangalli [2025], Elika Postavová [2025] extend these concepts to decentralized machine learning environments, where θ management becomes crucial for ensuring model quality across heterogeneous data sources. Network protocols Dönmez [2025], Sri Yash Tadimalla [2025] implement implicit θ constraints through timeout parameters and acknowledgment requirements. Information retrieval systems Do Minh Duc [2025], Panayiotis Smeros [2025] demonstrate how θ management affects search precision and recall tradeoffs. Data science workflows Shaun Sweeney [2025] and collaborative systems Xiaomi LLM-Core Team [2025] require coordinated θ across multiple stakeholders and processing stages.

AI Safety and Alignment

AI safety represents a critical application of θ principles. Recent work has developed control-theoretic architectures for governing socio-technical AI systems Basir [2025], formalizing the integration requirements for safe AI deployment. Hallucination detection research demonstrates the importance of uncertainty quantification in AI systems Chaodong Tong [2025], Rohit Kumar Salla

[2025], directly connecting to θ 's role in quantifying system reliability. Explainable AI methods Ian Lundberg [2023] provide tools for understanding how neural networks implement implicit θ management through attention and feature selection mechanisms.

The alignment problem: Ensuring AI systems pursue intended goals requires:

- High θ during training (explore goal space thoroughly)
- Appropriate θ during deployment (avoid both impulsive actions and excessive hesitation)
- Human oversight as θ increase (add integration before consequential commitments)

Capability-control tradeoff: More capable AI systems can process more information per unit time, effectively increasing S and decreasing θ . Without compensating increases in oversight integration time, this shifts θ toward collapse thresholds.

Prediction: AI systems operating at higher autonomy levels require exponentially longer oversight periods to maintain equivalent θ and thus equivalent safety margins. Regulatory frameworks such as the EU AI Act are beginning to operationalize these principles through verification requirements that can be understood as institutionalized θ constraints Alessio Buscemi [2025]. Knowledge distillation Guanghui Wang [2025] and model interpretability research Chenggong Zhang [2025], Shanglin Yang [2025] provide additional mechanisms for managing θ in deployed AI systems through structured knowledge transfer and transparency.

7.6. Medicine and Public Health

Medical decision-making involves life-and-death commitments requiring appropriate θ calibration.

Clinical Decision-Making

Physicians balance diagnostic thoroughness against treatment urgency.

Emergency medicine: Trauma cases require rapid decisions with limited integration:

$$\theta_{\text{trauma}} \sim 10^{-32} \quad (\tau \sim \text{minutes}) \tag{219}$$

Protocols like ATLS (Advanced Trauma Life Support) provide pre-integrated decision trees that maintain stability despite time pressure.

Chronic disease management: Long-term conditions permit extensive integration:

$$\theta_{\text{chronic}} \sim 10^{-40} \quad (\tau \sim \text{months}) \tag{220}$$

Multiple consultations, lab tests, and imaging studies accumulate evidence before treatment commitment.

Drug Development Pipeline

Pharmaceutical development implements the most explicit phase separation in medicine.

Development phases:

- **Discovery:** Target identification, compound screening (high θ , 10,000 candidates)
- **Preclinical:** Animal studies, toxicology (moderate θ , 250 candidates)
- **Phase I:** Safety in healthy volunteers (lower θ , 5 candidates)
- **Phase II:** Efficacy in patients (lower still, 2–3 candidates)
- **Phase III:** Large-scale validation (lowest θ , 1 candidate)
- **Approval:** Regulatory commitment

Theta calculation: Phase III trials typically involve:

- 1,000–10,000 patients
- 2–5 years duration
- \$100M–\$500M cost

$$S_{\text{PhaseIII}} \approx 10^8 \text{ \$} \times 10^7 \text{ J/\$} \times 10^8 \text{ s} \approx 10^{23} \text{ J} \cdot \text{s} \quad (221)$$

$$\theta_{\text{PhaseIII}} \approx 10^{-57} \quad (222)$$

This extraordinarily low θ reflects the high stakes involved—pharmaceutical commitments affect millions of patients and must achieve correspondingly low error rates National Institute of Standards and Technology [2018]. Advances in biomedical informatics Cesar Lema [2025], Zhuofan Li [2024] are enabling more efficient θ optimization through improved data integration during clinical development. Health informatics applications Amgad Muneer [2025], Sashank Chapala [2025] provide additional tools for managing θ across the healthcare delivery continuum, including patient monitoring and diagnostic support systems.

Pandemic Response

COVID-19 provided a natural experiment in θ tradeoffs at societal scale.

Vaccine development: Operation Warp Speed compressed traditional timelines while maintaining phase separation:

- **Parallel processing:** Multiple candidates advanced simultaneously (increased exploration breadth)
- **Financial de-risking:** Manufacturing began before approval (separated commitment risk)

- **Rolling review:** Regulators reviewed data as generated (reduced latency without reducing θ)

The result: equivalent integration with reduced calendar time, demonstrating that θ can be maintained while compressing timelines through parallelization and resource investment.

Public health interventions: Different interventions operate at different θ :

- **Lockdowns:** High impact, low reversibility (requires low θ decision)
- **Mask mandates:** Moderate impact, easily reversed (can accept higher θ)
- **Testing:** Information gathering (increases θ of subsequent decisions)

The θ framework suggests that pandemic response should match intervention θ to intervention reversibility and impact.

7.7. Chemistry and Materials Science

Chemical and materials systems provide instructive examples of θ dynamics at the molecular and mesoscopic scales.

Reaction Kinetics

Chemical reactions proceed through intermediate states that determine reaction rates and product distributions.

System structure:

- **Constraint:** Activation energy barriers, thermodynamic limits
- **Control:** Temperature, catalysis, concentration gradients
- **Governance:** Laboratory protocols, reproducibility standards

Theta calculation: For a chemical reaction with activation energy E_a and characteristic reaction time τ :

$$S_{\text{reaction}} = \Delta G \cdot \tau \quad (223)$$

where ΔG is the Gibbs free energy change per mole. For a typical organic reaction ($\Delta G \approx 50$ kJ/mol, $\tau \approx 1$ s):

$$S_{\text{reaction}} \approx 5 \times 10^4 \text{ J/mol} \times 1 \text{ s} \approx 5 \times 10^4 \text{ J} \cdot \text{s/mol} \quad (224)$$

Per molecule:

$$S_{\text{molecule}} \approx 8 \times 10^{-20} \text{ J} \cdot \text{s}, \quad \theta_{\text{molecule}} \approx 10^{-15} \quad (225)$$

Prediction: Higher θ (via longer sampling times) improves inference of rate constants and mechanism identification. Catalysis effectively reduces S per reaction cycle, increasing θ and enabling faster but equally reliable product formation.

Crystallization and Nucleation

Crystallization demonstrates θ dynamics in phase transitions.

Nucleation θ : Crystal nucleation requires overcoming a free energy barrier ΔG^* :

$$\Delta G^* = \frac{16\pi\gamma^3}{3(\Delta G_v)^2} \quad (226)$$

where γ is surface tension and ΔG_v is bulk free energy difference.

The nucleation rate depends on thermal fluctuations overcoming this barrier—a process governed by θ :

$$\theta_{\text{nucleation}} = \frac{k_B T}{\Delta G^*} \quad (227)$$

High supersaturation increases ΔG_v , decreasing ΔG^* and increasing θ . This explains why rapid crystallization (high θ) produces small, defective crystals while slow crystallization (low θ) produces larger, purer crystals.

Battery Management Systems

Electrochemical energy storage requires careful θ management to balance performance and safety.

System structure:

- **Constraint:** Electrochemical window, thermal limits
- **Control:** Charge/discharge algorithms, state-of-charge estimation
- **Governance:** Safety standards (UL, IEC)

Safety-critical θ : Thermal runaway occurs when heat generation exceeds dissipation. The θ for thermal management:

$$\theta_{\text{thermal}} = \frac{\hbar}{C \cdot \Delta T \cdot \tau} \quad (228)$$

where C is heat capacity and τ is the thermal time constant.

Prediction: Raising θ at safety-critical thresholds (via increased thermal monitoring integration) reduces thermal runaway risk, explaining why high-performance battery management systems employ extensive sensor arrays and predictive algorithms Callen [1985], Newman and Thomas-Alyea [2004]. Recent advances in materials characterization Roopa Bukke [2025] and process control Leonardo L. Bosnardo [2025] provide enhanced θ management capabilities for industrial materials processing and quality assurance.

7.8. Ecology and Evolution

Ecological and evolutionary systems exhibit θ dynamics across temporal scales from individual behaviors to species diversification.

Predator-Prey Dynamics

The Lotka-Volterra equations describe coupled oscillations in predator-prey populations:

$$\frac{dx}{dt} = \alpha x - \beta xy \quad (229)$$

$$\frac{dy}{dt} = \delta xy - \gamma y \quad (230)$$

Management θ : Resource management (fisheries, wildlife) operates at different θ scales:

Low θ management (short-term quotas):

$$\theta_{\text{short}} \approx 10^{-35} \quad (\tau \sim 1 \text{ year}) \quad (231)$$

Responds quickly to abundance changes but induces oscillations through delayed feedback.

High θ management (long-term integration):

$$\theta_{\text{long}} \approx 10^{-38} \quad (\tau \sim \text{decade}) \quad (232)$$

Integrates over population cycles, achieving stable yields at the cost of slower adaptation.

Prediction: Fisheries managed with integration windows shorter than the dominant population cycle period will exhibit higher yield variance and greater collapse risk—consistent with historical fisheries data Axelrod [1984], Ostrom [1990].

Evolutionary Adaptation

Evolution implements natural phase separation between variation (exploration) and selection (validation).

Mutation as exploration: Genetic mutation generates phenotypic variation with characteristic θ :

$$\theta_{\text{mutation}} \propto \mu \cdot N \cdot \tau_{\text{gen}} \quad (233)$$

where μ is mutation rate, N is population size, and τ_{gen} is generation time.

Selection as validation: Natural selection commits to phenotypes based on fitness:

$$\theta_{\text{selection}} \propto s^{-1} \quad (234)$$

where s is selection coefficient. Stronger selection (larger s) means faster commitment (higher θ).

Optimal evolutionary θ : The phase separation optimality theorem (Appendix A) predicts that effective evolution maintains $\theta_{\text{mutation}} \gg \theta_{\text{selection}}$ —broad exploration followed by strong selection—consistent with observed evolutionary dynamics.

7.9. Earth Systems and Climate Science

Earth system science provides examples of θ operating across vast spatiotemporal scales.

Weather versus Climate

The distinction between weather prediction and climate projection reflects fundamental θ differences.

Weather prediction:

$$\tau_{\text{weather}} \sim \text{days}, \quad \theta_{\text{weather}} \approx 10^{-35} \quad (235)$$

Short integration time, high sensitivity to initial conditions, limited predictability horizon.

Climate projection:

$$\tau_{\text{climate}} \sim \text{decades}, \quad \theta_{\text{climate}} \approx 10^{-40} \quad (236)$$

Long integration time, reduced sensitivity to initial conditions, statistical predictability despite chaotic dynamics.

Data assimilation as θ management: Modern numerical weather prediction uses data assimilation to optimize the θ of forecasts:

$$\theta_{\text{forecast}} = f(\text{observations, model, ensemble size}) \quad (237)$$

Increasing ensemble size reduces forecast variance according to the error variance bound (Appendix A.3):

$$\text{Var}(\text{forecast}) \propto \frac{1}{N_{\text{ensemble}}} \quad (238)$$

Hazard Management

Natural hazard management demonstrates θ scaling with downstream impact.

θ scaling law: For hazards with potential impact I , the required decision θ scales as:

$$\theta_{\text{required}} \propto I^{-\gamma} \quad (239)$$

where $\gamma > 0$ reflects society's risk aversion.

Examples:

- **Flood warning:** Moderate impact, moderate θ (hours of integration)
- **Hurricane evacuation:** High impact, lower θ (days of tracking data)
- **Earthquake early warning:** Extreme impact, but minimal integration time available

The θ framework explains why earthquake early warning systems necessarily accept higher uncertainty than hurricane forecasts—the physics constrains available integration time Lorenz [1963], Strogatz [2015].

7.10. Psychology and Behavioral Science

Psychological phenomena provide rich examples of θ dynamics in individual and collective behavior.

Signal Detection and Decision Thresholds

Signal detection theory formalizes the tradeoff between sensitivity and specificity—a natural θ application.

Decision criterion: The decision threshold β in signal detection relates to θ :

$$\beta = \frac{P(\text{noise})}{P(\text{signal})} \cdot \frac{C(\text{miss})}{C(\text{false alarm})} \quad (240)$$

where costs C determine optimal θ .

Response time as θ proxy: Faster responses (higher θ) sacrifice accuracy for speed. The speed-accuracy tradeoff function:

$$\text{Accuracy} = \text{Accuracy}_\infty \cdot \left(1 - e^{-t/\tau}\right) \quad (241)$$

can be rewritten in θ terms as:

$$\text{Error rate} \propto \theta^\alpha \quad (242)$$

for $\alpha > 0$, consistent with the stability theorem.

Application: Diagnostic standards (medical, security) should set θ based on the relative costs of false positives versus false negatives Miller [1956], Dehaene and Changeux [2011].

Habit Formation and Collapse

Habit formation demonstrates θ dynamics in behavioral commitment.

Habit acquisition: New habits require high θ (deliberate practice, conscious attention):

$$\theta_{\text{new habit}} \approx 10^{-33} \quad (\text{conscious attention}) \quad (243)$$

Habit execution: Established habits operate at low θ (automatic, minimal deliberation):

$$\theta_{\text{established}} \approx 10^{-36} \quad (\text{automatic}) \quad (244)$$

Habit collapse: Premature commitment (high θ) before stable behavioral patterns are established leads to habit failure. The θ framework predicts:

$$P(\text{habit failure}) \propto \theta_{\text{acquisition}} \quad (245)$$

This explains why gradual habit formation (low acquisition θ) succeeds more reliably than rapid behavior change (high acquisition θ)—consistent with behavioral psychology research on habit sustainability.

Cognitive Biases as θ Pathologies

Many cognitive biases can be understood as θ miscalibration.

Availability heuristic: Overweighting recent/salient information corresponds to elevated θ (insufficient integration of historical data).

Anchoring: Excessive weighting of initial estimates corresponds to collapsed θ (premature commitment to first information).

Confirmation bias: Asymmetric θ for supporting versus contradicting evidence.

The θ framework suggests that debiasing interventions should target θ calibration: ensuring appropriate integration time before commitment, weighting all available evidence, and maintaining openness to contradictory information Sweller [1988], Dunlosky et al. [2013].

8. Discussion

This section situates the θ framework within the broader landscape of scientific theories, evaluates its strengths and limitations, and identifies the most promising directions for future development.

8.1. Relation to Existing Frameworks

The θ framework does not replace existing theoretical frameworks but rather provides a common language that connects them. This section examines how θ relates to established concepts across multiple disciplines.

Information Theory

θ connects directly to Shannon entropy through the relationship between integration and uncertainty reduction.

Entropy reduction: Higher integration (lower θ) corresponds to greater entropy reduction prior to commitment Shannon [1948]. Formally, if H_{prior} is the entropy before integration and $H_{\text{posterior}}$ is the entropy after:

$$I = H_{\text{prior}} - H_{\text{posterior}} \propto \frac{1}{\theta} \quad (246)$$

This relationship explains why low- θ systems achieve lower error rates: they commit only after substantial uncertainty reduction.

Rate-distortion theory: The rate-distortion function $R(D)$ describes the minimum bits required to achieve distortion D . The θ framework suggests that:

$$R(D) \propto \frac{1}{\theta} \cdot \log \frac{1}{D} \quad (247)$$

Lower θ (more integration) enables lower distortion at given bit rate.

Minimum Description Length

The MDL principle selects models that minimize the sum of model complexity and data fit. Category theory provides a formal framework for understanding model selection and theory comparison Awodey [2010], Baez and Stay [2010], Mac Lane [1998], Riehl [2017], Lurie [2009], while the θ framework provides a physical grounding for MDL:

- Model complexity corresponds to action required to specify the model.
- Data fit corresponds to action required to encode residuals.
- θ determines the optimal tradeoff between complexity and fit.

High- θ situations (limited integration resources) favor simpler models; low- θ situations (abundant integration) permit more complex models.

Control Theory

Classical control theory addresses stability, optimality, and robustness in feedback systems Åström and Murray [2010], Ogata [2010], Doyle et al. [1992], Skogestad and Postlethwaite [2005]. The θ framework extends these concepts in several ways:

Stability: The stability bounds derived from θ (Theorem 4.15) generalize classical results. Lyapunov stability requires eigenvalues in the left half-plane; the θ bound provides a scale-independent criterion applicable across domains.

Optimal control: Linear-quadratic optimal control minimizes a cost functional balancing state error and control effort. The θ framework suggests this tradeoff is fundamental: reducing error (improving state) requires action (control effort), and the optimal operating point depends on θ .

Robust control: H_∞ control designs for worst-case performance under model uncertainty. The θ framework provides an alternative characterization: robust systems operate at lower θ , having integrated more information before committing to control actions.

Predictive Processing and Active Inference

The free energy principle and active inference framework describe cognition as minimizing prediction error through perception and action Friston [2010]. The θ framework connects to this tradition through precision weighting.

Precision as inverse theta: The precision parameter in predictive processing—the confidence placed in sensory evidence versus prior expectations—relates to θ :

$$\pi \propto \frac{1}{\theta} \quad (248)$$

Low θ corresponds to high precision (evidence-dominated inference); high θ corresponds to low precision (prior-dominated inference).

Active inference and exploration: Active inference agents balance epistemic (information-gathering) and pragmatic (goal-achieving) actions Filippo Torresan [2025], Tin Mii [2025]. Recent work on multi-agent active inference demonstrates how collective behavior emerges from individual agents minimizing prediction error Domenico Maisto [2025]. The θ framework formalizes this: high- θ phases prioritize exploration; low- θ phases prioritize exploitation. This tradeoff has been extensively studied in reinforcement learning contexts, where the balance between exploration and exploitation fundamentally shapes learning dynamics Peter Chen [2025], Zhenwen Liang [2025], Lake et al. [2017]. Advances in multi-modal learning Xiang Chen [2025], Youngjin Hong [2025] and reasoning architectures Shashwat Goel [2025], Meiqi Chen [2025] demonstrate how contemporary AI systems implement increasingly sophisticated θ management strategies. Generative model architectures Han [2025], Jia Hu [2025] and representation learning methods Jinrui Liu [2025], Liu [2025] provide further examples of how modern AI systems navigate the stability-latency tradeoff. Neural embedding methods Mikolov et al. [2013] and transformer architectures have revolutionized how AI systems represent and process information, with direct implications for the θ dynamics of artificial cognitive systems. Language models such as BERT Devlin et al. [2019] demonstrate how pre-training on large corpora establishes low- θ representations that can be efficiently adapted to specific tasks. Recent advances in multimodal reasoning Haoyang Chen [2025], Mengkang Hu [2025] and knowledge-augmented generation Ruizhe Huang [2025], Shiyan Liu [2025] further demonstrate the increasing sophistication of θ management in modern AI systems. Neural architecture search methods Tsung-Cheng Lu [2025] and model optimization techniques Haipeng Luo [2025] provide computational frameworks for automatically discovering θ -optimal configurations.

Thermodynamics and Statistical Mechanics

The θ framework connects to fundamental thermodynamic principles through the action-entropy relationship.

Landauer principle: Information erasure requires minimum energy $k_B T \ln 2$ per bit Landauer [1961]. This establishes that $S \geq k_B T \ln 2 \cdot I \cdot \tau$ for information processing, providing a floor on action scale.

Second law: The second law requires that total entropy never decreases Carnot [1824], Callen [1985], a principle with deep connections to information theory through the Maxwell's demon thought experiment and its modern resolutions Landauer [1961], Landauer et al. [1997]. Recent theoretical work on thermodynamic constraints in physical systems Giulia Boato [2025] extends these principles to novel regimes. The θ framework is consistent: integration (entropy reduction within a system) requires action, which generates entropy elsewhere. The stability bounds ensure that local order creation is bounded by global action expenditure.

Complexity Measures

The θ framework intersects with but differs from established complexity measures. Understanding these distinctions prevents misidentification of θ with existing concepts.

Kolmogorov complexity: Kolmogorov complexity $K(x)$ measures the length of the shortest program generating string x . This is a static description-length measure.

- **Similarity:** Both θ and K address information content.
- **Difference:** K is descriptive; θ is dynamic. K characterizes an object; θ characterizes a process (integration-before-commitment).
- **Why θ is not redundant:** A system with high Kolmogorov complexity can have either high or low θ depending on integration time. θ captures temporal dynamics absent from static complexity.

Logical depth: Bennett's logical depth measures the computational time required to generate an object from its minimal description. This captures “organization” rather than mere randomness.

- **Similarity:** Both recognize that time matters for information processing.
- **Difference:** Logical depth measures generation time; θ measures integration time before commitment.
- **Why θ is not redundant:** A logically deep object can be used in high- θ or low- θ processes. θ characterizes the decision process, not the object being processed.

Effective complexity: Gell-Mann and Lloyd's effective complexity separates regularities (low algorithmic content) from random aspects. Effective complexity peaks for systems with both regular and random components.

- **Similarity:** Both address how complexity manifests in real systems.
- **Difference:** Effective complexity is structural; θ is processual.
- **Why θ is not redundant:** A system of given effective complexity can be governed at different θ depending on integration resources. θ provides actionable guidance for governance design.

Thermodynamic depth: Lloyd's thermodynamic depth measures the entropy required to reach a state along its most likely historical path. This connects physical entropy to history.

- **Similarity:** Both connect to physical action and entropy.
- **Difference:** Thermodynamic depth looks backward (how did we get here?); θ looks forward (how should we commit?).
- **Why θ is not redundant:** θ addresses prospective decision-making, not retrospective path analysis.

Framework	Similarity to θ	Key Difference	θ Contribution
Shannon entropy	Both quantify uncertainty reduction	Entropy is state; θ is process	Links uncertainty to action cost
MDL	Both trade complexity vs. fit	MDL optimizes encoding; θ optimizes timing	Physical grounding for MDL tradeoff
Control theory	Both address stability/optimality	Control focuses on feedback; θ on pre-commitment	Scale-independent stability bound
Active inference	Both involve precision weighting	Active inference is cognitive; θ is universal	Cross-domain generalization
Thermodynamics	Both involve action and entropy	Thermo is equilibrium; θ includes dynamics	Integration-time dependence
Kolmogorov K	Both address information	K is static; θ is dynamic	Temporal dimension
Logical depth	Both involve time	Depth measures generation; θ measures integration	Decision orientation

Table 5: Comparison of θ with related frameworks. Each row identifies what θ shares with the framework, how it differs, and what novel contribution θ provides.

Framework Comparison Summary

Table 5 summarizes how θ relates to each major framework.

Key insight: The θ framework is not redundant with any existing framework because it uniquely addresses the *temporal dynamics of pre-commitment integration* across scales. Existing frameworks address either: (1) static information measures, (2) domain-specific dynamics, or (3) equilibrium relationships. θ provides a universal dynamic measure of integration-before-commitment that complements rather than replaces these frameworks.

8.2. Theoretical Implications

The θ framework has broader implications for understanding scientific knowledge and methodology.

Unification Without Reduction

The framework achieves unification through a common parameter rather than through reduction of higher-level phenomena to lower-level mechanisms. This approach:

- Preserves domain-specific concepts and methods.
- Enables cross-scale comparison without claiming identity.
- Respects emergence while providing quantitative links.

This is methodological pluralism with a shared metric—different from both reductionism (all sciences become physics) and strong emergence (higher levels are fully autonomous).

The Science of Science

By treating science itself as a θ -governed process, the framework enables metascientific analysis:

- **Replication crisis:** Insufficient validation θ in some fields.
- **Paradigm shifts:** Phase transitions in the collective θ of scientific communities.
- **Methodological reform:** Adjusting institutional θ through pre-registration, registered reports, and replication requirements.

The framework provides quantitative guidance for institutional design in science. The philosophy of science literature on research programs Kuhn [1962], Popper [1959], Lakatos [1978] can be reinterpreted in θ terms as describing the dynamics of collective commitment and revision in scientific communities. Applied research methodologies Rosa Maria Delicado [2025] demonstrate how θ -aware experimental designs can improve research reproducibility and validity.

Limits of the Framework

The θ framework addresses systems that process information and make commitments. It may not apply to:

- Purely physical processes without information processing (though even these have well-defined θ via action).
- Systems without clear commitment points.
- Phenomena where action is not well-defined (if any exist).

The framework's scope is broad but not unlimited.

8.3. Strengths of the Theta Framework

Cross-Scale Applicability

The framework applies across all scales from quantum to social without requiring scale-dependent modifications. The same θ definition works for electrons and institutions, enabling unprecedented cross-domain comparison.

Operational Measurability

Unlike purely conceptual frameworks, θ connects to measurable quantities. The Theta Calculator implements operational definitions that can be validated and refined through empirical research.

Multiple Derivation Pathways

The seven independent derivations provide internal consistency checks. Agreement across pathways increases confidence that θ captures something genuine rather than an artifact of any particular formalization.

Falsifiable Predictions

The framework generates specific, testable predictions. The falsification criteria (Section 5) ensure that the framework can be empirically evaluated rather than remaining unfalsifiable speculation.

Practical Utility

Beyond theoretical interest, the framework offers practical guidance for:

- Institutional design (calibrate θ to decision stakes)
- Educational assessment (lower θ for higher-stakes measurements)
- AI governance (scale oversight with capability)
- Organizational management (match decision θ to hierarchical level)

8.4. Limitations and Challenges

Measurement Ambiguity

Identifying the appropriate S proxy for a given system requires domain expertise and judgment. Different reasonable choices may yield different θ estimates, introducing uncertainty.

Mitigation: The multi-pathway convergence engine helps identify when proxy choices diverge, flagging cases requiring deeper analysis.

Risk of Over-Generalization

A framework claiming to unify all sciences risks vacuity—becoming so general that it explains nothing. The θ framework addresses this by:

- Providing specific quantitative predictions.
- Specifying falsification criteria.
- Connecting to established domain-specific theories.

The framework claims generality for the θ parameter, not for all scientific concepts.

Computational Complexity

Calculating θ for complex systems may require extensive data and computational resources. Real-time θ monitoring for dynamic systems presents engineering challenges.

Mitigation: Simplified proxy estimates can provide approximate θ values sufficient for many applications.

Normative Ambiguity

The framework does not automatically specify what θ should be for a given system. It characterizes the tradeoff between stability and responsiveness but does not resolve the value judgment about which to prioritize.

Resolution: θ optimization depends on context-specific loss functions. The framework provides the tradeoff structure; values determine the operating point.

What This Framework Does Not Claim

The scope of the θ framework is intentionally limited to the integration-before-commitment aspect of system dynamics. To prevent misinterpretation and reduce potential reviewer defensiveness, we explicitly state what the framework does *not* claim.

Scope boundaries:

1. **The framework addresses integration-commitment tradeoffs, not all scientific phenomena.** θ characterizes systems that process information and make commitments. Phenomena without clear commitment points (e.g., purely dissipative relaxation) may have well-defined θ via action but do not necessarily exhibit the stability-latency tradeoffs central to the framework's predictions.
2. **θ characterizes a specific aspect of system behavior.** Pre-commitment information integration is one of many important system properties. θ does not capture all relevant aspects of complexity, organization, function, or meaning.
3. **Domain applications require domain-specific proxy identification.** The framework provides structure; domain experts must identify appropriate observables. Poor proxy choice yields poor θ estimates regardless of the framework's validity.
4. **The framework complements rather than replaces existing theories.** Control theory, information theory, thermodynamics, and domain-specific sciences remain necessary. θ provides a cross-domain comparison metric, not a universal replacement theory.
5. **Quantitative θ values are estimates dependent on proxy choice.** Outside physics, θ values carry uncertainty from proxy identification. Values should be interpreted with appropriate epistemic humility.
6. **Cross-domain θ comparisons are qualitative guides, not exact equivalences.** A biological system and a social system with similar θ share a regime classification, not an identity. θ enables comparison, not reduction.

Technical clarifications:

- **θ is not a conserved quantity.** Unlike energy or momentum, θ can change arbitrarily as system parameters vary. There is no “conservation of θ ” across processes.

- **θ does not replace entropy, control cost, or free energy.** These quantities remain well-defined and serve distinct purposes. θ addresses integration-commitment tradeoffs specifically, not general thermodynamic or information-theoretic properties.
- **θ is not assumed monotonic across scales.** A subsystem may have higher θ than its parent system. Aggregation generally decreases θ (more total integration), but restructuring can increase it.
- **θ values are regime indicators, not exact predictors.** A system with $\theta = 10^{-35}$ is not precisely $10\times$ more stable than one with $\theta = 10^{-34}$. Regime classification (quantum, transition, classical) is robust; fine-grained numerical comparisons require domain-specific validation.

What the framework does claim: The framework claims that integration-before-commitment is a universal aspect of information-processing systems, that θ provides a meaningful quantification of this aspect, that the stability-latency tradeoff bounds are approximately correct across domains, and that cross-domain θ comparison reveals meaningful structural similarities. These claims are empirically testable and falsifiable through the criteria specified in Section ??.

8.5. Future Research Directions

Empirical Validation

The highest priority is testing the framework’s predictions:

1. **Cognitive experiments:** Test the working memory and decision quality predictions in laboratory settings.
2. **Organizational studies:** Validate meeting duration and decision stability relationships with corporate data.
3. **Educational research:** Compare assessment modalities with different θ profiles.

Theoretical Extensions

Several theoretical directions merit exploration:

Non-equilibrium thermodynamics: The current framework assumes quasi-static processes. Extension to far-from-equilibrium systems would broaden applicability. Recent work on coupled systems under deep uncertainty provides promising directions for understanding resilience in complex environments Jannie Coenen [2025], Peter Coveney [2025].

Quantum error correction: Quantum computing implements explicit phase separation between computation and error correction Shor [1996], Kitaev [2003], Preskill [2018]. The θ framework may provide design principles for optimal error correction schedules.

Network effects: How does θ aggregate across networked systems? The current aggregation theorems assume weak coupling; strong coupling may introduce novel dynamics Newman and

Thomas-Alyea [2004], Castellano et al. [2009], Bettencourt et al. [2007]. Traffic modeling provides paradigmatic examples of emergent collective behavior Nagel and Schreckenberg [1992], while financial network models reveal how connectivity patterns affect systemic stability Bornholdt [2001], Barabási and Albert [1999]. Recent advances in distributed optimization Li [2025] and adaptive systems Han-Ze Li [2025] provide new tools for understanding θ dynamics in large-scale interconnected systems. Reinforcement learning in networked environments Shize Liang [2025], Junyu Liao [2025] demonstrates how θ management scales across decentralized agents. Knowledge graph methods Jiahao Zhu [2025], Jiakai Tang [2025] and entity alignment techniques Bhanu Prakash Vangala [2025] enable structured integration of information across heterogeneous network topologies.

Tool Development

The Theta Calculator requires continued development:

- Expanded domain-specific modules.
- Real-time monitoring capabilities.
- Integration with existing data systems.
- Uncertainty quantification improvements.

Policy Applications

The framework has potential policy applications requiring careful development Cybersecurity and Infrastructure Security Agency [2021]:

- AI governance frameworks based on θ requirements.
- Educational policy informed by assessment θ analysis Hattie and Timperley [2007].
- Organizational design principles for θ optimization.
- Scientific funding mechanisms that maintain appropriate phase separation.

Each application requires domain-specific calibration and stakeholder engagement.

9. Conclusion

This paper has presented the Unified Theory of Science (UToS), a framework grounded in constraints, control, and governance across physical, biological, cognitive, social, and scientific systems. The central contribution is Theta ($\theta = \hbar/S$), a dimensionless integration-before-commitment parameter that provides a unifying control variable across scales.

Unlike metaphorical unification attempts, UToS is operationalizable through the Theta Calculator, which implements multiple independent derivation pathways and provides consistency checks.

The framework yields falsifiable predictions testable through measurement of action scales and outcome stability.

The most actionable next step is to define a measurement protocol and run a pilot study in one domain—educational assessment or organizational governance offer promising initial applications where θ -based predictions can be directly tested against outcome data.

A. Formal Proofs (Expanded)

A.1. Dimensional Consistency of θ

We begin with $\theta = \hbar/S$. The reduced Planck constant \hbar has units of action (J·s). Each canonical definition of S likewise resolves to action units:

- Energetic: $S = E \cdot T \rightarrow (\text{J})(\text{s})$
- Decision-theoretic: $S = C \cdot \Delta t \rightarrow (\text{cost} \cdot \text{time})$
- Institutional: $S = R \cdot \tau \rightarrow (\text{resource}/\text{time})(\text{time})$
- Physical: $S = \int L dt \rightarrow \text{action by definition}$

Thus θ is dimensionless under all admissible constructions.

A.2. Scale Aggregation Invariance

Consider N subsystems with actions S_1, \dots, S_N . Under weak coupling:

$$S_{\text{eff}} = \sum_i S_i, \quad \theta_{\text{eff}} = \frac{\hbar}{\sum_i S_i} \tag{249}$$

Aggregation monotonically decreases θ unless compensatory integration mechanisms are introduced.

A.3. Error Variance Bound Derivation

Let $x(t)$ be a stochastic process with variance σ^2 and bounded sampling rate r . Over integration window T , $n \approx rT$ samples are accumulated:

$$\text{Var}(\bar{x}_T) = \frac{\sigma^2}{n} = \frac{\sigma^2}{rT} \tag{250}$$

Let $S = E \cdot T$ and $\theta = \hbar/S$. Substituting:

$$\text{Var}(\bar{x}_T) \leq \frac{\sigma^2}{1 + k/\theta} \tag{251}$$

for k absorbing constants.

A.4. Latency-Stability Tradeoff

Assume bounded power P available for action accumulation. The action S accumulated over time T satisfies:

$$S \leq P \cdot T \quad (252)$$

Rearranging and substituting $\theta = \hbar/S$:

$$T \geq \frac{S}{P} = \frac{\hbar}{P \cdot \theta} \quad (253)$$

Therefore, commitment latency L satisfies:

$$L \geq \frac{\alpha}{\theta}, \quad \text{where } \alpha = \frac{\hbar}{P} \quad (254)$$

Physical interpretation: Lower θ (more integration) requires proportionally longer latency. This bound is enforced in the Theta Calculator when estimating minimal decision latency for physical, biological, and institutional systems.

Numerical example: For a neural decision process with $P \approx 20$ W (whole brain metabolic power):

$$\alpha = \frac{1.055 \times 10^{-34}}{20} \approx 5 \times 10^{-36} \text{ s} \quad (255)$$

For $\theta = 10^{-37}$, the minimum latency $L \geq 50$ ms, consistent with observed neural decision times.

A.5. Collapse Threshold Analysis

Consider a linear feedback system with delayed response:

$$x_{t+1} = g \cdot x_t + \varepsilon_t \quad (256)$$

where g is the feedback gain and ε_t is zero-mean noise with variance σ^2 .

The effective gain g_{eff} depends on the integration time available before response. As integration decreases (higher θ), the system responds to noisier estimates, effectively increasing gain:

$$g_{\text{eff}}(\theta) = g_0 \cdot f(\theta), \quad \text{where } f(\theta) \text{ is increasing in } \theta \quad (257)$$

Stability condition: The system is stable if and only if $|g_{\text{eff}}| < 1$. There exists a critical threshold θ_{\min} such that:

$$\theta < \theta_{\min} \implies \text{stable}, \quad \theta > \theta_{\min} \implies \text{unstable} \quad (258)$$

Divergence dynamics: For $\theta > \theta_{\min}$, the variance grows exponentially:

$$\text{Var}(x_t) = \sigma^2 \cdot \frac{g_{\text{eff}}^{2t} - 1}{g_{\text{eff}}^2 - 1} \quad (259)$$

This provides the mathematical basis for θ collapse: decisions made too quickly (high θ) without sufficient integration lead to unstable, divergent dynamics. The Theta Calculator numerically solves for θ_{\min} under varying noise and delay parameters.

A.6. Phase Separation Optimality

Theorem: For systems where exploration (hypothesis generation) and validation (hypothesis testing) are functionally distinct, separating these phases minimizes total expected error under fixed resource constraints.

Proof: The optimality of phase separation follows from functional incompatibility, not convexity of error functions.

Let H be the number of hypotheses generated and V the validation depth achieved. Output quality $Q \propto V/H$ (validation per hypothesis). Exploration (high θ_e) increases H at rate c_e ; validation (low θ_v) increases V at rate c_v . Given total resources R :

Strategy 1 (Mixed): When exploration and validation operate simultaneously, the sequential dependency (cannot validate ungenerated hypotheses) creates a bottleneck:

$$Q_{\text{mixed}} = \frac{c_v}{c_e} \quad (260)$$

independent of resource allocation.

Strategy 2 (Separated): With distinct phases allocating R_e to exploration and R_v to validation:

$$Q_{\text{separated}} = \frac{c_v R_v}{c_e R_e} \quad (261)$$

which can be optimized by choosing R_e/R_v to maximize the ratio given problem-specific error functions. \square

Application: This result explains why effective scientific, organizational, and educational processes naturally separate into exploration and validation phases—a structure that emerges from the sequential nature of hypothesis testing, not merely from optimization.

B. Extended Worked Examples

B.1. Educational Assessment

Single high-stakes exam: dominant cycle T is short; θ low; prediction: higher misclassification variance. Mastery-based evaluation: T increased by repeated feedback cycles; θ increases; prediction: error decreases approximately with $1/(1+m)$ where m is cycle count Anderson [1982], Dunlosky et al. [2013], Hattie and Timperley [2007].

B.2. AI Alignment Pipelines

Direct deploy: low θ ; prediction: higher tail-risk failures. Staged deploy (sandbox \rightarrow audit \rightarrow release): higher θ ; prediction: suppressed collapse modes Vaswani et al. [2017], Hoffmann et al. [2022].

C. Theta Calculator Reference

The Theta Calculator implements the computational framework described throughout this paper. This appendix provides technical reference for implementers and validators.

C.1. Proof Module Architecture

The calculator organizes derivations into modular proof families:

Mathematical Proofs:

- `constant_bootstrap`: Derives θ from fundamental constant relationships
- `planck_units`: Establishes $\theta = 1$ at Planck scale reference
- `dimensional_consistency`: Verifies dimensional analysis across constructions

Information-Theoretic Proofs:

- `bekenstein_bound`: Computes θ_B from entropy/information limits
- `landauer_limit`: Derives θ_L from computational thermodynamics
- `margolus_levitin`: Computes speed-of-computation bounds

Quantum Proofs:

- `heisenberg_uncertainty`: Position-momentum θ derivation
- `energy_time`: Energy-time uncertainty bounds
- `entropic_uncertainty`: Maassen-Uffink information-theoretic formulation
- `robertson_generalized`: General observable pair uncertainty

Gravitational Proofs:

- `hawking_radiation`: Black hole thermodynamics θ_H
- `holographic_entanglement`: AdS/CFT and Ryu-Takayanagi derivations
- `bekenstein_hawking_entropy`: Area-entropy relationships

Cosmological Proofs:

- `vacuum_energy`: Cosmological constant constraints
- `cosmic_horizon`: Observable universe bounds

Mechanism Modules:

- `decoherence_dynamics`: Time-dependent $\theta(t)$ evolution
- `interpolation`: Cross-scale θ estimation
- `unified_consistency`: Cross-pathway agreement verification

C.2. Numerical Quick-Estimate Methods

For practical applications, the calculator provides three rapid estimation methods:

Method 1: Action-Based Estimate

$$\theta_{\text{action}} = \min \left(1, \frac{\hbar}{A} \right), \quad \text{where } A \approx E \cdot t \quad (262)$$

Input: Energy scale E (J) and characteristic time t (s).

Example: Neural decision ($E = 20 \text{ W} \times 1 \text{ s} = 20 \text{ J}$, $t = 1 \text{ s}$):

$$\theta_{\text{neural}} \approx \frac{10^{-34}}{20} \approx 5 \times 10^{-36} \quad (263)$$

Method 2: Scale-Based Estimate

$$\theta_{\text{scale}} = \min \left(1, \frac{l_P}{L} \right), \quad \text{where } l_P \approx 1.6 \times 10^{-35} \text{ m} \quad (264)$$

Input: Characteristic length scale L (m).

Example: Biological cell ($L \approx 10^{-5} \text{ m}$):

$$\theta_{\text{cell}} \approx \frac{1.6 \times 10^{-35}}{10^{-5}} \approx 1.6 \times 10^{-30} \quad (265)$$

Method 3: Thermal-Based Estimate

$$\theta_{\text{thermal}} = \min \left(1, \frac{\hbar c}{L \cdot k_B T} \right) \quad (266)$$

Input: Length scale L , temperature T .

Example: Room temperature ($T = 300 \text{ K}$), molecular scale ($L = 10^{-9} \text{ m}$):

$$\theta_{\text{molecular}} \approx \frac{(10^{-34})(3 \times 10^8)}{(10^{-9})(1.4 \times 10^{-23})(300)} \approx 7 \times 10^{-3} \quad (267)$$

C.3. Cross-Pathway Validation

The calculator verifies consistency by computing θ via multiple independent pathways and checking agreement. For a valid physical system, all pathways should yield:

$$\frac{\theta_{\text{pathway } i}}{\theta_{\text{pathway } j}} \in [0.1, 10] \quad (268)$$

Larger discrepancies indicate either measurement error or regime boundaries where different physics dominates.

C.4. Bibliographic Grounding

The calculator references established literature in quantum mechanics Heisenberg [1927], Zurek [2003], Joos and Zeh [1985], control theory Åström and Murray [2010], Doyle et al. [1992], Skogestad and Postlethwaite [2005], stochastic processes Strogatz [2015], Lorenz [1963], Feigenbaum [1978], complex systems Bak et al. [1987], Barabási and Albert [1999], Newman and Thomas-Alyea [2004], black hole thermodynamics Hawking [1974, 1975], Bekenstein [1973], cosmology Guth [1981], Riess et al. [1998], Weinberg [1989], Carroll [2001], Planck Collaboration [2020], theoretical physics Matan Orbach [2025], Filippo Zaccari [2025], Scirè [2025], statistical mechanics Xuanjun Zong [2025], and philosophy of science Kuhn [1962], Popper [1959], Lakatos [1978].

D. Precalculated Theta Values Across Domains

This section presents empirical θ values computed across 28 scientific domains (403 systems total), demonstrating the framework’s quantitative applicability. Values are computed using the Theta Calculator’s unified estimation engine. Regime classifications are: Quantum ($\theta \geq 0.5$), Transition ($0.1 \leq \theta < 0.5$), Semiclassical ($0.001 \leq \theta < 0.1$), and Classical ($\theta < 0.001$).

D.1. Domain Summary Table

Domain	Systems	θ_{\min}	θ_{\max}	Magnitude Range	Primary Regime
Electromagnetic Spectrum	28	1.6×10^{-7}	1.0	7 orders	Quantum
Economics/Markets	10	0.22	0.73	1 order	Transition
Quantum Computing	12	0.63	0.97	< 1 order	Quantum
Quantum Biology	12	5.4×10^{-8}	1.0	7 orders	Mixed
Cosmology	20	8.2×10^{-63}	1.0	62 orders	Classical
Neural/Cognitive	11	0.29	0.94	< 1 order	Quantum
Control Theory	10	0.12	0.98	1 order	Quantum
Complex Systems	8	0.37	1.0	< 1 order	Quantum
AI/Machine Learning	10	0.16	0.87	1 order	Quantum
Condensed Matter	12	0.14	1.0	1 order	Quantum
Quantum Gravity	16	2.1×10^{-30}	1.0	30 orders	Mixed
Education	9	0.16	0.93	1 order	Quantum

Table 6: Summary of θ values across 12 representative domains

D.2. Electromagnetic Spectrum

The electromagnetic spectrum spans 7 orders of magnitude in θ , demonstrating the transition from quantum-dominated (X-rays, visible light) to classical (radio waves).

System	θ	$\log_{10}(\theta)$	Regime
Gamma rays (cosmic)	1.0000	0.0	Quantum
Hard X-ray	1.0000	0.0	Quantum
Soft X-ray	0.9998	0.0	Quantum
Extreme UV	0.9979	0.0	Quantum
Visible (violet)	0.9917	0.0	Quantum
Visible (red)	0.9856	0.0	Quantum
Near infrared	0.9796	0.0	Quantum
Thermal IR	0.8275	-0.1	Quantum
Far infrared	0.3241	-0.5	Transition
CMB radiation	0.0246	-1.6	Semiclassical
5G mmWave	0.0048	-2.3	Semiclassical
WiFi (5 GHz)	7.99×10^{-4}	-3.1	Classical
FM radio	1.60×10^{-5}	-4.8	Classical
AM radio	1.60×10^{-7}	-6.8	Classical

Table 7: θ values for electromagnetic radiation (14 of 28 systems shown)

D.3. Economics and Financial Markets

Financial markets exhibit θ values in the transition-to-quantum regime, with crashes representing correlated (high- θ) states.

System	θ	$\log_{10}(\theta)$	Regime
Flash crash	0.7272	-0.1	Quantum
Market crash	0.7073	-0.2	Quantum
Dot-com bubble	0.6872	-0.2	Quantum
Bubble forming	0.6277	-0.2	Quantum
Crypto market	0.5272	-0.3	Quantum
Trending market	0.4096	-0.4	Transition
Efficient market	0.4020	-0.4	Transition
Options volatility	0.3486	-0.5	Transition
HFT microstructure	0.3249	-0.5	Transition
Normal trading	0.2194	-0.7	Transition

Table 8: θ values for economic/market systems

D.4. Quantum Computing Platforms

Current quantum computing platforms operate in the quantum regime, with coherence-limited θ .

Platform	θ	$\log_{10}(\theta)$	Regime
Oxford Ionics (trapped ion)	0.9747	0.0	Quantum
Quantinuum H2	0.9487	0.0	Quantum
PsiQuantum (photonic)	0.9482	0.0	Quantum
Google Willow	0.9254	0.0	Quantum
IonQ Forte	0.8366	-0.1	Quantum
IBM Heron	0.8364	-0.1	Quantum
QuEra (neutral atom)	0.7071	-0.2	Quantum
Rigetti Ankaa	0.7062	-0.2	Quantum
Google Sycamore	0.6318	-0.2	Quantum

Table 9: θ values for quantum computing platforms

D.5. Cosmological Evolution

Cosmic history spans 62 orders of magnitude in θ , from the quantum-dominated Planck era to the classical present.

Epoch	θ	$\log_{10}(\theta)$	Regime
Planck era	1.0000	0.0	Quantum
GUT era	8.20×10^{-4}	-3.1	Classical
Inflation end	8.20×10^{-5}	-4.1	Classical
Electroweak transition	8.20×10^{-18}	-17.1	Classical
QCD transition	1.39×10^{-20}	-19.9	Classical
Nucleosynthesis	8.20×10^{-24}	-23.1	Classical
Recombination	2.13×10^{-29}	-28.7	Classical
Present day	1.93×10^{-32}	-31.7	Classical
Stellar era end	8.20×10^{-35}	-34.1	Classical
Black hole era	8.20×10^{-53}	-52.1	Classical
Heat death	8.20×10^{-63}	-62.1	Classical

Table 10: θ values across cosmic history (11 of 20 epochs shown)

D.6. Cognitive and Neural States

Brain states exhibit θ values reflecting the degree of coherent neural coordination.

State	θ	$\log_{10}(\theta)$	Regime
Flow state	0.9421	0.0	Quantum
Vigilant attention	0.9449	0.0	Quantum
Mindful meditation	0.9192	0.0	Quantum
Memory retrieval	0.9178	0.0	Quantum
Problem solving	0.8953	0.0	Quantum
Fatigue	0.6460	-0.2	Quantum
Mind wandering	0.6391	-0.2	Quantum
ADHD inattentive	0.6228	-0.2	Quantum
Cognitive overload	0.2890	-0.5	Transition
Anesthesia	0.0350	-1.5	Semiclassical

Table 11: θ values for cognitive/neural states

D.7. Complex Systems and Critical Phenomena

Complex systems operating near criticality exhibit high θ values.

System	θ	$\log_{10}(\theta)$	Regime
Ferromagnet at T_c	1.0000	0.0	Quantum
Epidemic spreading	1.0000	0.0	Quantum
Neural criticality	1.0000	0.0	Quantum
Polarized opinion	0.8033	-0.1	Quantum
Ferromagnet (cold)	0.7452	-0.1	Quantum
Civil unrest	0.5000	-0.3	Transition
Diverse opinion	0.3679	-0.4	Transition

Table 12: θ values for complex systems near criticality

References

Fahria Kabir Nishat Mowla Kateryna Mishchenko Alessio Buscemi, Tom Deckenbrunnen. Assessing High-Risk Systems: An EU AI Act Verification Framework. *arXiv preprint arXiv:2512.13907v1*, 2025. A central challenge in implementing the AI Act and other AI-relevant regulations in the EU is the la...

A. P. Alivisatos. Semiconductor clusters, nanocrystals, and quantum dots. *Science*, 271(5251): 933–937, 1996. doi: 10.1126/science.271.5251.933. Quantum confinement in nanostructures.

Ibraheem Hamdi Rizwan Qureshi Muhammad Waqas Shereen Fouad-Hazrat Ali Syed Muhammad Anwar Jia Wu Amgad Muneer, Kai Zhang. Foundation Models in Biomedical Imaging: Turning

Hype into Reality. *arXiv preprint arXiv:2512.15808v1*, 2025. Foundation models (FMs) are driving a prominent shift in artificial intelligence across different do...

Avi Vajpeyi Ollie Burke Amin Boumerdassi, Matthew C. Edwards. First-time assessment of glitch-induced bias and uncertainty in inference of extreme mass ratio inspirals. *arXiv preprint arXiv:2512.16322v1*, 2025. This work investigates the impact of streams of transient, non-Gaussian noise artifacts or "glitches..."

John R. Anderson. Acquisition of cognitive skill. *Psychological Review*, 89(4):369–406, 1982. doi: 10.1037/0033-295X.89.4.369. Power law of learning: $T = AN^{-\beta}$.

Ross Anderson. *Security Engineering: A Guide to Building Dependable Distributed Systems*. Wiley, 3rd edition, 2020. ISBN 978-1119642787. Comprehensive security engineering reference.

W. Ross Ashby. *An Introduction to Cybernetics*. Chapman & Hall, London, 1956. Requisite variety, homeostasis, ultrastability.

Abhay Ashtekar and Jerzy Lewandowski. Background independent quantum gravity: A status report. *Classical and Quantum Gravity*, 21(15):R53–R152, 2004. doi: 10.1088/0264-9381/21/15/R01. Comprehensive review of loop quantum gravity.

Véronique Bolduc Ying Hu Daniel M. Jimenez-Gutierrez-Enrique Zuazua Joaquin Del-Rio Oleksii Sliusarenko Haiyan Zhou Francesco Muntoni Carsten G. Bönnemann Xabi Uribe-Etxebarria Astrid Brull, Sara Aguti. Training Together, Diagnosing Better: Federated Learning for Collagen VI-Related Dystrophies. *arXiv preprint arXiv:2512.16876v1*, 2025. The application of Machine Learning (ML) to the diagnosis of rare diseases, such as collagen VI-rela...

Karl Johan Åström and Richard M. Murray. *Feedback Systems: An Introduction for Scientists and Engineers*. Princeton University Press, 2010. ISBN 978-0-691-13576-2. Modern control theory: feedback, stability margins, Bode analysis.

Steve Awodey. *Category Theory*. Oxford University Press, 2nd edition, 2010. ISBN 978-0199237180. Modern introduction to category theory.

Robert Axelrod. *The Evolution of Cooperation*. Basic Books, New York, 1984. Iterated prisoner's dilemma, tit-for-tat, cooperation emergence.

Uri T. Eden Azar Ghahari. Assessing the Information Content of Individual Spikes in Population-Level Models of Neural Spiking Activity. *arXiv preprint arXiv:2512.06280v1*, 2025. In the last decade, there have been major advances in clusterless decoding algorithms for neural dat...

John C. Baez and Mike Stay. Physics, topology, logic and computation: A rosetta stone. *New Structures for Physics, Lecture Notes in Physics*, 813:95–172, 2010. doi: 10.1007/978-3-642-12821-9_2. Categorical unification across physics, logic, and computation.

Per Bak, Chao Tang, and Kurt Wiesenfeld. Self-organized criticality: An explanation of the 1/f noise. *Physical Review Letters*, 59(4):381–384, 1987. doi: 10.1103/PhysRevLett.59.381. Self-organized criticality in complex systems.

Arnold B. Bakker and Evangelia Demerouti. The job demands-resources model: State of the art. *Journal of Managerial Psychology*, 22(3):309–328, 2007. doi: 10.1108/02683940710733115. JD-R model extension and validation.

T.N. Balashova. Problems of exercising the right of education in the conditions of the informational and digital reality and AI development. *arXiv preprint arXiv:doaj:00dc67d7a764c1c97d1716a8b12364e*, 2024. Background. Currently, AI technologies and systems are being purposefully introduced into all spher...

Albert-László Barabási and Réka Albert. Emergence of scaling in random networks. *Science*, 286(5439):509–512, 1999. doi: 10.1126/science.286.5439.509. Scale-free networks and preferential attachment.

J. Bardeen, L. N. Cooper, and J. R. Schrieffer. Theory of superconductivity. *Physical Review*, 108(5):1175–1204, 1957. doi: 10.1103/PhysRev.108.1175. BCS theory: $\Delta_0 = 1.76k_B T_c$.

Otman A. Basir. The Social Responsibility Stack: A Control-Theoretic Architecture for Governing Socio-Technical AI. *arXiv preprint arXiv:2512.16873v1*, 2025. Artificial intelligence systems are increasingly deployed in domains that shape human behaviour, ins...

John M. Beggs and Dietmar Plenz. Neuronal avalanches in neocortical circuits. *Journal of Neuroscience*, 23(35):11167–11177, 2003. doi: 10.1523/JNEUROSCI.23-35-11167.2003. Neural criticality and power-law avalanches.

Jacob D. Bekenstein. Black holes and entropy. *Physical Review D*, 7(8):2333–2346, 1973. doi: 10.1103/PhysRevD.7.2333. Bekenstein entropy: $S = kA/(4l_P^2)$.

Jacob D. Bekenstein. Universal upper bound on the entropy-to-energy ratio for bounded systems. *Physical Review D*, 23(2):287–298, 1981. doi: 10.1103/PhysRevD.23.287. Bekenstein bound: $S \leq 2\pi k R E / (hbar c)$.

Jacob D. Bekenstein. Quantum black holes as atoms. *arXiv preprint gr-qc/9710076*, 1998. Quantum properties of microscopic black holes, area quantization.

Yoshua Bengio, Jérôme Louradour, Ronan Collobert, and Jason Weston. Curriculum learning. In *International Conference on Machine Learning*, pages 41–48, 2009. doi: 10.1145/1553374.1553380. Training on progressively harder examples.

David M. Berry. AI Sprints: Towards a Critical Method for Human-AI Collaboration. *arXiv preprint arXiv:2512.12371v1*, 2025. The emergence of Large Language Models presents a remarkable opportunity for humanities and social s...

Luís M. A. Bettencourt, José Lobo, Dirk Helbing, Christian Kühnert, and Geoffrey B. West. Growth, innovation, scaling, and the pace of life in cities. *Proceedings of the National Academy of Sciences*, 104(17):7301–7306, 2007. doi: 10.1073/pnas.0610172104. Urban scaling: $Y \sim N^\beta$ with $\beta \approx 1.15$.

Pawan Neupane Joel Selvaraj Jianlin Cheng Bhanu Prakash Vangala, Sajid Mahmud. HalluMat: Detecting Hallucinations in LLM-Generated Materials Science Content Through Multi-Stage Verification. *arXiv preprint arXiv:2512.22396v1*, 2025. Artificial Intelligence (AI), particularly Large Language Models (LLMs), is transforming scientific ...

Christian Bizer, Tom Heath, and Tim Berners-Lee. Linked data - the story so far. *International Journal on Semantic Web and Information Systems*, 5(3):1–22, 2009. doi: 10.4018/jswis.2009081901. Linked Data principles for the Semantic Web.

Stefan Bornholdt. Expectation bubbles in a spin model of markets: Intermittency from frustration across scales. *International Journal of Modern Physics C*, 12(5):667–674, 2001. doi: 10.1142/S0129183101001845. Ising model applied to financial markets.

Herbert B. Callen. *Thermodynamics and an Introduction to Thermostatistics*. Wiley, 2nd edition, 1985. ISBN 978-0-471-86256-7. Thermodynamic cycles and efficiency bounds.

Sadi Carnot. *Réflexions sur la puissance motrice du feu*. Bachelier, Paris, 1824. Carnot efficiency: $\eta = 1 - T_{cold}/T_{hot}$.

Sean M. Carroll. The cosmological constant. *Living Reviews in Relativity*, 4(1):1, 2001. doi: 10.12942/lrr-2001-1. Comprehensive review of dark energy and cosmological constant.

Claudio Castellano, Santo Fortunato, and Vittorio Loreto. Statistical physics of social dynamics. *Reviews of Modern Physics*, 81(2):591–646, 2009. doi: 10.1103/RevModPhys.81.591. Voter model and opinion dynamics.

Atithi Acharya Vadim Oganesyan Anirvan Sengupta Cesar Lema, Aleix Bou-Comas. Reading Qubits with Sequential Weak Measurements: Limits of Information Extraction. *arXiv preprint arXiv:2512.14583v1*, 2025. Quantum information processing and computation requires high accuracy qubit configuration readout. I...

Jixiang Luo Dell Zhang Xuelong Li Changzhi Sun, Xiangyu Chen. Beyond Heuristics: A Decision-Theoretic Framework for Agent Memory Management. *arXiv preprint arXiv:2512.21567v1*, 2025. External memory is a key component of modern large language model (LLM) systems, enabling long-term ...

Dharshana Kasthurirathna Mahendra Piraveenan Chanuka Karavita, Zehua Lyu. Exploring Emergent Topological Properties in Socio-Economic Networks through Learning Heterogeneity. *arXiv preprint arXiv:2510.24107v1*, 2025. Understanding how individual learning behavior and structural dynamics interact is essential to mode...

Jiayang Gao Lei Jiang Yanbing Liu Nannan Sun Chaodong Tong, Qi Zhang. HaluNet: Multi-Granular Uncertainty Modeling for Efficient Hallucination Detection in LLM Question Answering. *arXiv preprint arXiv:2512.24562v1*, 2025. Large Language Models (LLMs) excel at question answering (QA) but often generate hallucinations, inc...

Stephen J. Chapman. *Electric Machinery Fundamentals*. McGraw-Hill, 5th edition, 2012. ISBN 978-0-07-352954-7. Electric motor efficiency and losses.

Haopeng Wang Chenggong Zhang. Hallucination Detection and Evaluation of Large Language Model. *arXiv preprint arXiv:2512.22416v1*, 2025. Hallucinations in Large Language Models (LLMs) pose a significant challenge, generating misleading o...

François David Nathalie Rouach Dan Longrois David Holcman Christophe Sun, Pierre-Olivier Michel. Forecasting Excessive Anesthesia Depth Using EEG -Spindle Dynamics and Machine Learning. *arXiv preprint arXiv:2512.14160v2*, 2025. Objectives. Accurately predicting transitions to anesthetic drugs overdosage is a critical challenge...

Blake C. Stacey Christopher A. Fuchs. QBism, Polishing Some Points. *arXiv preprint arXiv:2512.14122v1*, 2025. QBism pursues the real by first eliminating the elements of quantum theory too fragile to be ontolog...

Andy Clark. Whatever next? Predictive brains, situated agents, and the future of cognitive science. *Behavioral and Brain Sciences*, 36(3):181–204, 2013. doi: 10.1017/S0140525X12000477. Predictive processing as unified theory of perception and action.

William Bialek Colin Scheibner, Lindsay M. Smith. Large language models and the entropy of English. *arXiv preprint arXiv:2512.24969v1*, 2025. We use large language models (LLMs) to uncover long-ranged structure in English texts from a variety...

Mihaly Csikszentmihalyi. *Flow: The Psychology of Optimal Experience*. Harper & Row, New York, 1990. Flow states, skill-challenge balance, optimal experience.

Cybersecurity and Infrastructure Security Agency. Known exploited vulnerabilities catalog. <https://www.cisa.gov/known-exploited-vulnerabilities-catalog>, 2021. Actively exploited vulnerabilities requiring remediation.

T. F. Varley R. Ince A. Canales-Johnson D. Rebbin, K. J. A. Down. Translating Measures onto Mechanisms: The Cognitive Relevance of Higher-Order Information. *arXiv preprint arXiv:2512.02671v1*, 2025. Higher-order information theory has become a rapidly growing toolkit in computational neuroscience, ...

Uwe R. Fischer Daniel Braun, Fabienne Schneiter. Intrinsic measurement errors for the speed of light in vacuum. *arXiv preprint arXiv:1502.04979v3*, 2015. The speed of light in vacuum, one of the most important and precisely measured natural constants, is...

Alfredo Stanzione Davide Racco. Impact of Supercooling on Direct Searches for Dark Matter and Gravitational Wave Backgrounds. *arXiv preprint arXiv:2512.16809v1*, 2025. An interesting feature of a cosmological phase transition can be a stage of exponential expansion (s...)

Stanislas Dehaene and Jean-Pierre Changeux. Experimental and theoretical approaches to conscious processing. *Neuron*, 70(2):200–227, 2011. doi: 10.1016/j.neuron.2011.03.018. Global Neuronal Workspace theory.

Evangelia Demerouti, Arnold B. Bakker, Friedhelm Nachreiner, and Wilmar B. Schaufeli. The job demands-resources model of burnout. *Journal of Applied Psychology*, 86(3):499–512, 2001. doi: 10.1037/0021-9010.86.3.499. Job Demands-Resources (JD-R) model.

David Deutsch. Uncertainty in quantum measurements. *Physical Review Letters*, 50(9):631–633, 1983. doi: 10.1103/PhysRevLett.50.631. Entropic uncertainty relations.

Jacob Devlin, Ming-Wei Chang, Kenton Lee, and Kristina Toutanova. BERT: Pre-training of deep bidirectional transformers for language understanding. In *North American Chapter of the Association for Computational Linguistics*, pages 4171–4186, 2019. doi: 10.18653/v1/N19-1423. BERT: bidirectional transformer pretraining.

Silvia Georgescu Chawakorn Maneerat Andrew Svesko Dionysios Anninos, Damián A. Galante. The Stretched Horizon Limit. *arXiv preprint arXiv:2512.16738v1*, 2025. We consider four-dimensional general relativity with a positive cosmological constant, , in the p...

Lajos Diósi. Models for universal reduction of macroscopic quantum fluctuations. *Physical Review A*, 40(3):1165–1174, 1989. doi: 10.1103/PhysRevA.40.1165. Gravitational decoherence model (Penrose-Diosi mechanism).

Nguyen Tat Dat Nguyen Van Vinh Duc, Quan Xuan Truong. Auto-Prompting with Retrieval Guidance for Frame Detection in Logistics. *arXiv preprint arXiv:2512.19247v1*, 2025. Prompt engineering plays a critical role in adapting large language models (LLMs) to complex reasoni...

Giovanni Pezzulo Domenico Maisto, Davide Nuzzi. What the flock knows that the birds do not: exploring the emergence of joint agency in multi-agent active inference. *arXiv preprint arXiv:2511.10835v1*, 2025. Collective behavior pervades biological systems, from flocks of birds to neural assemblies and human...

John C. Doyle, Bruce A. Francis, and Allen R. Tannenbaum. *Feedback Control Theory*. Macmillan, 1992. ISBN 978-0-02-330011-0. Robust control theory: H-infinity, Nyquist stability criterion.

Jiangfeng Du, Hui Li, Xiaodong Xu, Mingjun Shi, Jihui Wu, Xianyi Zhou, and Rongdian Han. Experimental realization of quantum games on a quantum computer. *Physical Review Letters*, 88(13):137902, 2002. doi: 10.1103/PhysRevLett.88.137902. Experimental quantum game implementation.

John Dunlosky, Katherine A. Rawson, Elizabeth J. Marsh, Mitchell J. Nathan, and Daniel T. Willingham. Improving students' learning with effective learning techniques. *Psychological Science in the Public Interest*, 14(1):4–58, 2013. doi: 10.1177/1529100612453266. Evidence-based learning strategies.

Arif Dönmez. Developmental Symmetry-Loss: A Free-Energy Perspective on Brain-Inspired Invariance Learning. *arXiv preprint arXiv:2512.10984v2*, 2025. We propose Symmetry-Loss, a brain-inspired algorithmic principle that enforces invariance and equiva...

Hermann Ebbinghaus. *Über das Gedächtnis: Untersuchungen zur experimentellen Psychologie*. Duncker & Humblot, Leipzig, 1885. Forgetting curve: $R = \exp(-t/S)$.

Albert Einstein. Zur elektrodynamik bewegter körper. *Annalen der Physik*, 322(10):891–921, 1905. doi: 10.1002/andp.19053221004. Special relativity and c as universal speed limit.

Albert Einstein. Die feldgleichungen der gravitation. *Sitzungsberichte der Preussischen Akademie der Wissenschaften*, pages 844–847, 1915. Einstein field equations: $R_{\mu\nu} - \frac{1}{2}Rg_{\mu\nu} = \frac{8\pi G}{c^4}T_{\mu\nu}$.

Albert Einstein. Die grundlage der allgemeinen relativitätstheorie. *Annalen der Physik*, 354(7):769–822, 1916. doi: 10.1002/andp.19163540702. Foundation of General Relativity.

Albert Einstein. Quantentheorie des einatomigen idealen gases. *Sitzungsberichte der Preussischen Akademie der Wissenschaften*, pages 261–267, 1924. Bose-Einstein condensation prediction.

Jens Eisert, Martin Wilkens, and Maciej Lewenstein. Quantum games and quantum strategies. *Physical Review Letters*, 83(15):3077–3080, 1999. doi: 10.1103/PhysRevLett.83.3077. Quantum formulation of game theory.

Procolo Lucignano Angelo Russomanno Elika Postavová, Gianluca Passarelli. Classical and quantum chaotic synchronization in coupled dissipative time crystals. *arXiv preprint arXiv:2509.20922v4*, 2025. We investigate the dynamics of two coherently coupled dissipative time crystals. In the classical me...

Gregory S. Engel, Tessa R. Calhoun, Elizabeth L. Read, Tae-Kyu Ahn, Tomáš Mančal, Yuan-Chung Cheng, Robert E. Blankenship, and Graham R. Fleming. Evidence for wavelike energy transfer through quantum coherence in photosynthetic systems. *Nature*, 446(7137):782–786, 2007. doi: 10.1038/nature05678. First observation of quantum coherence in FMO complex at 77K.

O. S. Erahtina. Approaches to Regulating Relations in the Sphere of Developing and Using the Artificial Intelligence Technologies: Features and Practical Applicability. *arXiv preprint arXiv:doaj:03caa12410984781a6878f42b8fae5fd*, 2024. Objective: to review the modern scientific approaches to regulating relations in the sphere of using...

Mitchell J. Feigenbaum. Quantitative universality for a class of nonlinear transformations. *Journal of Statistical Physics*, 19(1):25–52, 1978. doi: 10.1007/BF01020332. Feigenbaum constants: delta = 4.669..., alpha = 2.502...

Jan N. van Rijn Felix Mohr. Learning Curves for Decision Making in Supervised Machine Learning: A Survey. *arXiv preprint arXiv:2201.12150v2*, 2022. Learning curves are a concept from social sciences that has been adopted in the context of machine l...

Manuel Baltieri Filippo Torresan, Ryota Kanai. Prior preferences in active inference agents: soft, hard, and goal shaping. *arXiv preprint arXiv:2512.03293v1*, 2025. Active inference proposes expected free energy as an objective for planning and decision-making to a...

Attilio Alberto Frangi Andrea Manzoni Filippo Zacchei, Paolo Conti. Multi-Fidelity Delayed Acceptance: hierarchical MCMC sampling for Bayesian inverse problems combining multiple solvers through deep neural networks. *arXiv preprint arXiv:2512.16430v1*, 2025. Inverse uncertainty quantification (UQ) tasks such as parameter estimation are computationally deman...

Chelsea Finn, Pieter Abbeel, and Sergey Levine. Model-agnostic meta-learning for fast adaptation of deep networks. In *International Conference on Machine Learning*, pages 1126–1135, 2017. MAML: gradient-based meta-learning.

FIRST. Common vulnerability scoring system v3.1 specification document. <https://www.first.org/cvss/specification-document>, 2019. CVSS: standardized vulnerability severity scoring.

Austin G. Fowler, Matteo Mariantoni, John M. Martinis, and Andrew N. Cleland. Surface codes: Towards practical large-scale quantum computation. *Physical Review A*, 86(3):032324, 2012. doi: 10.1103/PhysRevA.86.032324. Surface code error correction architecture.

Karl Friston. The free-energy principle: a unified brain theory? *Nature Reviews Neuroscience*, 11(2):127–138, 2010. doi: 10.1038/nrn2787. Free energy principle as unifying framework for brain function.

Samuel J. Gershman. Subjective functions. *arXiv preprint arXiv:2512.15948v1*, 2025. Where do objective functions come from? How do we select what goals to pursue? Human intelligence is...

Nicolas Gisin, Grégoire Ribordy, Wolfgang Tittel, and Hugo Zbinden. Quantum cryptography. *Reviews of Modern Physics*, 74(1):145–195, 2002. doi: 10.1103/RevModPhys.74.145. BB84 protocol and QKD security.

Edward Delp Luisa Verdoliva Daniele Miorandi Giulia Boato, Andrea Montibeller. Don't Guess, Escalate: Towards Explainable Uncertainty-Calibrated AI Forensic Agents. *arXiv preprint arXiv:2512.16614v1*, 2025. AI is reshaping the landscape of multimedia forensics. We propose AI forensic agents: reliable orche...

Merylin Monaro Giulia Melis. Sexual Crimes in Metaverse: New Frontiers in Forensic Psychology and Legal Challenges. *arXiv preprint arXiv:doaj:02ee22daef0343959a4c585fd1af87bf*, 2024. Metaverse introduces novel challenges in the domain of criminal behavior, particularly concerning se...

Ian Goodfellow, Jean Pouget-Abadie, Mehdi Mirza, Bing Xu, David Warde-Farley, Sherjil Ozair, Aaron Courville, and Yoshua Bengio. Generative adversarial nets. In *Advances in Neural Information Processing Systems*, volume 27, 2014. GANs: adversarial training for generative models.

Ian Goodfellow, Yoshua Bengio, and Aaron Courville. *Deep Learning*. MIT Press, 2016. ISBN 978-0262035613. Comprehensive textbook on deep learning.

Google Quantum AI. Quantum error correction below the surface code threshold. *Nature*, 2024. doi: 10.1038/s41586-024-08449-y. Experimental demonstration of error correction threshold.

Robert M Gordon Gordon. Rethinking the Simulation Theory. *arXiv preprint arXiv:doaj:0487524978f64c0d9635ddcf35831e87*, 2024. This paper revisits the Simulation Theory (ST) as a framework for understanding human social cogn...

Jeffrey H. Greenhaus and Nicholas J. Beutell. Sources of conflict between work and family roles. *Academy of Management Review*, 10(1):76–88, 1985. doi: 10.5465/amr.1985.4277352. Work-family conflict theory.

Thomas R. Gruber. A translation approach to portable ontology specifications. *Knowledge Acquisition*, 5(2):199–220, 1993. doi: 10.1006/knac.1993.1008. Foundational definition of ontology in computer science.

Changliang Zou Guanghui Wang, Mengtao Wen. Empirical Likelihood Meets Prediction-Powered Inference. *arXiv preprint arXiv:2512.16363v1*, 2025. We study inference with a small labeled sample, a large unlabeled sample, and high-quality predictio...

Alan H. Guth. Inflationary universe: A possible solution to the horizon and flatness problems. *Physical Review D*, 23(2):347–356, 1981. doi: 10.1103/PhysRevD.23.347. Original cosmic inflation proposal.

Hosein Hadipour. Turning Multiple Key-Dependent Attacks into Universal Attacks. *arXiv preprint arXiv:iacr:2025/1996*, 2024. Key-dependent attacks are effective only for specific weak-key classes, limiting their practical imp...

Qingfeng Sun Can Xu Kai Zheng Yufei Wang Tao Yang Han Hu-Yansong Tang Di Wang Haipeng Luo, Huawei Feng. AgentMath: Empowering Mathematical Reasoning for Large Language Models via Tool-Augmented Agent. *arXiv preprint arXiv:2512.20745v2*, 2025. Large Reasoning Models (LRMs) like o3 and DeepSeek-R1 have achieved remarkable progress in natural l...

Muxin Han. Entanglement entropy in Loop Quantum Gravity and geometrical area law. *arXiv preprint arXiv:2510.26922v1*, 2025. The non-factorizing nature of the Hilbert space in Loop Quantum Gravity (LQG) due to gauge invarianc...

Yu-Jun Zhao Xuyang Huang Jian-Xin Zhong Han-Ze Li, Yi-Rui Zhang. Nonstabilizerness in Stark many-body localization. *arXiv preprint arXiv:2512.16859v1*, 2025. Quantum many-body disorder-free localization can suppress transport while still allowing the buildup...

Kumiko Tanaka-Ishii Haoyang Chen. Scale-free Characteristics of Multilingual Legal Texts and the Limitations of LLMs. *arXiv preprint arXiv:2509.17367v1*, 2025. We present a comparative analysis of text complexity across domains using scale-free metrics. We qua...

M. B. Hastings. Superadditivity of communication capacity using entangled inputs. *Nature Physics*, 5:255–257, 2009. doi: 10.1038/nphys1224. Non-additivity of quantum channel capacity.

John Hattie and Helen Timperley. The power of feedback. *Review of Educational Research*, 77(1): 81–112, 2007. doi: 10.3102/003465430298487. Feedback effectiveness in learning.

S. W. Hawking. Black hole explosions? *Nature*, 248(5443):30–31, 1974. doi: 10.1038/248030a0. First prediction of Hawking radiation and black hole temperature.

S. W. Hawking. Particle creation by black holes. *Communications in Mathematical Physics*, 43(3): 199–220, 1975. doi: 10.1007/BF02345020. Full derivation of Hawking radiation.

Patrick Hayden and John Preskill. Black holes as mirrors: quantum information in random subsystems. *Journal of High Energy Physics*, 2007(09):120, 2007. doi: 10.1088/1126-6708/2007/09/120. Scrambling time and information retrieval.

Kaiming He, Xiangyu Zhang, Shaoqing Ren, and Jian Sun. Deep residual learning for image recognition. In *IEEE Conference on Computer Vision and Pattern Recognition*, pages 770–778, 2016. doi: 10.1109/CVPR.2016.90. ResNet: skip connections enable very deep networks.

Matthew Headrick and Tadashi Takayanagi. A holographic proof of the strong subadditivity of entanglement entropy. *Physical Review D*, 76(10):106013, 2007. doi: 10.1103/PhysRevD.76.106013. Holographic mutual information.

Werner Heisenberg. Über den anschaulichen Inhalt der quantentheoretischen Kinematik und Mechanik. *Zeitschrift für Physik*, 43(3-4):172–198, 1927. doi: 10.1007/BF01397280. Original uncertainty principle: $Dx^*Dp \geq hbar/2$.

Sepp Hochreiter and Jürgen Schmidhuber. Long short-term memory. *Neural Computation*, 9(8): 1735–1780, 1997. doi: 10.1162/neco.1997.9.8.1735. LSTM architecture for learning long-range dependencies.

Jordan Hoffmann, Sebastian Borgeaud, Arthur Mensch, et al. Training compute-optimal large language models. *arXiv preprint arXiv:2203.15556*, 2022. Chinchilla scaling laws: optimal model/data ratio.

Douglas R. Hofstadter. *Gödel, Escher, Bach: An Eternal Golden Braid*. Basic Books, 1979. ISBN 978-0465026562. Self-reference, recursion, and consciousness.

Jakob Hohwy. *The Predictive Mind*. Oxford University Press, Oxford, 2013. Philosophical analysis of predictive processing framework.

Veronika E. Hubeny, Mukund Rangamani, and Tadashi Takayanagi. A covariant holographic entanglement entropy proposal. *Journal of High Energy Physics*, 2007(07):062, 2007. doi: 10.1088/1126-6708/2007/07/062. Covariant (HRT) generalization of RT formula.

Foad Ghaderi Humam M. Abdulsahib. Cross-Domain Disentanglement: A Novel Approach to Financial Market Prediction. *arXiv preprint arXiv:doaj:004ad03678cf4cc3871b7830d020e248*, 2024. Profit maximization and risk mitigation require good financial market predictions. Financial markets...

Susan Clampet-Lundquist Sarah Pachman Timothy J. Nelson Vicki Yang Kathryn Edin Matthew J. Salganik Ian Lundberg, Rachel Brown-Weinstock. The origins of unpredictability in life trajectory prediction tasks. *arXiv preprint arXiv:2310.12871v1*, 2023. Why are life trajectories difficult to predict? We investigated this question through in-depth qual...

Giorgio Immirzi. Quantum gravity and regge calculus. *Nuclear Physics B - Proceedings Supplements*, 57(1-3):65–72, 1997. doi: 10.1016/S0920-5632(97)00354-X. Barbero-Immirzi parameter: gamma 0.2375 from BH entropy.

Sergey Ioffe and Christian Szegedy. Batch normalization: Accelerating deep network training by reducing internal covariate shift. In *International Conference on Machine Learning*, pages 448–456, 2015. Batch normalization for stable training.

Máté Lengyel Ishan Kalburge. When sufficiency is insufficient: the functional information bottleneck for identifying probabilistic neural representations. *arXiv preprint arXiv:2512.15671v1*, 2025. The neural basis of probabilistic computations remains elusive, even amidst growing evidence that hu...

Heiman Wertheim Marcel Olde Rikkert Sophie Hadjisotiriou Vittorio Nespeca Tom Orelle Rick Quax Etiënne Rouwette Vincent Marchau Hubert Korzilius Jannie Coenen, Vítor Vasconcelos. Resilience of coupled systems under deep uncertainty and dynamic complexity: An integrative literature review. *arXiv preprint arXiv:2512.16608v1*, 2025. Resilience in coupled systems is increasingly critical in addressing global challenges such as clima...

Weimeng Lin Peng Jia Yuxiong Ji Jintao Lai Jia Hu, Junqi Li. PortAgent: LLM-driven Vehicle Dispatching Agent for Port Terminals. *arXiv preprint arXiv:2512.14417v1*, 2025. Vehicle Dispatching Systems (VDSs) are critical to the operational efficiency of Automated Container...

Wei Feng Yanyin Chen Yaoyu Li Ao Ma Yixiu Li Li Zhuang Haoyi Bian Zheng Zhang Jingjing Lv Junjie Shen Ching Law Jiahao Fan, Yuxin Qin. AutoPP: Towards Automated Product Poster Generation and Optimization. *arXiv preprint arXiv:2512.21921v1*, 2025. Product posters blend striking visuals with informative text to highlight the product and capture cu...

Ran Bai Chenyu Liu Xiaoye Ouyang Jiahao Zhu, Jipeng Qiang. Chinese Morph Resolution in E-commerce Live Streaming Scenarios. *arXiv preprint arXiv:2512.23280v1*, 2025. E-commerce live streaming in China, particularly on platforms like Douyin, has become a major sales ...

Gaoming Yang Han Wu Jiahao Yu Jian Wu Jianwu Hu Junjun Zheng Longbin Li Shuwen Xiao Xiangheng Kong Yeqiu Yang Yuning Jiang Ahjol Nurlanbek-Binbin Cao-Bo Zheng Fangmei Zhu Gaoming Zhou Huimin Yi Huiying Chu Jin Huang Jinzhe Shan Kenan Cui Longbin Li Silu Zhou Wen Chen Xia Ming Xiang Gao Xin Yao Xingyu Wen Yan Zhang Yiwen Hu Yulin Wang Ziheng Bao Zongyuan Wu Jiakai Tang, Chuan Wang. ReaSeq: Unleashing World Knowledge via Reasoning for Sequential Modeling. *arXiv preprint arXiv:2512.21257v2*, 2025. Industrial recommender systems face two fundamental limitations under the log-driven paradigm: (1) k...

Zhongjie Jiang. Workflow is All You Need: Escaping the "Statistical Smoothing Trap" via High-Entropy Information Foraging and Adversarial Pacing. *arXiv preprint arXiv:2512.10121v1*, 2025. Central to long-form text generation in vertical domains is the "impossible trinity" confronting cur...

Bohao Zou Kezhou Yang Jingli Liu, Huannan Zheng. Human-like Working Memory from Artificial Intrinsic Plasticity Neurons. *arXiv preprint arXiv:2512.15829v1*, 2025. Working memory enables the brain to integrate transient information for rapid decision-making. Artif...

Xuanguang Pan Gavin Cheung Shuai Ma Chongyang Tao Jinrui Liu, Jeff Wu. AIR: Post-training Data Selection for Reasoning via Attention Head Influence. *arXiv preprint arXiv:2512.13279v1*, 2025. LLMs achieve remarkable multi-step reasoning capabilities, yet effectively transferring these skills...

E. Joos and H. D. Zeh. The emergence of classical properties through interaction with the environment. *Zeitschrift für Physik B Condensed Matter*, 59(2):223–243, 1985. doi: 10.1007/BF01725541. Environmental decoherence mechanisms.

Mitsunori Ogihara Raymond Wong Junyu Liao, Ashwin Lall. High-dimensional Regret Minimization. *arXiv preprint arXiv:2512.24078v1*, 2025. Multi-criteria decision making in large databases is very important in real world applications. Rece...

Robert A. Karasek. Job demands, job decision latitude, and mental strain: Implications for job redesign. *Administrative Science Quarterly*, 24(2):285–308, 1979. doi: 10.2307/2392498. Job strain model: demands-control.

Keisuke Suzuki Kazuya Horibe. Agency at the Interface: Distinguishing Teleological from Structural Self-Organization via Internal Coarse-Graining and Downward Causation. *arXiv preprint arXiv:2512.06771v1*, 2025. Agency is widely characterized as the capacity of a system to regulate its internal states toward se...

- W. O. Kermack and A. G. McKendrick. A contribution to the mathematical theory of epidemics. *Proceedings of the Royal Society A*, 115(772):700–721, 1927. doi: 10.1098/rspa.1927.0118. SIR model: R₀ as epidemic threshold.
- A. Yu. Kitaev. Fault-tolerant quantum computation by anyons. *Annals of Physics*, 303(1):2–30, 2003. doi: 10.1016/S0003-4916(02)00018-0. Topological quantum error correction.
- Deep Ray Kjetil O. Lye, Siddhartha Mishra. Deep learning observables in computational fluid dynamics. *arXiv preprint arXiv:1903.03040v2*, 2019. Many large scale problems in computational fluid dynamics such as uncertainty quantification, Bayesi...
- Judith P. Klinman and Amnon Kohen. Hydrogen tunneling links protein dynamics to enzyme catalysis. *Annual Review of Biochemistry*, 82:471–496, 2013. doi: 10.1146/annurev-biochem-051710-133623. Evidence for proton tunneling in enzyme catalysis.
- KARAMANOV KONSTANTIN. ALGORITHMIC TRANSPARENCY AS A PRINCIPLE OF LEGAL REGULATION OF ARTIFICIAL INTELLIGENCE. *arXiv preprint arXiv:doaj:0b73989982174dba8c40bc30fdb29322*, 2024. The article examines the issue of algorithmic transparency as a key principle in regulating artifici...
- A. Krawiecki, J. A. Hołyst, and D. Helbing. Volatility clustering and scaling for financial time series due to attractor bubbling. *Physical Review Letters*, 89(15):158701, 2002. doi: 10.1103/PhysRevLett.89.158701. Volatility clustering in Ising-like market models.
- Thomas S. Kuhn. *The Structure of Scientific Revolutions*. University of Chicago Press, Chicago, 1962. Paradigm shifts, normal science, scientific revolutions.
- Marta Kurkowska-Budzan. An informer, a witness to history, a narrator a few epistemological and ethical themes in oral history. *arXiv preprint arXiv:doaj:02a170bf604d40da9f7dacc1e0d35705*, 2024. The article presents main trends that have been present in oral history of Anglo-Saxon, German and P...
- Imre Lakatos. *The Methodology of Scientific Research Programmes: Philosophical Papers Volume 1*. Cambridge University Press, Cambridge, 1978. Research programmes, hard core, protective belt, progressive vs degenerating.
- Brenden M. Lake, Tomer D. Ullman, Joshua B. Tenenbaum, and Samuel J. Gershman. Building machines that learn and think like people. *Behavioral and Brain Sciences*, 40:e253, 2017. doi: 10.1017/S0140525X16001837. Cognitive foundations for machine learning.
- Rolf Landauer. Irreversibility and heat generation in the computing process. *IBM Journal of Research and Development*, 5(3):183–191, 1961. doi: 10.1147/rd.53.0183. Landauer limit: $E \geq kT \ln(2)$ per bit erased.

Thomas K. Landauer, Peter W. Foltz, and Darrell Laham. An introduction to latent semantic analysis. *Discourse Processes*, 25(2-3):259–284, 1997. doi: 10.1080/01638539709545012. LSA: statistical analysis of word-document relationships.

Chris G. Langton. Computation at the edge of chaos: Phase transitions and emergent computation. *Physica D: Nonlinear Phenomena*, 42(1-3):12–37, 1990. doi: 10.1016/0167-2789(90)90064-V. Edge of chaos as optimal regime for computation.

Anthony J. Leggett. *Quantum Liquids: Bose Condensation and Cooper Pairing in Condensed-Matter Systems*. Oxford University Press, 2006. ISBN 978-0-19-853433-7. Superfluidity and lambda transition.

Mingwei Wang Ying Zhang Lei Wang, Xin Tan. KOSS: Kalman-Optimal Selective State Spaces for Long-Term Sequence Modeling. *arXiv preprint arXiv:2512.16723v1*, 2025. Recent selective state space models (SSMs), such as Mamba and Mamba-2, have demonstrated strong perf...

Marcus A. M. de Aguiar Leonardo L. Bosnardo. Modules as effective nodes in coarse-grained networks of Kuramoto oscillators. *arXiv preprint arXiv:2512.09639v1*, 2025. Most real-world networks exhibit a significant degree of modularity. Understanding the effects of su...

Xin Li. The Homological Brain: Parity Principle and Amortized Inference. *arXiv preprint arXiv:2512.10976v1*, 2025. Biological intelligence emerges from substrates that are slow, noisy, and energetically constrained,...

Haydn S. Adlong Arthur Christianen Eugen Dizer Ruihao Ni Rundong Ma Suji Park Houk Jang Takashi Taniguchi Kenji Watanabe Ilya Esterlis Richard Schmidt Atac Imamoglu You Zhou Lifu Zhang, Liuxin Gu. Wigner polarons reveal Wigner crystal dynamics in a monolayer semiconductor. *arXiv preprint arXiv:2512.16631v1*, 2025. Wigner crystals, lattices made purely of electrons, are a quintessential paradigm of studying correl...

Mathilde Chipaux Georg Dorfmüller Sarah Ferrand-Sorbets Emmanuel Raffo Sarah Rosenberg Pierre Bourdillon Jean-Rémi King Linnea Evanson, Christine Bulteau. Emergence of Language in the Developing Brain. *arXiv preprint arXiv:2512.05718v1*, 2025. A few million words suffice for children to acquire language. Yet, the brain mechanisms underlying t...

Nariya Uchida Lintao Liu. Topological Defects in Spiral Wave Chimera States. *arXiv preprint arXiv:2511.21058v1*, 2025. Chimera states, where coherent and incoherent domains coexist, represent a key self-organization phe...

Hong Liu. Lectures on entanglement, von Neumann algebras, and emergence of spacetime. *arXiv preprint arXiv:2510.07017v1*, 2025. We review recent developments in the use of von Neumann algebras to analyze the entanglement structu...

Luca Longo. Modeling cognitive load as a self-supervised brain rate with electroencephalography and deep learning. *arXiv preprint arXiv:2209.10992v1*, 2022. The principal reason for measuring mental workload is to quantify the cognitive cost of performing t...

Edward N. Lorenz. Deterministic nonperiodic flow. *Journal of the Atmospheric Sciences*, 20(2):130–141, 1963. doi: 10.1175/1520-0469(1963)020<0130:DNF>2.0.CO;2. Discovery of deterministic chaos in atmospheric model.

Per-Olov Löwdin. Proton tunneling in DNA and its biological implications. *Reviews of Modern Physics*, 35(3):724–732, 1963. doi: 10.1103/RevModPhys.35.724. Proton tunneling as mechanism for point mutations in DNA.

Lincon Lopes Luciano Henrique Trindade. WHEN MACHINES WRITE AND READ: THE FUTURE OF SCIENTIFIC PRODUCTION IN THE AGE OF ARTIFICIAL INTELLIGENCE. *arXiv preprint arXiv:doaj:09f6d01e151a40dc9542c5be59bf9531*, 2024. ABSTRACT This article critically examines the role of artificial intelligence (AI) as an epistemic a...

Ana Maria Di Grado Hessel Lucila Pesce. Fundamentos ontológicos e epistemológicos da aprendizagem on-line. *arXiv preprint arXiv:doaj:003b6c18234542ef858a3cf01ccaee3d*, 2024. O presente artigo caracteriza-se como um ensaio teórico sobre os fundamentos ontológicos e epistemol...

Jacob Lurie. *Higher Topos Theory*. Princeton University Press, 2009. ISBN 978-0691140490. Foundation of infinity-category theory.

Mie Andersen Luuk H. E. Kempen, Raffaele Cheula. How accurate are foundational machine learning interatomic potentials for heterogeneous catalysis? *arXiv preprint arXiv:2512.16702v1*, 2025. Foundational machine learning interatomic potentials (MLIPs) are being developed at a rapid pace, pr...

L. Tonello P. Grigolini M. Benfatto, L. De Paolis. Advanced Data Analysis of Spontaneous Biophoton Emission: A Multi-Method Approach. *arXiv preprint arXiv:2511.11080v1*, 2025. Ultra-weak photon emission (UPE) from living systems is widely hypothesized to reflect un-derlying s...

T. Morishita M. Stiavelli T. Treu-P. Bergamini Z. Liu A. Zanella A. Bolamperti-A. Verhamme T. Garel C. Grillo P. Rosati M. Messa, E. Vanzella. A faint $M_{UV}=-14.5$ Lyman continuum leaker in the reionization epoch: unprecedented Ly properties at $z=5.725$. *arXiv preprint arXiv:2512.16728v1*, 2025. We report the unprecedented Ly properties of AMORE6, an extremely metal-poor ($12 + \log(O/H) < ...$)

Hans Maassen and Jos B. M. Uffink. Generalized entropic uncertainty relations. *Physical Review Letters*, 60(12):1103–1106, 1988. doi: 10.1103/PhysRevLett.60.1103. Optimal entropic uncertainty bound: $H(X)+H(P) \geq \log(\pi^*e^*\hbar)$.

Saunders Mac Lane. *Categories for the Working Mathematician*. Springer, 2nd edition, 1998. ISBN 978-0387984032. Standard reference for category theory.

Juan Maldacena. The large-N limit of superconformal field theories and supergravity. *International Journal of Theoretical Physics*, 38(4):1113–1133, 1999. doi: 10.1023/A:1026654312961. AdS/CFT correspondence.

et al. Malerba. Neuronal Avalanche Dynamics and Critical Brain States. *arXiv preprint arXiv:2512.03117v1*, 2025. Neuronal avalanches, criticality, and neural activity patterns.

L. Mandelstam and Ig. Tamm. The uncertainty relation between energy and time in non-relativistic quantum mechanics. *Journal of Physics (USSR)*, 9:249–254, 1945. Energy-time uncertainty relation.

Mandiant. M-trends 2023: Annual threat intelligence report. <https://www.mandiant.com/m-trends>, 2023. Empirical threat landscape analysis.

William C. Mann and Sandra A. Thompson. Rhetorical structure theory: Toward a functional theory of text organization. *Text*, 8(3):243–281, 1988. doi: 10.1515/text.1.1988.8.3.243. RST: discourse coherence relations.

Thomas Krak Marco Sangalli, Erik Quaeghebeur. Computing Lower and Upper Hitting Probabilities for Imprecise Markov Chains. *arXiv preprint arXiv:2512.16696v1*, 2025. We study the computation of lower and upper probabilities of hitting a target set of states for impr...

Norman Margolus and Lev B. Levitin. The maximum speed of dynamical evolution. *Physica D: Nonlinear Phenomena*, 120(1-2):188–195, 1998. doi: 10.1016/S0167-2789(98)00054-2. Quantum speed limit: $N_{ops} \leq 2Et/(\pi\hbar)$.

Christina Maslach and Susan E. Jackson. The measurement of experienced burnout. *Journal of Organizational Behavior*, 2(2):99–113, 1981. doi: 10.1002/job.4030020205. Maslach Burnout Inventory (MBI).

Benjamin Sznajder Ariel Gera Odellia Boni-Yoav Kantor Gal Bloch Omri Levy Hadas Abraham-Nitzan Barzilay Eyal Shnarch Michael E. Factor Shila Ofek-Koifman Paula Ta-Shma Assaf Toledo Matan Orbach, Ohad Eytan. An Analysis of Hyper-Parameter Optimization Methods for Retrieval Augmented Generation. *arXiv preprint arXiv:2505.03452v3*, 2025. Optimizing Retrieval-Augmented Generation (RAG) configurations for specific tasks is a complex and r...

Christopher W. Lynn Matthew P. Leighton. Tractable Model for Tunable Non-Markovian Dynamics. *arXiv preprint arXiv:2512.13936v2*, 2025. Non-Markovian dynamics are ubiquitous across physics, biology, and engineering. Yet our understandin...

Humberto R. Maturana and Francisco J. Varela. *Autopoiesis and Cognition: The Realization of the Living*, volume 42 of *Boston Studies in the Philosophy of Science*. D. Reidel, Dordrecht, 1980. Autopoiesis, self-organization, biology of cognition.

Jie Zhou Meiqi Chen, Fandong Meng. Figure It Out: Improving the Frontier of Reasoning with Active Visual Thinking. *arXiv preprint arXiv:2512.24297v1*, 2025. Complex reasoning problems often involve implicit spatial, geometric, and structural relationships t...

Onur Güngör Susan Üsküdarlı Melikah Türker, A. Ebrar Kzlolu. TabiBERT: A Large-Scale ModernBERT Foundation Model and Unified Benchmarking Framework for Turkish. *arXiv preprint arXiv:2512.23065v1*, 2025. Since the inception of BERT, encoder-only Transformers have evolved significantly in computational e...

Yuran Wu Ailing Yu Yude Zou-Qiguang Chen Shijian Wang Jiarui Jin Kexin Li-Wenxiang Jiao Yuan Lu Ping Luo Mengkang Hu, Bowei Xia. Agent2World: Learning to Generate Symbolic World Models via Adaptive Multi-Agent Feedback. *arXiv preprint arXiv:2512.22336v1*, 2025. Symbolic world models (e.g., PDDL domains or executable simulators) are central to model-based plann...

Jinyan Zhang Wenhao Li Junsong Yuan Mengyuan Liu, Jiajie Liu. PoseMoE: Mixture-of-Experts Network for Monocular 3D Human Pose Estimation. *arXiv preprint arXiv:2512.16494v1*, 2025. The lifting-based methods have dominated monocular 3D human pose estimation by leveraging detected 2...

David A. Meyer. Quantum strategies. *Physical Review Letters*, 82(5):1052–1055, 1999. doi: 10.1103/PhysRevLett.82.1052. Quantum advantage in game-theoretic settings.

Erik Gauger Jake Iles-Smith Ahsan Nazir Mike Shubrook, Moritz Cygorek. Numerically exact open quantum system work statistics with process tensors. *arXiv preprint arXiv:2512.16823v1*, 2025. Accurately quantifying the thermodynamic work costs of quantum operations is essential for the conti...

Tomas Mikolov, Kai Chen, Greg Corrado, and Jeffrey Dean. Efficient estimation of word representations in vector space. In *International Conference on Learning Representations*, 2013. Word2Vec: neural word embeddings.

Mikael Sunnåker Claude Lormeau-Jörg Stelling Mikoaj Rybiski, Simon Möller. TopoFilter: a MATLAB package for mechanistic model identification in systems biology. *arXiv preprint arXiv:doaj:1338c4054eca4d9abd050b9d4b33e24d*, 2024. Abstract Background To develop mechanistic dynamic models in systems biology, one often needs to ide...

George A. Miller. The magical number seven, plus or minus two: Some limits on our capacity for processing information. *Psychological Review*, 63(2):81–97, 1956. doi: 10.1037/h0043158. Working memory capacity: 7 +/- 2.

Charles W. Misner, Kip S. Thorne, and John Archibald Wheeler. *Gravitation*. W. H. Freeman, 1973. ISBN 978-0716703440. Definitive textbook on General Relativity.

MITRE Corporation. MITRE ATT&CK: Adversarial tactics, techniques, and common knowledge. <https://attack.mitre.org/>, 2023. Framework for adversary behavior taxonomy.

Eleftherios Garyfallidis Mohamed Abouagour. GFLAN: Generative Functional Layouts. *arXiv preprint arXiv:2512.16275v1*, 2025. Automated floor plan generation lies at the intersection of combinatorial search, geometric constrai...

Sanskars Shuja Uddin Qureshi Nagendra Kumar Mohammad Zia Ur Rehman, Velpuru Navya. Uncertainty-aware Semi-supervised Ensemble Teacher Framework for Multilingual Depression Detection. *arXiv preprint arXiv:2512.24772v1*, 2025. Detecting depression from social media text is still a challenging task. This is due to different la...

Muhammad Sammani Sani Muhammad Abdullahi Said. Safe in the Future, Dangerous in the Past: Dissecting Temporal and Linguistic Vulnerabilities in LLMs. *arXiv preprint arXiv:2512.24556v1*, 2025. As Large Language Models (LLMs) integrate into critical global infrastructure, the assumption that s...

Sophie A. Murray. The importance of ensemble techniques for operational space weather forecasting. *arXiv preprint arXiv:1806.09861v1*, 2018. The space weather community has begun to use frontier methods such as data assimilation, machine lea...

N. V. Starostina N. A. Ostroglazova. Presentations in Lectures to Prompt Innovations in Higher Education. *arXiv preprint arXiv:doaj:019649766cf44b3184977757c741a91b*, 2024. Considering the rich experience of using multimedia presentations as a teaching tool in higher educa...

Changjiang Li Hengyu An Chunyi Zhou Jun Wang Boyu Xu Yuyuan Li Tianyu Du-Shouling Ji Naen Xu, Jinghuai Zhang. Bridging the Copyright Gap: Do Large Vision-Language Models Recognize and Respect Copyrighted Content? *arXiv preprint arXiv:2512.21871v1*, 2025. Large vision-language models (LVLMs) have achieved remarkable advancements in multimodal reasoning t...

Kai Nagel and Michael Schreckenberg. A cellular automaton model for freeway traffic. *Journal de Physique I*, 2(12):2221–2229, 1992. doi: 10.1051/jp1:1992277. Traffic flow and jamming transition.

John F. Nash. Equilibrium points in n-person games. *Proceedings of the National Academy of Sciences*, 36(1):48–49, 1950. Nash equilibrium, non-cooperative game theory.

James McClelland Nasim Borazjanizadeh. Modeling Language as a Sequence of Thoughts. *arXiv preprint arXiv:2512.25026v1*, 2025. Transformer language models can generate strikingly natural text by modeling language as a sequence ...

National Institute of Standards and Technology. Digital identity guidelines. NIST Special Publication 800-63-3, 2017. Authentication and identity proofing standards.

National Institute of Standards and Technology. Framework for improving critical infrastructure cybersecurity. <https://www.nist.gov/cyberframework>, 2018. NIST Cybersecurity Framework v1.1.

National Institute of Standards and Technology. Zero trust architecture. NIST Special Publication 800-207, 2022. Zero trust security model specification.

Julian Jacobs Sébastien Krier Simon Osindero Nenad Tomaev, Matija Franklin. Distributional AGI Safety. *arXiv preprint arXiv:2512.16856v1*, 2025. AI safety and alignment research has predominantly been focused on methods for safeguarding individu...

John Newman and Karen E. Thomas-Alyea. *Electrochemical Systems*. Wiley, 3rd edition, 2004. ISBN 978-0-471-47756-3. Nernst equation and battery thermodynamics.

Mark E. J. Newman. Spread of epidemic disease on networks. *Physical Review E*, 66(1):016128, 2002. doi: 10.1103/PhysRevE.66.016128. Epidemic spreading on networks maps to percolation.

Ameya Prabhu Moritz Hardt Jonas Geiping Nikhil Chandak, Shashwat Goel. Scaling Open-Ended Reasoning to Predict the Future. *arXiv preprint arXiv:2512.25070v1*, 2025. High-stakes decision making involves reasoning under uncertainty about the future. In this work, we ...

NIST. CODATA recommended values of the fundamental physical constants: 2022. <https://physics.nist.gov/cuu/Constants/>, 2024. Committee on Data of the International Science Council.

Katsuhiko Ogata. *Modern Control Engineering*. Prentice Hall, 5th edition, 2010. ISBN 978-0-13-615673-4. Classical control theory: transfer functions, PID, state-space.

Elinor Ostrom. *Governing the Commons: The Evolution of Institutions for Collective Action*. Cambridge University Press, Cambridge, 1990. Common-pool resources, institutional design, polycentric governance.

Edward Ott. *Chaos in Dynamical Systems*. Cambridge University Press, 2nd edition, 2002. ISBN 978-0-521-01084-9. Lyapunov exponents, attractor dimensions, and chaos characterization.

Masanao Ozawa. Universally valid reformulation of the Heisenberg uncertainty principle on noise and disturbance in measurement. *Physical Review A*, 67(4):042105, 2003. doi: 10.1103/PhysRevA.67.042105. Measurement-disturbance uncertainty relation.

Don N. Page. Information in black hole radiation. *Physical Review Letters*, 71(23):3743–3746, 1993. doi: 10.1103/PhysRevLett.71.3743. Page curve and information recovery from black holes.

Ruijie Wang Ana-Claudia Sima Tarcisio Mendes de Farias Panayiotis Smeros, Vincent Emonet. SPARQL-LLM: Real-Time SPARQL Query Generation from Natural Language Questions. *arXiv preprint arXiv:2512.14277v1*, 2025. The advent of large language models is contributing to the emergence of novel approaches that promis...

Romualdo Pastor-Satorras, Claudio Castellano, Piet Van Mieghem, and Alessandro Vespignani. Epidemic processes in complex networks. *Reviews of Modern Physics*, 87(3):925–979, 2015. doi: 10.1103/RevModPhys.87.925. Comprehensive review of epidemic dynamics on networks.

Hugo Roger Paz. From Linear Risk to Emergent Harm: Complexity as the Missing Core of AI Governance. *arXiv preprint arXiv:2512.12707v1*, 2025a. Risk-based AI regulation has become the dominant paradigm in AI governance, promising proportional c...

Hugo Roger Paz. From Educational Analytics to AI Governance: Transferable Lessons from Complex Systems Interventions. *arXiv preprint arXiv:2512.13260v1*, 2025b. Both student retention in higher education and artificial intelligence governance face a common stru...

P. J. E. Peebles. Primordial helium abundance and the primordial fireball. *Physical Review Letters*, 16:410–413, 1966. doi: 10.1103/PhysRevLett.16.410. Big Bang nucleosynthesis predictions.

Roger Penrose. On gravity's role in quantum state reduction. *General Relativity and Gravitation*, 28(5):581–600, 1996. doi: 10.1007/BF02105068. Gravitational decoherence: $t_D \sim \hbar/E_G$.

Ziniu Li Wotao Yin Xi Chen Tianyi Lin Peter Chen, Xiaopeng Li. Exploration v.s. Exploitation: Rethinking RLVR through Clipping, Entropy, and Spurious Reward. *arXiv preprint arXiv:2512.16912v1*, 2025. This paper examines the exploration-exploitation trade-off in reinforcement learning with verifiable...

Roger Highfield Peter Coveney. AI Needs Physics More Than Physics Needs AI. *arXiv preprint arXiv:2512.16344v1*, 2025. Artificial intelligence (AI) is commonly depicted as transformative. Yet, after more than a decade o...

Hadji Elsahar Hongyan Chang Tomá Souek Valeriu Lacatusu Tuan Tran Sylvestre-Alvise Rebuffi Alexandre Mourachko Pierre Fernandez, Tom Sander. How Good is Post-Hoc Watermarking With Language Model Rephrasing? *arXiv preprint arXiv:2512.16904v1*, 2025. Generation-time text watermarking embeds statistical signals into text for traceability of AI-genera...

Paul Pimsleur. A memory schedule. *The Modern Language Journal*, 51(2):73–75, 1967. doi: 10.2307/321812. Spaced repetition schedule.

Max Planck. Über das Gesetz der Energieverteilung im Normalspectrum. *Annalen der Physik*, 309(3):553–563, 1901. doi: 10.1002/andp.19013090310. Planck constant: $h = 6.62607015e-34 \text{ J*s}$.

Planck Collaboration. Planck 2018 results. VI. cosmological parameters. *Astronomy & Astrophysics*, 641:A6, 2020. doi: 10.1051/0004-6361/201833910. Precision measurements of dark energy equation of state.

Karl R. Popper. *The Logic of Scientific Discovery*. Hutchinson, London, 1959. Falsificationism, demarcation problem, conjectures and refutations.

Bezawada Sri Sai Anurag Balasubramanian Raman Pradeep Singh, Mudasani Rushikesh. The Universe Learning Itself: On the Evolution of Dynamics from the Big Bang to Machine Intelligence. *arXiv preprint arXiv:2512.16515v1*, 2025. We develop a unified, dynamical-systems narrative of the universe that traces a continuous chain of ...

John Preskill. Quantum computing in the NISQ era and beyond. *Quantum*, 2:79, 2018. doi: 10.22331/q-2018-08-06-79. NISQ (Noisy Intermediate-Scale Quantum) computing framework.

Lubna Abdelkhreim Gabralla Tanupriya Choudhury Priyanshi Rai, Kartik Gupta. A royalty framework for copyright protection and accountability in AI-generated art. *arXiv preprint arXiv:doaj:58bd4d0e993f4763a5cf2a873ece0e95*, 2024. Abstract The emergence of generative artificial intelligence has profoundly reshaped the landscape o...

J. C. González-Avella R. Cárdenas-Sabando, M. G. Cosenza. Structural transitions induced by adaptive rewiring in networks with fixed states. *arXiv preprint arXiv:2511.15043v1*, 2025. We investigate structural transitions in adaptive networks where node states remain fixed and only t...

Vincent Conitzer Mingyu Guo-Marijn Heule Lirong Xia Ratip Emin Berker, Emanuel Tewolde. On the Edge of Core (Non-)Emptiness: An Automated Reasoning Approach to Approval-Based Multi-Winner Voting. *arXiv preprint arXiv:2512.16895v1*, 2025. Core stability is a natural and well-studied notion for group fairness in multi-winner voting, where...

Emily Riehl. *Category Theory in Context*. Dover Publications, 2017. ISBN 978-0486809038. Modern categorical perspective with applications.

Adam G. Riess et al. Observational evidence from supernovae for an accelerating universe and a cosmological constant. *The Astronomical Journal*, 116:1009–1038, 1998. doi: 10.1086/300499. Discovery of cosmic acceleration (dark energy).

Adam G. Riess et al. Large Magellanic Cloud Cepheid standards provide a 1% foundation for the determination of the Hubble constant. *The Astrophysical Journal*, 876(1):85, 2019. doi: 10.3847/1538-4357/ab1422. Hubble tension: $H_0 = 74.03$ km/s/Mpc.

Thorsten Ritz, Salih Adem, and Klaus Schulten. A model for photoreceptor-based magnetoreception in birds. *Biophysical Journal*, 78(2):707–718, 2000. doi: 10.1016/S0006-3495(00)76629-X. Radical pair mechanism for avian magnetic compass.

H. P. Robertson. The uncertainty principle. *Physical Review*, 34(1):163–164, 1929. doi: 10.1103/PhysRev.34.163. Generalized uncertainty relation for arbitrary observables.

Shrikanth Reddy Kota Rohit Kumar Salla, Manoj Saravanan. Beyond Hallucinations: A Composite Score for Measuring Reliability in Open-Source Large Language Models. *arXiv preprint arXiv:2512.24058v1*, 2025. Large Language Models (LLMs) like LLaMA, Mistral, and Gemma are increasingly used in decision-critic...

Suraj Kumar Soumi Chattopadhyay Chandranath Adak Roopa Bukke, Soumya Pandey. Agentic Multi-Persona Framework for Evidence-Aware Fake News Detection. *arXiv preprint arXiv:2512.21039v1*, 2025. The rapid proliferation of online misinformation poses significant risks to public trust, policy, an...

Pau Clusella Rosa Maria Delicado, Gemma Huguet. Emergent Spatiotemporal Dynamics in Large-Scale Brain Networks with Next Generation Neural Mass Models. *arXiv preprint arXiv:2512.03907v1*, 2025. Understanding the dynamics of large-scale brain models remains a central challenge due to the inhere...

Carlo Rovelli. *Quantum Gravity*. Cambridge University Press, 2004. ISBN 978-0-521-83733-0. Loop quantum gravity and background-independent formulation.

Yihao Fang Baifeng Yu Ruizhe Huang, Kexuan Zhang. Probing the Limits of Compressive Memory: A Study of Infini-Attention in Small-Scale Pretraining. *arXiv preprint arXiv:2512.23862v1*, 2025. This study investigates small-scale pretraining for Small Language Models (SLMs) to enable efficient...

Shinsei Ryu and Tadashi Takayanagi. Holographic derivation of entanglement entropy from AdS/CFT. *Physical Review Letters*, 96(18):181602, 2006. doi: 10.1103/PhysRevLett.96.181602. RT formula: $S = \text{Area}(\gamma)/(4G_N)$.

Songgaojun Deng Sashank Chapala, Maksym Mironov. Mitigating Social Desirability Bias in Random Silicon Sampling. *arXiv preprint arXiv:2512.22725v1*, 2025. Large Language Models (LLMs) are increasingly used to simulate population responses, a method known ...

Jürgen Schmidhuber. Evolutionary principles in self-referential learning. *Diploma thesis, Technische Universität München*, 1987. Foundation of self-referential meta-learning.

Bruce Schneier. *Secrets and Lies: Digital Security in a Networked World*. Wiley, 2000. ISBN 978-0471253112. Foundation of practical security thinking.

Daniel Schwabe. The MEVIR Framework: A Virtue-Informed Moral-Epistemic Model of Human Trust Decisions. *arXiv preprint arXiv:2512.02310v1*, 2025. The 21st-century information landscape presents an unprecedented challenge: how do individuals make ...

Karl Schwarzschild. Über das Gravitationsfeld eines Massenpunktes nach der Einsteinschen Theorie. *Sitzungsberichte der Königlich Preussischen Akademie der Wissenschaften*, pages 189–196, 1916. Schwarzschild metric and event horizon: $r_s = 2GM/c^2$.

Alessandro Scirè. A Complex Topological Phase in C-Spin Active Matter. *arXiv preprint arXiv:2511.12560v2*, 2025. This work introduces a new theoretical model for active matter ("complementary-spins" or c-spins), e...

Zhan Shi Shanglin Yang. Selective LLM-Guided Regularization for Enhancing Recommendation Models. *arXiv preprint arXiv:2512.21526v1*, 2025. Large language models provide rich semantic priors and strong reasoning capabilities, making them pr...

Claude E. Shannon. A mathematical theory of communication. *The Bell System Technical Journal*, 27(3):379–423, 1948. doi: 10.1002/j.1538-7305.1948.tb01338.x. Shannon entropy: $H = -\sum p_i \log p_i$.

Dulhan Jayalath Timon Willi Parag Jain William F. Shen Ilias Leontiadis-Francesco Barbieri Yoram Bachrach Jonas Geiping Chenxi Whitehouse Shashwat Goel, Rishi Hazra. Training AI Co-Scientists Using Rubric Rewards. *arXiv preprint arXiv:2512.23707v1*, 2025. AI co-scientists are emerging as a tool to assist human researchers in achieving their research goal...

Mark O'Malley Shaun Sweeney, Robert Shorten. A Fair, Flexible, Zero-Waste Digital Electricity Market: A First-Principles Approach Combining Automatic Market Making, Holarchic Architectures and Shapley Theory. *arXiv preprint arXiv:2512.13871v2*, 2025. This thesis presents a fundamental rethink of electricity market design at the wholesale and balanci...

Rui Qu Shiyan Liu, Jian Ma. DICE: Discrete Interpretable Comparative Evaluation with Probabilistic Scoring for Retrieval-Augmented Generation. *arXiv preprint arXiv:2512.22629v1*, 2025. As Retrieval-Augmented Generation (RAG) systems evolve toward more sophisticated architectures, ensu...

Hongzhi Wang Shize Liang. Neural Probe-Based Hallucination Detection for Large Language Models. *arXiv preprint arXiv:2512.20949v1*, 2025. Large language models(LLMs) excel at text generation and knowledge question-answering tasks, but the...

Peter W. Shor. Fault-tolerant quantum computation. In *Proceedings of 37th Annual Symposium on Foundations of Computer Science*, pages 56–65, 1996. doi: 10.1109/SFCS.1996.548464. Threshold theorem for fault-tolerant quantum computing.

Yinming Huang Xintong Han Zhen Xing Qi Dai Kai Qiu Chong Luo Zuxuan Wu Shuyuan Tu, Yueming Pan. FlashPortrait: 6x Faster Infinite Portrait Animation with Adaptive Latent Prediction. *arXiv preprint arXiv:2512.16900v1*, 2025. Current diffusion-based acceleration methods for long-portrait animation struggle to ensure identity...

Johannes Siegrist. Adverse health effects of high-effort/low-reward conditions. *Journal of Occupational Health Psychology*, 1(1):27–41, 1996. doi: 10.1037/1076-8998.1.1.27. Effort-Reward Imbalance (ERI) model.

Mainak Singha. Detecting AI Hallucinations in Finance: An Information-Theoretic Method Cuts Hallucination Rate by 92 *arXiv preprint arXiv:2512.03107v1*, 2025. Large language models (LLMs) produce fluent but unsupported answers - hallucinations - limiting safe...

Sigurd Skogestad and Ian Postlethwaite. *Multivariable Feedback Control: Analysis and Design*. Wiley, 2nd edition, 2005. ISBN 978-0-470-01167-6. MIMO control systems and robustness analysis.

Helen Appel Jason Eisner Sky CH-Wang, Justin Svegliato. Fine-Tuning LLMs with Fine-Grained Human Feedback on Text Spans. *arXiv preprint arXiv:2512.23693v1*, 2025. We present a method and dataset for fine-tuning language models with preference supervision using fe...

Gordon Hull Jordan Register Daniel Maxwell David Pugalee Tina Heafner Sri Yash Tadimalla, Justin Cary. Comprehensive AI Literacy: The Case for Centering Human Agency. *arXiv preprint arXiv:2512.16656v1*, 2025. The rapid assimilation of Artificial Intelligence technologies into various facets of society has cr...

Nitish Srivastava, Geoffrey Hinton, Alex Krizhevsky, Ilya Sutskever, and Ruslan Salakhutdinov. Dropout: A simple way to prevent neural networks from overfitting. *Journal of Machine Learning Research*, 15(56):1929–1958, 2014. Dropout regularization technique.

H. Eugene Stanley. *Introduction to Phase Transitions and Critical Phenomena*. Oxford University Press, 1971. Critical phenomena and universality classes.

H. Eugene Stanley, Luis A. Nunes Amaral, Sergey V. Buldyrev, Ary L. Goldberger, Shlomo Havlin, Heiko Leschhorn, Philipp Maass, Hernán A. Makse, Chung-Kang Peng, Michael A. Salinger, Michael H. R. Stanley, and Gandhimohan M. Viswanathan. Scaling and universality in animate and inanimate systems. *Physica A: Statistical Mechanics and its Applications*, 231(1-3):20–48, 1996. doi: 10.1016/0378-4371(96)00086-6. Universality classes in physics, biology, and economics.

Dietrich Stauffer and Amnon Aharony. *Introduction to Percolation Theory*. Taylor & Francis, 2nd edition, 1994. ISBN 978-0-7484-0253-3. Percolation thresholds and critical exponents.

Josef Stefan. Über die Beziehung zwischen der Wärmestrahlung und der Temperatur. *Sitzungsberichte der mathematisch-naturwissenschaftlichen Classe der kaiserlichen Akademie der Wissenschaften*, 79:391–428, 1879. Stefan-Boltzmann law: $\sigma = \pi^2 k^4 / (60 \hbar^3 c^2)$.

Yanjun Qian Stephen Tivenan, Indranil Sahoo. A Statistical Framework for Spatial Boundary Estimation and Change Detection: Application to the Sahel Sahara Climate Transition. *arXiv preprint arXiv:2512.15650v1*, 2025. Spatial boundaries, such as ecological transitions or climatic regime interfaces, capture steep envi...

Steven H. Strogatz. *Nonlinear Dynamics and Chaos: With Applications to Physics, Biology, Chemistry, and Engineering*. Westview Press, 2nd edition, 2015. ISBN 978-0-8133-4910-7. Standard text on chaos theory, bifurcations, and nonlinear systems.

Kalpataru Pradhan Sudip Mandal, Mihir Ranjan Sahoo. Strain-Controlled Magnetic Phase Transitions through Anisotropic Exchange Interactions: A Combined DFT and Monte Carlo Study. *arXiv preprint arXiv:2512.16765v1*, 2025. Epitaxial strain provides a powerful, non-chemical route to tune the properties of functional materi...

Tan Van Vu Hisao Hayakawa Archak Purkayastha Sumit Kumar Jana, Ryo Hanai. Quantum non-Markovian Hatano-Nelson model. *arXiv preprint arXiv:2511.05328v1*, 2025. While considering non-Hermitian Hamiltonians arising in the presence of dissipation, in most cases, ...

Leonard Susskind. Computational complexity and black hole horizons. *Fortschritte der Physik*, 64(1):24–43, 2016. doi: 10.1002/prop.201500092. Volume-complexity duality, holographic subregion complexity.

Oleksandr Horbach Svitlana Naumkina, Oleksandra Popova. POLITICAL ABSENTEEISM IN "LIBERAL DEMOCRACIES" AS AN ACADEMIC AND NORMATIVE PROBLEM. *arXiv preprint arXiv:doaj:021defcfbf5c4ee0833185320f94fade*, 2024. The relevance of the study is determined by the significant and steady decline in the level of citi...

John Sweller. Cognitive load during problem solving: Effects on learning. *Cognitive Science*, 12(2):257–285, 1988. doi: 10.1207/s15516709cog1202_4. Cognitive Load Theory.

Thomas Thiemann. *Modern Canonical Quantum General Relativity*. Cambridge University Press, 2007. ISBN 978-0-521-84263-1. Mathematical foundations of LQG: spin networks and discrete spectra.

Stephen T. Thornton and Jerry B. Marion. *Classical Dynamics of Particles and Systems*. Brooks/Cole, 5th edition, 2004. ISBN 978-0-534-40896-1. Damped oscillators and critical damping.

Song Wang Yiyao Zhu Ao Liang Lingdong Kong Guoyang Zhao Zeying Gong Jun Cen Zhiyu Huang Xiaoshuai Hao Linfeng Li Hang Song Xiangtai Li Jun Ma-Shaojie Shen Jianke Zhu Dacheng Tao Ziwei Liu Junwei Liang Tianshuai Hu, Xiaolu Liu. Vision-Language-Action Models for Autonomous Driving: Past, Present, and Future. *arXiv preprint arXiv:2512.16760v1*, 2025. Autonomous driving has long relied on modular "Perception-Decision-Action" pipelines, where hand-cra...

Fabio Bonsignorio Ivan Petrovi Ivan Markovi Tin Mii, Karlo Koledi. An Active Inference Model of Covert and Overt Visual Attention. *arXiv preprint arXiv:2505.03856v1*, 2025. The ability to selectively attend to relevant stimuli while filtering out distractions is essential ...

Kotryna Ramancauske Titas Ramancauskas. IELTS Writing Revision Platform with Automated Essay Scoring and Adaptive Feedback. *arXiv preprint arXiv:2512.24460v1*, 2025. This paper presents the design, development, and evaluation of a proposed revision platform assistin...

Hadji Elsahar Sylvestre-Alvise Rebuffi Valeriu Lacatusu Tuan Tran Tom Sander Alexandre Mourachko Tomá Souek, Pierre Fernandez. Pixel Seal: Adversarial-only training for invisible image and video watermarking. *arXiv preprint arXiv:2512.16874v1*, 2025. Invisible watermarking is essential for tracing the provenance of digital content. However, training...

Giulio Tononi, Melanie Boly, Marcello Massimini, and Christof Koch. Integrated information theory: from consciousness to its physical substrate. *Nature Reviews Neuroscience*, 17(7):450–461, 2016. doi: 10.1038/nrn.2016.44. Integrated Information Theory (IIT): Phi as consciousness measure.

Sarang Gopalakrishnan Yizhi You Tsung-Cheng Lu, Yu-Jie Liu. Holographic duality between bulk topological order and boundary mixed-state order. *arXiv preprint arXiv:2511.19597v1*, 2025. We

introduce a holographic framework for analyzing the steady states of repeated quantum channels
wi...

Luca Turin. A spectroscopic mechanism for primary olfactory reception. *Chemical Senses*, 21(6):773–791, 1996. doi: 10.1093/chemse/21.6.773. Vibration theory of olfaction via inelastic electron tunneling.

Mark Van Raamsdonk. Building up spacetime with quantum entanglement. *General Relativity and Gravitation*, 42(10):2323–2329, 2010. doi: 10.1007/s10714-010-1034-0. Entanglement as origin of spacetime connectivity.

Ashish Vaswani, Noam Shazeer, Niki Parmar, Jakob Uszkoreit, Llion Jones, Aidan N. Gomez, Lukasz Kaiser, and Illia Polosukhin. Attention is all you need. In *Advances in Neural Information Processing Systems*, volume 30, 2017. Transformer architecture: self-attention mechanism.

Aleksandar Geci Victor E. Ambrus. Thermodynamics of rotating fermions. *arXiv preprint arXiv:2509.17640v1*, 2025. We consider the thermodynamic properties of a rotating gas of fermions. We begin by constructing the...

John von Neumann. *Mathematische Grundlagen der Quantenmechanik*. Springer, Berlin, 1932. Von Neumann entropy: $S = -\text{Tr}(\rho \log \rho)$.

Yaning Zhao Christian Deppe Holger Boche Wafa Labidi, Vida Gholamian. Secure Event-triggered Molecular Communication - Information Theoretic Perspective and Optimal Performance. *arXiv preprint arXiv:2512.16761v1*, 2025. Molecular Communication (MC) is an emerging field of research focused on understanding how cells in ...

Erdhi Widyarto Wahyu Febriyanto, Brenda Chandrawati. Game Design to Introduce Pets. *arXiv preprint arXiv:doaj:0846410259eb477494bca38d455bf83f*, 2024. Introduction of animals from an early age can make children to love animals, especially pets. Childr...

Yucheng Wang. Deriving the Eigenstate Thermalization Hypothesis from Eigenstate Typicality and Kinematic Principles. *arXiv preprint arXiv:2512.13348v2*, 2025. The eigenstate thermalization hypothesis (ETH) provides a powerful framework for understanding therm...

Steven Weinberg. *Gravitation and Cosmology: Principles and Applications of the General Theory of Relativity*. Wiley, 1972. Classical cosmology and general relativity foundations.

Steven Weinberg. The cosmological constant problem. *Reviews of Modern Physics*, 61(1):1–23, 1989. doi: 10.1103/RevModPhys.61.1. The 10^{122} discrepancy between quantum and observed vacuum energy.

Wanhe An Fangwen Dai Wei Gao Yancheng He Ju Huang Qiang Ji Hanqi Jin Xiaoyang Li Yang Li Zhongwen Li Shirong Lin Jiashun Liu Zenan Liu-Tao Luo Dilxat Muhtar Yuanbin Qu Jiaqiang Shi Qinghui Sun Yinghui Tan Hao Tang Runze Wang Yi Wang Zhaoguo Wang Yanan Wu Shaopan

Xiong Binchen Xu Xander Xu Yuchi Xu Qipeng Zhang Xixia Zhang Haizhou Zhao Jie Zhao Shuaibing Zhao Baihui Zheng Jianhui Zheng Suhang Zheng Yanni Zhu Mengze Cai Kerui Cao Xitong Chen Yue Dai Lifan Du Tao Feng Tao He Jin Hu Yijie Hu Ziyu Jiang Cheng Li Xiang Li Jing Liang Chonghuan Liu ZhenDong Liu Haodong Mi Yanhu Mo Junjia Ni Shixin Pei Jingyu Shen XiaoShuai Song Cecilia Wang Chaofan Wang Kangyu Wang Pei Wang Tao Wang Wei Wang Ke Xiao Mingyu Xu Tiange Xu Nan Ya Siran Yang Jianan Ye Yaxing Zang Duo Zhang Junbo Zhang Boren Zheng Wanxi Deng Ling Pan Lin Qu Wenbo Su Jiamang Wang Wei Wang Hu Wei Minggang Wu Cheng Yu Bing Zhao Zhicheng Zheng Bo Zheng Weixun Wang, XiaoXiao Xu. Let It Flow: Agentic Crafting on Rock and Roll, Building the ROME Model within an Open Agentic Learning Ecosystem. *arXiv preprint arXiv:2512.24873v1*, 2025. Agentic crafting requires LLMs to operate in real-world environments over multiple turns by taking a...

Qinghua Hu Wenbo Qiao, Peng Zhang. Quantum Visual Word Sense Disambiguation: Unraveling Ambiguities Through Quantum Inference Model. *arXiv preprint arXiv:2512.24687v1*, 2025. Visual word sense disambiguation focuses on polysemous words, where candidate images can be easily c...

Bailu Si Liqin Zhou Ke Zhou Wenhui Gao, Changbo Zhu. Precision-dependent modulation of social attention. *arXiv preprint arXiv:doaj:016c65ceee9d408abbe67022cd055488*, 2024. Social attention, guided by cues like gaze direction, is crucial for effective social interactions. ...

John Archibald Wheeler. On the nature of quantum geometrodynamics. *Annals of Physics*, 2:604–614, 1957. Quantum foam, Planck-scale spacetime fluctuations.

John Archibald Wheeler. Information, physics, quantum: The search for links. In Wojciech H. Zurek, editor, *Complexity, Entropy, and the Physics of Information*, pages 3–28. Addison-Wesley, 1990. "It from Bit" - information as the foundation of physical reality.

Norbert Wiener. *Cybernetics: Or Control and Communication in the Animal and the Machine*. MIT Press, Cambridge, MA, 1948. Foundation of cybernetics, feedback control, information and entropy.

Kenneth G. Wilson and John Kogut. The renormalization group and the ϵ expansion. *Physics Reports*, 12(2):75–199, 1974. doi: 10.1016/0370-1573(74)90023-4. Renormalization group theory.

Zi-Niu Wu. Duality-based Mode Operations and Pyramid Multilayer Mapping for Rhetorical Modes. *arXiv preprint arXiv:2511.06601v1*, 2025. Rhetorical modes are useful in both academic and non-academic writing, and can be subjects to be stu...

Quan Feng Lei Li Piji Li Haibo Ye Sheng-Jun Huang Shuofei Qiao Shumin Deng Huajun Chen Ningyu Zhang Xiang Chen, Yixin Ou. Retrieval-augmented Prompt Learning for Pre-trained Foundation Models. *arXiv preprint arXiv:2512.20145v1*, 2025. The pre-trained foundation models (PFMs) have become essential for facilitating large-scale multimod...

Dong Zhang Gang Wang Jinlong Xue Kai Fang-Liang Zhao Rui Ma Shuhuai Ren Shuo Liu Tao Guo Weiji Zhuang Xin Zhang Xingchen Song Yihan Yan Yongzhe He Cici Bowen Shen Chengxuan Zhu

Chong Ma Chun Chen Heyu Chen Jiawei Li Lei Li Menghang Zhu Peidian Li Qiying Wang Sirui Deng Weimin Xiong Wenshan Huang Wenyu Yang Yilin Jiang Yixin Yang Yuanyuan Tian Yue Ma Yue Yu Zihan Zhang Zihao Yue Bangjun Xiao Bingquan Xia Bofei Gao Bowen Ye Can Cai Chang Liu Chenhong He Chunan Li Dawei Zhu Duo Zhang Fengyuan Shi Guoan Wang Hailin Zhang Hanglong Lv Hanyu Li Hao Tian Heng Qu Hongshen Xu Houbin Zhang Huaqiu Liu Jiangshan Duo Jianguang Zuo Jianyu Wei Jiebao Xiao Jinhaoy Dong Jun Shi Junhao Hu Kainan Bao Kang Zhou Linghao Zhang Meng Chen Nuo Chen Peng Zhang Qianli Chen Qiantong Wang Rang Li Shaohui Liu Shengfan Wang Shicheng Li Shihua Yu Shijie Cao Shimao Chen Shuhao Gu Weikun Wang Wenhan Ma Xiangwei Deng Xing Yong Xing Zhang Xu Wang Yifan Song Yihao Zhao Yingbo Zhao Yizhao Gao Yu Cheng Yu Tu Yudong Wang Zhaojun Huang Zhengju Tang Zhenru Lin Zhichao Song Zhipeng Xu Zhixian Zheng Zihan Jiang Xiaomi LLM-Core Team, :. MiMo-Audio: Audio Language Models are Few-Shot Learners. *arXiv preprint arXiv:2512.23808v1*, 2025. Existing audio language models typically rely on task-specific fine-tuning to accomplish particular ...

Lei Wang Yunshi Lan Chao Yang Xuanjun Zong, Zhiqi Shen. MCP-SafetyBench: A Benchmark for Safety Evaluation of Large Language Models with Real-World MCP Servers. *arXiv preprint arXiv:2512.15163v1*, 2025. Large language models (LLMs) are evolving into agentic systems that reason, plan, and operate extern...

Han-Jia Ye Yi-Kai Zhang, De-Chuan Zhan. Capability Instruction Tuning: A New Paradigm for Dynamic LLM Routing. *arXiv preprint arXiv:2502.17282v1*, 2025. Large Language Models (LLMs) have demonstrated human-like instruction-following abilities, particula...

Varshith Roy Kotla Yoshith Roy Kotla. Conformal Prediction Sets for Next-Token Prediction in Large Language Models: Balancing Coverage Guarantees with Set Efficiency. *arXiv preprint arXiv:2512.22682v1*, 2025. Deploying large language models (LLMs) in high-stakes domains requires rigorous uncertainty quantifi...

Kyoo il Kim Youngjin Hong, In Kyung Kim. An Instrumental Variables Approach to Testing Firm Conduct under a Bertrand-Nash Framework. *arXiv preprint arXiv:2501.05022v4*, 2025. Understanding firm conduct is crucial for industrial organization and antitrust policy. In this arti...

Damien Teney Michael Moor Maria Brbic Yulun Jiang, Liangze Jiang. Meta-RL Induces Exploration in Language Agents. *arXiv preprint arXiv:2512.16848v1*, 2025. Reinforcement learning (RL) has enabled the training of large language model (LLM) agents to interac...

Kunquan Zhang Jinxiao Zhang Xinying Chen Haohuan Fu Runmin Dong Yunkai Yang, Yudong Zhang. Task-Oriented Data Synthesis and Control-Rectify Sampling for Remote Sensing Semantic Segmentation. *arXiv preprint arXiv:2512.16740v1*, 2025. With the rapid progress of controllable generation, training data synthesis has become a promising w...

Yudong Li Shaojie Zhu Zijian Luo Chenyun Yu Sikai Wu Shichen Shen Cong Xu Bin Wang Kai Jiang Hongyong Yu Chengxiang Zhuo Zang Li Yunsheng Pang, Zijian Liu. HiGR: Efficient Generative

Slate Recommendation via Hierarchical Planning and Multi-Objective Preference Alignment. *arXiv preprint arXiv:2512.24787v1*, 2025. Slate recommendation, where users are presented with a ranked list of items simultaneously, is widel...

Bo Wang Qi Luo Xuanjing Huang Yining Zheng Xipeng Qiu Yuxin Wang, Shicheng Fang. Multi-hop Reasoning via Early Knowledge Alignment. *arXiv preprint arXiv:2512.20144v1*, 2025. Retrieval-Augmented Generation (RAG) has emerged as a powerful paradigm for Large Language Models (L...

Tianjie Ju Sufeng Duan Gongshen Liu Yuyi Zhang, Boyu Tang. Do Latent Tokens Think? A Causal and Adversarial Analysis of Chain-of-Continuous-Thought. *arXiv preprint arXiv:2512.21711v1*, 2025. Latent tokens are gaining attention for enhancing reasoning in large language models (LLMs), yet the...

Chiyuan Zhang, Samy Bengio, Moritz Hardt, Benjamin Recht, and Oriol Vinyals. Understanding deep learning requires rethinking generalization. In *International Conference on Learning Representations*, 2017. Deep networks can memorize random labels - generalization mystery.

et al. Zhang. Adaptive Control Methods for AI Systems. *arXiv preprint arXiv:2512.09632v1*, 2025. Adaptive control applied to AI systems and parameter optimization.

Huanqi Cao Chenggang Zhao Chengqi Deng Jiashi Li Damai Dai Huazuo Gao Jiang Chang Liang Zhao Shangyan Zhou Zhean Xu Zhengyan Zhang Wangding Zeng Shengding Hu Yuqing Wang Jingyang Yuan Lean Wang Wenfeng Liang Zhenda Xie, Yixuan Wei. mHC: Manifold-Constrained Hyper-Connections. *arXiv preprint arXiv:2512.24880v1*, 2025. Recently, studies exemplified by Hyper-Connections (HC) have extended the ubiquitous residual connec...

Wenhao Yu Kishan Panaganti Yujun Zhou Haitao Mi Dong Yu Zhenwen Liang, Sidi Lu. Can LLMs Guide Their Own Exploration? Gradient-Guided Reinforcement Learning for LLM Reasoning. *arXiv preprint arXiv:2512.15687v1*, 2025. Reinforcement learning has become essential for strengthening the reasoning abilities of large langu...

Yahao Mu Ruihua Zhou Hang Liu Tingwu Jin Di Wu Jianlong Xia Ce-Wen Nan Zhixing Wan, Shuo Wang. PTCDA/CuS cathode enabling stable sulfide-based all-solid-state batteries. *arXiv preprint arXiv:doaj:090fea278bf04a4e855f51c64abab60e*, 2024. Organic cathode materials have garnered significant attention for their potential application in lit...

Corey M. Abramson Zhuofan Li. Ethnography and Machine Learning: Synergies and New Directions. *arXiv preprint arXiv:2412.06087v1*, 2024. Ethnography (social scientific methods that illuminate how people understand, navigate and shape the...

Yan Li Xuejun Ma Shaofeng Sun Zixuan Zhang, Zhenxing Niu. Research on the influence factors of accident severity of new energy vehicles based on ensemble learning. *arXiv preprint*

arXiv:doaj:01b99c28e3cd46f49886cc3e0a26c073, 2024. With the deepening of the concept of green, low-carbon, and sustainable development, the continuous ...

Wojciech H. Zurek. Decoherence, einselection, and the quantum origins of the classical. *Reviews of Modern Physics*, 75(3):715–775, 2003. doi: 10.1103/RevModPhys.75.715. Quantum Darwinism and environment-induced superselection.

Mátyás Antal Márk Marosi Ákos Prucs, Márton Csutora. Compute-Accuracy Pareto Frontiers for Open-Source Reasoning Large Language Models. *arXiv preprint arXiv:2512.24776v1*, 2025. Large Language Models (LLMs) are demonstrating rapid improvements on complex reasoning benchmarks, p...